66-6994

PIKAL, Michael Jon, 1939-

APPARENT MOLAL VOLUMES AND VISCOSITIES OF SOME AQUEOUS RARE-EARTH CHLORIDE SOLUTIONS AT 25°C.

Iowa State University of Science and Technology
Ph.D., 1966
Chemistry, physical

University Microfilms, Inc., Ann Arbor, Michigan

APPARENT MOLAL VOLUMES AND VISCOSITIES OF SOME AQUEOUS RARE-EARTH CHLORIDE SOLUTIONS AT 25°C.

by

Michael Jon Pikal

A Dissertation Submitted to the
Graduate Faculty in Partial Fulfillment of
The Requirements for the Degree of
DOCTOR OF PHILOSOPHY

Major Subject: Physical Chemistry

Approved:

Signature was redacted for privacy.
In Charge of Major Work

Signature was redacted for privacy.
Head of Major Department

Signature was redacted for privacy.
Dean of Graduate College

Iowa State University
Of Science and Technology
Ames, Iowa

1966

TABLE OF CONTENTS

I. INTRODUCTION

Electrolytic solutions have been the subject of scientific research for nearly a century, but in spite of considerable progress, a fundamental understanding of electrolytes at moderate and high concentrations remains one of the major unsolved problems in physical chemistry. Part of the difficulty in developing a comprehensive theory of electrolytes has been the lack of an adequate theory describing complex liquids such as water. Mostly due to the success of the Debye-Hückel theory (1), a popular model for the solvent has been one in which the solvent is regarded as a structureless continuum with a certain dielectric constant. This simplified model is generally quite successful in treating the concentration dependence of many properties of dilute solutions. However, it has become increasingly evident that the structure of the solvent and specific ion-solvent interactions have a significant influence on the properties of a concentrated electrolyte and on many properties of an electrolyte at infinite dilution. Indeed, a significant proportion of the recent research effort is devoted to an elucidation of the structure of water and the nature of ion-water interactions (2).

The lanthanide, or rare-earth, elements offer a unique opportunity to study ion-solvent interactions of highly charged ions as a function of ionic radius. The rare-earths form a number of salts that are readily soluble in water, and under

normal conditions, the rare-earth ion exists only in the plus three valence state. Chemically, the tripositive rare-earth ions resemble each other, and in aqueous media, tend to hydrolyze and associate with the anion much less than other tripositive ions. This lack of appreciable hydrolysis and association for many of the rare-earth salts in dilute solution makes a theoretical analysis of the experimental data a great deal easier. Furthermore, the increasing nuclear charge across the rare-earth series exerts a greater attraction for the electron shells as the atomic number increases, causing a gradual decrease in ionic radius with increasing atomic number of the tripositive rare-earth ion. It is this property that allows a critical study of ion-solvent interactions as a function of ionic radius.

Thermodynamic and transport properties of aqueous rare-earth salts have been extensively investigated by Spedding and co-workers over the past fifteen years (3,4,5,6). These studies have shown that for properties that can be measured accurately in dilute solutions, the data are generally compatible with interionic attraction theory. One possible exception may be the concentration dependence of the apparent molal volume, as investigated by Ayers (7), where significant deviations from the simple limiting law were found at low concentrations. However, the uncertainty in the value of the theoretical limiting slope at the time and the lack of data for the rare-earth salts in the middle of the series prevented

definite conclusions from being drawn.

Perhaps the most interesting result of these investigations is the irregular behavior shown by many of the solution properties when plotted as a function of ionic radius. In particular, the apparent molal volumes at infinite dilution determined by Ayers do not show the expected regular decrease as the radius of the rare-earth ion decreases. Rather, the apparent molal volumes show the expected decrease from La to Nd, and from Er to Yb, but the data indicate the apparent molal volumes for Er^{+3} and Nd^{+3} are nearly the same. It was suggested by Spedding and Ayers (7) that this irregular change of apparent molal volumes at infinite dilution could result from a change in the water co-ordination number of the rare-earth ions. The data of Saeger and Spedding (6) indicate that the apparent molal volumes of the rare-earth ions at infinite dilution decrease from La to Nd, increase from Nd to about Gd, and decrease from Gd to Yb. According to Saeger and Spedding, their results suggest a gradual change in preferred co-ordination number takes place over a number of rare-earths near the middle of the series.

The apparent molal volume, ϕ_V, is defined by,

$$\phi_V = \frac{V - n_1 \bar{V}_1^o}{n_2} , \qquad (1.1)$$

where V is the total volume of a solution composed of n_2 moles of solute and n_1 moles of solvent having a molar volume, $\bar{V}_1^o$. The partial molal volume, $\bar{V}_2$, may be calculated from Equation

1.1 and expressed as,

$$\bar{V}_2 = \left(\frac{\partial V}{\partial n_2}\right)_{T,P,n_1} = n_2 \frac{\partial \phi_v}{\partial n_2} + \phi_v \qquad (1.2)$$

and since the molality, m, is directly proportional to n_2,

$$\bar{V}_2 = m \frac{\partial \phi_v}{\partial m} + \phi_v \, . \qquad (1.3)$$

The apparent molal volume at infinite dilution, ϕ_v^o, is identically equal to the partial molal volume at infinite dilution, $\bar{V}_2^o$. The partial molal volume at infinite dilution may be visualized as the change in volume of a nearly infinite quantity of solvent upon addition of one mole of solute, and therefore depends on the intrinsic volume of the ions and ion-solvent interactions. During the course of this research, apparent molal volume data were obtained for dilute aqueous solutions of $PrCl_3$, $SmCl_3$, $GdCl_3$, $TbCl_3$, $DyCl_3$, $HoCl_3$, and $ErCl_3$. Chapter IV of this thesis presents these experimental results and a study of the apparent molal volumes of dilute rare-earth chlorides and nitrates in aqueous solution. This investigation was an extension of earlier work by Spedding and Ayers (7) and by Saeger and Spedding (6). The partial molal volumes at infinite dilution obtained by Saeger and Spedding were the result of an empirical extrapolation from relatively high concentrations and may contain large extrapolation errors. Therefore, it seemed advisable to employ the experimental method of Spedding and Ayers to measure the apparent molal volumes of a number of dilute rare-earth chloride solu-

tions spanning the rare-earth series. More accurate values of the partial molal volume at infinite dilution could then be obtained. Furthermore, the additional data obtained in this research may be expected to be helpful in a further study of the concentration dependence of the apparent molal volumes of dilute aqueous rare-earth salts.

The second part of this thesis is an extension of earlier work on transport properties (3,6) to include viscosity measurements. In particular, the relative viscosities of aqueous solutions of $LaCl_3$, $NdCl_3$, $SmCl_3$, $TbCl_3$, $DyCl_3$, $HoCl_3$, and $ErCl_3$ were measured, at 25°C., as a function of concentration from 0.05 molal to saturation.

The coefficient of viscosity, or simply viscosity, of a fluid is a measure of the internal resistance to flow exhibited by a fluid whenever there is relative motion between adjacent layers of the fluid. The definition of viscosity is perhaps best illustrated by considering two parallel plates separated by a fluid, one of the plates being held stationary and the other plate being in motion at a constant velocity in its own plane. If S is the force per unit area required to maintain the velocity of the moving plate, and dv/dx is the velocity gradient in the fluid in a direction perpendicular to the plates, the viscosity of a Newtonian fluid, η, may be defined by

$$\eta = S/(dv/dx). \qquad (1.4)$$

The absolute unit of viscosity is the poise, defined as the

viscosity of a material which requires a shearing force, S, of one dyne per square centimeter to maintain a velocity gradient of one centimeter per second between two parallel plates one centimeter apart. When discussing the viscosity behavior of solutions, it is useful to consider the relative viscosity, η_r, defined as the absolute viscosity of the solution divided by the absolute viscosity of the solvent at the same temperature.

The relative viscosity of dilute electrolytes has proven to be an effective method for studying ion-solvent interactions (8,9). Also, there is some reason for expecting the role of ion-ion interactions to be of minor importance in determining the relative viscosity of an electrolyte at high concentrations (10). Therefore, viscosity data for aqueous rare-earth salts might be expected to yield valuable information concerning ion-water interactions at high concentrations, as well as in dilute solutions.

II. ELECTROLYTIC SOLUTION THEORY

The objective of a theory of electrolytes is the calculation of macroscopic properties of the electrolyte as a function of temperature, pressure, and composition, which involves a statistical analysis of the interactions between large numbers of ions and solvent molecules. The theoretical calculation of the activity coefficient is of particular interest, since the laws of thermodynamics make it possible to calculate other thermodynamic functions once the expression for the activity coefficient is known. This chapter will consider the theoretical calculation of the activity coefficient and related thermodynamic properties. In particular, emphasis will be placed on a discussion of the assumptions involved rather than on a detailed mathematical derivation of the equations. The theoretical analysis of a transport property proceeds from the same basic ideas employed in the activity coefficient problem, except for the added complications of a non-equilibrium system (11,12). Therefore, the limitations that will be assigned to the theoretical expression for the activity coefficient apply for the non-equilibrium theories as well.

A. Early Concepts of Electrolytes

The basic difference between a solution of an electrolyte and that of a non-electrolyte is that an electrolytic solution contains ions, or charged particles. This important distinction was recognized as early as 1887 by Arrhenius (13). In an attempt to explain the existing experimental data on electro-

lytes, Arrhenius proposed that when an electrolyte dissolves, an equilibrium exists in solution between the undissociated solute molecules and the ions which arise from dissociation of the solute. According to the Arrhenius theory, the properties of an electrolyte may be explained by using the law of mass action to calculate the equilibrium between ions and solute molecules. Although the Arrhenius theory was quite successful in explaining the properties of what are now called weak electrolytes, it soon became obvious that the dissociation theory alone could not account for the properties of strong electrolytes like sodium chloride (14). J. J. van Laar (15) was the first to suggest the importance of the long range coulombic force between ions in explaining the characteristic properties of electrolytes. It was shortly realized (16,17,18) that the behavior of strong electrolytes in dilute solution could be qualitatively explained by assuming complete dissociation and considering the effect of the interionic coulombic forces. In 1912, Milner (19) attempted a quantitative solution of the electrolyte problem, assuming complete dissociation and considering only coulomb forces. By graphical methods he obtained a result that was essentially correct for dilute solutions. However, Milner's mathematical treatment was extremely involved, and his equations were not easily applied to experimental data.

B. The Debye-Hückel Theory

The present theory of electrolytes was born in 1923 when Debye and Hückel (1) derived a simple expression for the activ-

ity coefficient of a very dilute electrolyte. Debye and Hückel approached the problem by considering the mean distribution of charge around a given central ion in the solution, which may be called the "ionic atmosphere" of the central ion. Through use of this "ionic atmosphere" concept and the Poisson equation, they were able to circumvent most of the mathematical difficulties encountered by Milner and obtain a simple solution to the problem. Their result for the mean ionic activity coefficient, $\gamma_{\pm}$, may be written in the form,

$$\ln \gamma_{\pm} = - \frac{|z_+ z_-| e^2}{2DkT} \kappa \quad , \qquad (2.1)$$

where κ^{-1} is the mean radius of the "ionic atmosphere", defined by the equation

$$\kappa = \left[\frac{4\pi N e^2 (\nu_+ z_+^2 + \nu_- z_-^2) c}{DkT} \right]^{\frac{1}{2}} = bc^{\frac{1}{2}} . \qquad (2.2)$$

Equations 2.1 and 2.2 apply to an electrolyte which dissociates into ν_+ cations of charge ez_+ and ν_- anions of charge ez_-, where e is the absolute value of the electronic charge. The quantity, D, is the dielectric constant of the solvent, T is the absolute temperature, N is Avogadro's number, k is Boltzman's constant, and c is the concentration of the electrolyte in moles per liter.

The Debye-Hückel theory is an ingenious approximate method of evaluating the partition function for an electrolyte, and its validity rests upon the following assumptions:

1. The solute is completely dissociated into spherical, unpolarizable ions, which are all of the same size. These ions move in a continuous medium of dielectric constant, D.

The volume and dielectric constant of this medium are independent of temperature, pressure, and the presence of ions. All deviations from ideality are due to coulomb forces between the ions. Also, the ions are characterized by a distance of closest approach, a, which limits the electrostatic energy to finite values.

2. For a given configuration of ions, it is possible to define a smoothed electrostatic potential, $\psi(r)$, and smoothed charge density, $\rho(r)$, which obey Poisson's equation,

$$\nabla^2 \psi(r) = \frac{-4\pi}{D} \rho(r) , \qquad (2.3)$$

where r is the distance from a central ion, i.

The average electrostatic potential, $\overline{\psi(r)}^{i}$, may be related to the average charge density, $\overline{\rho(r)}^{i}$, by summing Equation 2.3 over all accessible configurations of ions, except i, to obtain the equation,

$$\nabla^2 \overline{\psi(r)}^{i} = \frac{-4\pi}{D} \overline{\rho(r)}^{i} . \qquad (2.4)$$

The Boltzman equation may then be used to express the average charge density in terms of W_{ij}, defined as the average free energy of an ion j at distance r from a given ion i, which gives,

$$\overline{\rho(r)}^{i} = \frac{1}{V} \sum_{j} ez_j \exp(-W_{ij}/kT) . \qquad (2.5)$$

Here, V is the total volume of the system, and ez_j is the charge of the j ion. Combination of Equations 2.4 and 2.5 results in the expression,

$$\nabla^2 \overline{\psi(r)}^{i} = \frac{-4\pi}{DV} \sum_j ez_j \exp(-W_{ij}/kT) . \qquad (2.6)$$

Equation 2.6 is exact for the model assumed apart from the smoothing error introduced by applying Equation 2.3 (20). The fundamental statistical approximation of the Debye-Hückel theory is to assume the equality,

$$W_{ij} = z_j e \overline{\psi(r)}^{i} . \qquad (2.7)$$

This approximation is often called the assumption of linear superposition. Equations 2.6 and 2.7 lead to the Poisson-Boltzman equation,

$$\nabla^2 \overline{\psi(r)}^{i} = \frac{-4\pi}{DV} \sum_j ez_j \exp(-z_j e \overline{\psi(r)}^{i}/kT). \qquad (2.8)$$

4. For the purpose of obtaining a simple solution for $\overline{\psi(r)}^{i}$, Debye and Hückel made the further assumption,

$$\exp(-z_j e \overline{\psi(r)}^{i}/kT) \cong 1 - z_j e \overline{\psi(r)}^{i}/kT , \qquad (2.9)$$

which is valid when $z_j e \overline{\psi(r)}^{i}/kT \ll 1$. Using the approximation indicated by Equation 2.9 and the principle of electrical neutrality, Equation 2.8 leads to the linearized Poisson-Boltzman equation

$$\nabla^2 \overline{\psi(r)}^{i} = \kappa^2 \overline{\psi(r)}^{i} , \qquad (2.10)$$

where κ has been defined by Equation 2.2. Equation 2.10 may then be solved for $\overline{\psi(r)}^{i}$ (20). After making the assumption,

$\kappa a \ll 1$, the derivation of Equation 2.1 from $\frac{i}{\psi(r)}$ is straightforward, and no further assumptions or approximations needed, provided the physical model defined earlier is retained (20).

The Debye-Hückel limiting law, given by Equation 2.1, is often referred to erroneously as valid for point charges. In fact, a system of point charges is unstable and could not exist (21). The original work of Debye and Hückel (1) made use of rather unorthodox statistical mechanics, and as a result, the assumptions involved in their treatment were not immediately obvious. Using the same basic method and assumptions used by Debye and Hückel, Fowler and Guggenheim (20) gave a more complete derivation, indicating the various assumptions, and arrived at Equation 2.11 for the mean ionic activity coefficient.

$$\ln \gamma_{\pm} = \frac{-|z_+ z_-| e^2}{2DkT} \frac{\kappa}{1 + \kappa a} . \qquad (2.11)$$

Equation 2.11 reduces to the Debye-Hückel limiting law, Equation 2.1, by making the assumption $\kappa a \ll 1$, which is valid for extremely dilute solutions. However, it is important to note that the derivation of Equation 2.11 does not require any assumptions in addition to those already necessary to derive the limiting law. Actually, derivation of the limiting law proceeds from Equation 2.11 by use of the further approximation, $\kappa a \ll 1$ (20).

Although the distance of closest approach, a, does have

a precise theoretical significance, the Debye-Hückel theory does not predict its exact value for a given electrolyte. Consequently, the exact value of a to be used in Equation 2.11 must be determined by either intelligent guessing or by choosing the value of a which best represents the experimental data. Neither of these procedures for evaluating a is entirely satisfactory. The most rigorous method of testing the Debye-Hückel theory would be to use experimental data at such low concentrations that Equation 2.11 becomes independent of a and reduces to the limiting law. Unfortunately, this method is normally impossible in practice, and the Debye-Hückel theory is usually compared with experimental data by using Equation 2.11 and the value of a which best represents the data. If the value of a determined from the data is reasonable, the data is said to agree with the Debye-Hückel theory. The definition of a implies that a reasonable value of a must be close to the mean ionic diameter, or slightly greater if the ions are strongly hydrated. Experimental activity coefficient data for dilute aqueous solutions of strong electrolytes are generally well represented by Equation 2.11 and reasonable values of a (11). However, for a few electrolytes, the data can be represented by Equation 2.11 only by using values of a that are much too small (11,20). Activity coefficient data for the rare-earth chlorides, obtained by Spedding and co-workers (22,23,24,25), are consistent with Equation 2.11 for all concentrations up to about 0.05 molar,

provided the a parameter is suitably adjusted for each salt. These a parameters are roughly equal to the sum of the rare-earth and chloride ionic radii, plus the diameter of a water molecule, suggesting the rare-earth ions are strongly hydrated.

C. Critique of the Debye-Hückel Theory

The validity of the Debye-Hückel theory is dependent upon the validity of the various assumptions made during its development. These approximations have already been described. The purpose of the following discussion will be to examine these assumptions in more detail and to determine the physical conditions necessary for the theory to be a good approximation.

1. Mathematical and statistical approximations

The Poisson equation applies rigorously only to a continuous charge distribution, and its application to a given configuration of ions is not strictly valid. Therefore, the use of Equation 2.3 is an approximation which assumes the discrete charges on the ions can be smoothed into a continuous distribution without thereby spreading them over regions within which the electrostatic potential varies greatly (20). This smoothing process will be more successful the greater the ionic radii of the ions (20).

The assumption of linear superposition, described by Equation 2.7 implies that the average force acting on a third ion, k, in the neighborhood of two other ions, i and j, is the sum of the average forces which would act on ion k if

ions i and j acted separately (26). This assumption is a good one for low concentrations, small charges, and large ionic diameters, but as soon as higher terms in the Poisson-Boltzman equation become important, linear superposition is no longer valid (27). Consequently, only the linearized Poisson-Boltzman equation, Equation 2.10, is consistent with the linear superposition assumption. The assumption of linear superposition introduces errors which are of the same order in ionic charge as the non-linear terms in the Poisson-Boltzman equation, so the limiting law is not affected by the errors introduced by this assumption (26).

Since $\overset{i}{\psi}(r) \propto 1/r$, the approximation described by Equation 2.9 is a very bad one for small values of r. As the concentration decreases, the number of close encounters of ions will also decrease, and in the limit of infinite dilution, Equation 2.9 will be valid. However, at finite concentrations there will be occasional "ion-pair" formation when two ions of opposite charge approach one another within a certain radius, q, characteristic of the ions and the solvent. The effect of this "ion-pair" formation will be to lower the activity coefficient and will be more serious for small highly charged ions in a medium of low dielectric constant (20). For large ions, the effect of "ion-pair" formation is negligible. A simple way of extending the Debye-Hückel theory to include the effect of "ion-pair" formation was proposed by Bjerrum (28).

Bjerrum considered separately the case where two ions came closer than the distance, $q = |e_i e_j| / 2DkT$. This treatment is described by Harned and Owen (11) and by Fowler and Guggenheim (20). Basically, Bjerrum's treatment for symmetrical electrolytes involves application of the Debye-Hückel theory for the ions outside of q, using q as the distance of closest approach, and ignoring the effect of the electrostatic field of the two ions inside of q on the remaining ions. Bjerrum's separate consideration of close ionic encounters therefore allows Equation 2.9 to be a good approximation for the remaining ions. Furthermore, Bjerrum's treatment has the important feature of being self-consistent and is particularly successful for solutions of small ions in media of low dielectric constant (20).

Another method of avoiding the limitations imposed by Equation 2.9 would be to include higher terms in the series expansion of the exponential. This is the approach taken by Gronwall, La Mer, and Sandved (29), who evaluated higher order terms in the Poisson-Boltzman equation. They found that the higher order terms did not affect the limiting law but became important at finite concentrations for small ions. For electrolytes where application of the Debye-Hückel theory gave unreasonably small a values, application of the Gronwall-La Mer-Sandved extension resulted in more reasonable values for this parameter. However, their treatment is not self-consistent and therefore cannot be exact (20). Negative deviations for Equation 2.11 are probably due to the neglect of higher

order terms in the Poisson-Boltzman equation, and for systems where negative deviations are observed, a more exact solution of the Poisson-Boltzman equation probably gives a better approximation than the Debye-Hückel theory. However, a large number of electrolytes exhibit positive deviations from the Debye-Hückel theory, which cannot be explained on the basis of higher order terms in the Poisson-Boltzman equation (30).

2. The physical model

The physical model assumed by Debye and Hückel was defined by the first assumption. It seems obvious that this model is not an exact description of an electrolyte, and the effect of these assumptions on the theoretical expression for the activity coefficient may be serious.

Contrary to the Debye-Hückel model, the volume of a real solution is temperature and pressure dependent and is also influenced by the presence of ions. Consequently, the electrical free energy computed from the Debye-Hückel theory corresponds more closely to the Gibbs free energy, rather than to the Helmholtz free energy (20). Also, it is a better approximation to assume the volume of a solution has the same temperature and pressure dependence as the pure solvent, rather than to ignore the temperature dependence entirely. These modifications of the Debye-Hückel model are extremely important when calculating other thermodynamic quantities from the free energy.

The use of the Poisson equation, described in assumption

number two, assumes the dielectric constant of the solvent is independent of the distance from the ion. Also, in the averaging process used to derive Equation 2.4, it was assumed that the dielectric constant is independent of the particular ionic configuration. While these assumptions are valid for the idealized solvent assumed by Debye and Hückel, they are only approximations for a real solvent. The presence of charged ions in a real solvent may be expected to exert a considerable influence on the solvent molecules in the immediate vicinity of the ions, such that the average dielectric constant is no longer independent of the distance from the ion. Therefore, the dielectric constant, D, that appears in Equation 2.3 is, in fact, an average over all solvent molecules (20), which will be dependent upon the particular configuration of the ions. Since this average dielectric constant is dependent upon the ionic configuration, the averaging of Equation 2.3 for a real solution gives,

$$\nabla^2 \overline{\psi(r)}^{i} = -4\pi \overline{\left(\rho(r)/D\right)}^{i} , \qquad (2.12)$$

Equation 2.4 is obtained by replacing $\overline{\left(\rho(r)/D\right)}^{i}$ by $\overline{\rho(r)}^{i} \Big/ \frac{1}{D}$ (31). Therefore, the dielectric constant that appears in Equation 2.4 is really a result of two separate averaging steps, first averaging over all the solvent configurations for a given ionic configuration, and then averaging over all ionic configurations except i. A rigorous result can be obtained

only by averaging over all accessable configurations, both solvent and ionic, in one step, and the result obtained by two successive partial averaging steps cannot give the exact result (20). Also, this average dielectric constant should be dependent on the concentration, which introduces complications when computing the electrical free energy from the electrostatic potential (20).

In spite of these statistical difficulties, when most of the solvent is unaffected by the presence of ions, as in a very dilute solution, it is a good approximation to use the dielectric constant of the pure solvent in the theoretical equations. However, the temperature and pressure dependence of the dielectric constant must be taken into consideration when computing other thermodynamic quantities from the electrical free energy. It may be expected that the deviations due to these approximations concerning the dielectric constant would be expressed in the form of a power series in c, with the first term being proportional to c (20). The limiting law would then be exact. In fact, the limiting law has been proven to be unaffected by the variation in effective dielectric constant around the ion (32,33). The deviations due to the "dielectric saturation" effect are approximately proportional to c at low concentrations and become important for highly charged ions and high temperatures at moderate concentrations.

The assumption of non-polarizable ions, therefore

neglecting short range forces, is a good approximation in dilute solution. The limiting law has been shown to be unaffected by deviations due to this approximation (27,34). However, short range repulsive forces will give a contribution of their own to the free energy, which will become important at higher concentrations. According to Onsager (27), the assumption of short range repulsion is necessary and sufficient to explain the observed rise of activity coefficients at high concentrations.

Treating the solvent as a continum may not be realistic, particularly for water as the solvent. Experimental (35,36) and theoretical (37) evidence suggest that all highly charged ions are strongly hydrated in aqueous solution and these hydrated ions behave as a single species. Robinson and Stokes (38) modified the Debye-Hückel model to account for hydration. Again, the limiting law was not affected, but the effects of hydration became extremely important at higher concentrations. They treated the hydration number, h, as an adjustable parameter and obtained excellent agreement with experiment, even for concentrated solutions. The physical model used by Robinson and Stokes was certainly more realistic at non-zero concentrations than the original Debye-Hückel model. However, their treatment suffers from the use of the Debye-Hückel expression for the ion-ion contribution to the free energy, which is certainly not valid for concentrated solutions. Their treatment also neglects the effect of short range

ion-ion repulsive forces resulting from polarization of the ions. However, for strongly hydrated ions, these short range forces may not be important since the hydration sphere may prevent close encounters of the ions.

It has been shown that neither lack of spherical symmetry (39) nor unequal size (40) of the ions affect the validity of the Debye-Hückel limiting law.

D. Conclusions

Theoretically, the validity of the Debye-Hückel theory has been firmly established as a limiting law and Equation 2.1 should be exact in the limit as c approaches zero. Generally, accurate experimental data for activity coefficients and other thermodynamic properties of dilute solutions confirm this conclusion (11). Equation 2.11 includes the effect of the a parameter and probably gives a good approximation for the deviations from the limiting law in dilute solutions, provided the solvent has a high dielectric constant and the a parameter is large. The a parameter would be large if either the ions are large or if the ions are strongly hydrated.

An accurate description of concentrated solutions must consider other effects, such as ion-solvent interactions, short range repulsive forces and "co-valent" complex formation, in addition to the coulomb forces between ions. Scatchard (41) has included non-coulomb interactions in an attempt to develop a theory for concentrated solutions. However, his

theory uses the Debye-Hückel approach to calculate the electrical free energy, which is of dubious validity in concentrated solutions. The linear superposition approximation is no longer valid in concentrated solutions, and recently Frank and Thompson (42) have argued that the entire "ionic atmosphere" concept is no longer valid above about 0.001 molar. Consequently, any theory of concentrated solutions which used the Debye-Hückel theory to calculate the electrical free energy must be treated with caution.

Mayer (43) and Poirier (44) have adapted the cluster theory of imperfect gases to ionic solutions. Their results verify the validity of the Debye-Hückel limiting law. The physical model used by Mayer was essentially the same as that used in the Debye-Hückel theory, so the equations derived are limited to dilute solutions. However, many of the statistical approximations inherent in the Debye-Hückel approach do not appear in Mayer's theory, so that, in principle, the cluster theory approach could be combined with a more realistic model to yield an acceptable theory for concentrated solutions. In practice, application of the cluster theory of solutions may be limited to dilute solutions because of the nearly impossible task of evaluating a slowly converging infinite series (45).

III. PREPARATION OF SOLUTIONS

The rare-earth chloride solutions used in this research were prepared by dissolving the rare-earth oxides in C. P. hydrochloric acid. The rare-earth oxides were obtained from the rare-earth separation group of the Ames Laboratory of the U. S. Atomic Energy Commission. The oxides were analyzed for the common metallic impurities by emission spectrography. The results of these analyses are given in Table 1.

The rare-earth chloride stock solutions were prepared by adding the dry oxides to a slightly less than equivalent amount of 6N acid. The excess oxide was removed by filtering the solutions through a fine sintered glass filter. A solution in this form contained some colloidal oxide, which was readily detected by the formation of a Tyndall cone from a small beam of light passing through the solution. Most of the colloidal oxide and other basic species were removed by adding acid to the solution until a pH of about three was reached. A small portion of the solution was removed and used to determine the equivalence point of the suspected hydrolysis reaction,

$$R^{+3} + H_2O \rightleftharpoons R(OH)^{+2} + H^+ , \qquad (3.1)$$

where R^{+3} is a rare-earth ion. The solution was titrated with 0.05N hydrochloric acid, and the equivalence point was determined by a plot of change in pH per milliliter of acid added, $\triangle pH/\triangle ml.$, against the average volume of acid added. The pH where $\triangle pH/\triangle ml.$ was a maximum was taken as the equivalence

Table 1. Spectrographic analysis of rare-earth oxides

Oxide	Impurities (percent)[a]		
	Fe	Ca	Other rare-earths
La_2O_3	< 0.007	< 0.01	< 0.08
Pr_6O_{11}	0.003	0.02	< 0.15
Nd_2O_3	< 0.009	< 0.03	< 0.20
Sm_2O_3[b]	0.006	0.06	< 0.03
Sm_2O_3[c]	< 0.003	0.02	< 0.10
Gd_2O_3	0.001	0.006	< 0.03
Tb_4O_7	< 0.005	0.04	< 0.05
Dy_2O_3[b]	< 0.01	< 0.03	< 0.10
Dy_2O_3[c]	0.01	< 0.03	< 0.15
Ho_2O_3	< 0.005	0.05	< 0.06
Er_2O_3[b]	< 0.002	0.01	< 0.01
Er_2O_3[c]	0.006	0.02	< 0.03

[a]The percentage impurities reported as "less than" are the lower limits of the analytical method, and the actual amount of impurity is probably much less than the amount indicated.

[b]Used only for apparent molal volume work.

[c]Used only for viscosity work.

pH.

The stock solution was then adjusted to its equivalence pH and heated for several hours to dissolve any remaining oxychloride or colloidal oxide. The solution was cooled and the pH adjusted again to the equivalence pH, and the solution was again heated for several hours. This procedure was repeated until the pH did not change from the equivalence pH. Solutions prepared in this way were found to be stable indefinitely and were free of colloidal oxide.

The stock solutions prepared for the apparent molal volume studies were usually about 2.7 molal. Secondary stock solutions of about 0.6 and 0.2 molal were prepared from weighed quantities of the primary stock solution and conductivity water. The conductivity water had been prepared by distilling tap distilled water from an alkaline potassium permanganate solution in a Barnsted Conductivity Still; the conductivity water had a specific conductance of less than 1×10^{-6} mho per centimeter.

The stock solutions prepared for viscosity studies were usually about 3.5 molal. Solutions more dilute than the stock solution were prepared, by weight, from the stock solution and conductivity water. The saturated solutions were prepared by allowing the concentrated stock solutions to evaporate in a desiccator until rare-earth chloride hydrate crystals formed. The saturated solution, in contact with the crystals, were then placed in a constant temperature bath at 25°C. and

continuously agitated for about two weeks before the solution was used. The concentration of the saturated solution was taken from the data of Saeger and Spedding (6) and the data of Spedding, Brown and Gray[1].

The stock solutions were analyzed for rare-earth content by either the "oxide method" or the "sulfate method". In the "sulfate method", a ten percent excess of three molar sulfuric acid was added to the rare-earth chloride solution, which precipitated most of the rare-earth ion as $R_2(SO_4)_3$. After about 12 hours, the solutions were heated under infrared lamps until most of the water had been evaporated. The dry precipitates were then ignited with a gas burner to drive off the excess sulfuric acid as SO_3 and water. When it appeared SO_3 was no longer being driven off, the precipitates were placed in an electric furnace and ignited to 500°C. Several ignitions were required before the precipitates, $R_2(SO_4)_3$, came to constant weight. Each analysis, made in triplicate, gave a mean deviation of less than 0.05 percent. This method was used for $PrCl_3$ and $TbCl_3$.

In the "oxide method", a ten percent excess of oxalic acid was added to the rare-earth chloride solution in each crucible, and the samples were heated to dryness under infrared lamps. The dry residues were moistened with conductivity

---

[1]Spedding, F. H., Brown, M., and Gray, K., Ames Laboratory of the A.E.C., Ames, Iowa. Apparent molal volumes of some aqueous rare-earth chloride solutions. Private communication. 1964.

water, and a small quantity of nitric acid was added to each crucible. The samples were again evaporated to dryness and ignited to the oxide, R_2O_3, at about 950°C. The mean deviation for a triplicate analysis was less than 0.05 percent in all cases. This method was used for all rare-earth chloride solutions except $PrCl_3$ and $TbCl_3$.

The stock solutions were analyzed for the chloride content by a potentiometric method, using a silver indicating electrode and a sleeve-type reference electrode with an ammonium nitrate bridge to the inner calomel electrode. About fifty grams of previously standardized silver nitrate (about 0.1N) was placed in a beaker, and a weighed excess of rare-earth chloride sample was added to the silver nitrate. This excess was then back titrated with the same silver nitrate, using a Sargent Model D Recording Titrator. The silver nitrate was standardized using the same procedure with a standard potassium chloride solution. This method gave a mean deviation of less than 0.1 percent in all cases.

A given chloride analysis agreed with the corresponding rare-earth analysis within about 0.1 percent. The concentration of a stock solution was calculated from the mean of the rare-earth analysis and the chloride analysis.

The potassium chloride, lithium chloride, lithium nitrate, and potassium chromate solutions, used in checking the accuracy of the experimental methods, were prepared from recrystallized reagent grade salts. The recrystallized salts were dried in

an electric oven at about 200°C. The potassium chloride, lithium nitrate, and potassium chromate solutions were prepared, by weight, from the anhydrous salt and conductivity water. The lithium chloride solution was prepared by dissolving the salt in conductivity water and determining the concentration by the potentiometric chloride method described earlier.

IV. APPARENT MOLAL VOLUMES

A. Historical

1. Experimental observations

Apparent molal volumes and their theoretical interpretation have long been an important subject of scientific research. In 1929, Masson (46) proposed that the concentration dependence of the apparent molal volume could be expressed by the simple relation,

$$\phi_V = \phi_V^o + sc^{\frac{1}{2}}, \qquad (4.1)$$

where ϕ_V^o and s were parameters specific for each electrolyte. Later, Geffchen (47) and Scott (48) verified Masson's equation for a large number of electrolytes. Although the values of ϕ_V^o and s determined from Masson's equation were specific for each electrolyte, systematic trends were evident. The values of the slope, s, were generally greater for high valence type electrolytes than for simple 1-1 electrolytes. For electrolytes with both a common ion and the same valence, the values of ϕ_V^o showed a general decrease as the ionic radius of the non-common ion decreased. For electrolytes with both a common ion and approximately the same radius for the other ion, the values of ϕ_V^o generally decreased as the valence of the non-common ion increased.

The tests of Masson's equation described above were based, for the most part, on relatively inaccurate data at moderate to high concentrations. Redlich (49) and later Redlich and Mayer (50) showed that the most accurate data did not verify

Masson's equation, except as a crude approximation. In fact, the best experimental data for apparent molal volumes showed convergence toward a common limiting slope for electrolytes of the same valence type. For 1-1 salts, it was shown that accurate data for dilute solutions could be represented by the equation,

$$\phi_V = \phi_V^o + 1.86c^{\frac{1}{2}} + hc, \qquad (4.2)$$

where ϕ_V^o and h are specific for each electrolyte.

If it can be assumed that the apparent molal volume at infinite dilution, ϕ_V^o, is an additive property of the individual ions, ϕ_V^o for a 1-1 electrolyte may be written as,

$$(\phi_V^o)_{MX} = (\phi_V^o)_{M^+} + (\phi_V^o)_{X^-} , \qquad (4.3)$$

where $(\phi_V^o)_{M^+}$ and $(\phi_V^o)_{X^-}$ are the apparent molal volumes at infinite dilution of the cation and anion, respectively. For a given temperature, Equation 4.3 implies additivity relationships of the form,

$$(\phi_V^o)_{MX} - (\phi_V^o)_{M'X} = (\phi_V^o)_{M^+} - (\phi_V^o)_{M^{+'}} , \qquad (4.4)$$

$$(\phi_V^o)_{MX} - (\phi_V^o)_{MX'} = (\phi_V^o)_{X^-} - (\phi_V^o)_{X^{-'}} , \qquad (4.5)$$

where the primed symbols represent a non-common ion. Equations 4.4 and 4.5 should be independent of the anion, X^-, and cation, M^+, respectively. For higher valence type electrolytes, equations analogous to Equation 4.3 may be written, which lead to additivity relationships similar to those expressed by Equations 4.4 and 4.5. Using the data of Baxter and Wallace (51), Scott (48) found the additivity laws

expressed by Equations 4.4 and 4.5 to be valid, within experimental error, for the alkali halides. It seems certain that the additivity laws must be obeyed if the ions are completely dissociated at infinite dilution, so, in practice, the additivity laws may be used as a check on the self-consistency of the data.

Since experimental measurements give only the value of ϕ_v^o for the total solute and not the individual ionic contributions, it is not possible, at present, to experimentally obtain ionic apparent molal volumes at infinite dilution. However, if the ionic apparent molal volume at infinite dilution of one ion can be estimated by some method, other ionic contributions to ϕ_v^o can be determined relative to this estimate by using the additivity relationships. Based on various assumptions, several methods have been used to obtain ionic apparent molal volumes at infinite dilution (52,53,54).

2. Theoretical concentration dependence

The theoretical limiting expression for the apparent molal volume as a function of concentration was derived in 1931 by Redlich and Rosenfeld (55). Basically, their derivation involved differentiating Equation 2.1 with respect to pressure, recognizing the pressure dependence of the volume and dielectric constant. Their result may be written as,

$$\phi_v = \phi_v^o + K\, W^{3/2}\, c^{\frac{1}{2}} , \qquad (4.6)$$

where,

$$W = \tfrac{1}{2} \sum_i \nu_i z_i^2 , \qquad (4.7)$$

and,

$$K = N^2e^2(8\pi/1000D^3RT)^{\frac{1}{2}} \left(\partial \ln D/\partial P - \beta/3\right) . \qquad (4.8)$$

In the above equations, P is the pressure and β is the compressibility of the solvent. The other symbols have their usual meanings. The dielectric constant refers to the value for the pure solvent, which will be restricted to water for this discussion.

In the past, there has been some uncertainty in the theoretical value of K, principally because of the uncertainty in the pressure derivative of the dielectric constant, $\partial \ln D/\partial P$. A recent review by Redlich and Mayer (50) considers this problem in some detail and concludes, on the basis of recent measurements of $\partial \ln D/\partial P$ by Owen and co-workers (56), that $K = 1.868$ for water at 25°C. This value of K agrees with Equation 4.2 and shows that this empirical expression has a theoretical foundation.

Since Equation 4.6 is based upon the Debye-Hückel theory with the approximation, $\kappa a \ll 1$, it can be expected to be valid only in very dilute solutions. Generally, accurate data for dilute solutions confirm Equation 4.6 as the correct limiting law (49,50). In fact, apparent molal volume data for some 1-1 salts still obey the limiting law at relatively high concentrations. For example, Redlich and Mayer (50) show that the data of Kruis (57) for sodium chloride is well represented by the limiting law up to about 0.5 molar. For potassium chloride and a large number of other electrolytes,

mostly 1-1 salts, ϕ_V data can be well represented by Equation 4.9 over rather wide concentration ranges (49,50).

$$\phi_V = \phi_V^o + 1.868\ W^{3/2}\ c^{\frac{1}{2}} + h\ c\ . \qquad (4.9)$$

In Equation 4.9, h is an empirical parameter which represents the deviations from the simple limiting law and is usually quite small. Redlich and Mayer (50) strongly recommend Equation 4.9 as an extrapolation equation. They contend that the use of an empirical power series in $c^{\frac{1}{2}}$ to represent the data, where the coefficient of the $c^{\frac{1}{2}}$ term is evaluated from the data, may lead to inaccurate values for the extrapolated quantity, ϕ_V^o, particularly if the range of extrapolation is large.

Accurate apparent molal volume data at very low concentrations is scarce for higher valence type electrolytes, but the available data seem to confirm the validity of the limiting law (50). For example, the strontium chloride data of Kruis (57) confirm the limiting law, although noticable negative deviations from the simple limiting law occur at concentrations above about 0.05 molar.

The limiting law includes the approximation, $\kappa a \ll 1$. This approximation is not valid at moderate concentration, particularly for higher valence type electrolytes. For example, at 0.01 molar, $\kappa a = 0.1$, for a 1-1 electrolyte with $a = 4$ Å, but for a 3-1 electrolyte under the same conditions, $\kappa a = 0.3$. Consequently, even if the Debye-Hückel assumptions

were good approximations above 0.01 molar, a 3-1 electrolyte may be expected to show deviations from the limiting law at most experimental concentrations.

Knowing the effect of the a parameter on the theoretical limiting law would obviously be of great value in interpreting apparent molal volume data. Owen and Brinkley (58) have derived a semi-theoretical equation for the apparent molal volume which does include the effect of the a parameter. Their equation may be written in the form,

$$\phi_V = \phi_V^o + K\, W^{3/2} T(\kappa a) c^{\frac{1}{2}} + \tfrac{1}{2} W_V \theta(\kappa a) c + \tfrac{1}{2} K_V\, c\,, \qquad (4.10)$$

$$T(x) = \frac{3}{x^3}\left[x^2/2 - x + \ln(1 + x) \right], \qquad (4.11)$$

$$= 1 - (3/4)x + (3/5)x^2 - \ldots;\ x \leqslant 1, \qquad (4.11a)$$

$$\theta(x) = \frac{4}{x^4}\left[x^2/2 - x + 3\ln(1 + x) + 1/(1 + x) - (1 + x) \right], \qquad (4.12)$$

$$= 1 - (8/5)x + (12/6)x^2 - \ldots;\ x \leqslant 1, \qquad (4.12a)$$

$$W_V = -2.303 \nu R\, T\, S_f\, A'\, \tfrac{1}{2}\left[\partial \ln D/\partial P - \beta - 2\,\partial \ln a/\partial P \right], \qquad (4.13)$$

$$A' = \Big(\sum_i \nu_i z_i^2 \Big)^{\frac{1}{2}} (4\pi N\, e^2/1000\, D\, k\, T)^{\frac{1}{2}}\, a. \qquad (4.14)$$

The symbol, S_f, refers to the theoretical limiting slope for the mean ionic activity coefficient, $\partial \ln \gamma_{\pm}/\partial c^{\frac{1}{2}}$, and is defined by Equations 2.1 and 2.2. The quantity, $\frac{1}{2} K_V$, is an empirical parameter to be evaluated from the experimental

data, and the other symbols have their usual meanings. If the empirical term involving K_V is omitted from Equation 4.10, the remaining terms can be derived from Equation 2.11 for the mean ionic activity coefficient and therefore have some theoretical justification. Retaining only these theoretical terms gives the equation,

$$\phi_V = \phi_V^o + K\, W^{3/2}\, \tau(\kappa a)c^{\frac{1}{2}} + \tfrac{1}{2}W_V\, \theta(\kappa a)c \ . \qquad (4.15)$$

The success of the Debye-Hückel theory in the form of Equation 2.11 suggests that Equation 4.15 should be a good approximation in dilute solution. In particular, for the rare-earth chlorides, there is reason to suspect that Equation 4.15 should be a good approximation up to about 0.05 molar.

The comparison of Equation 4.15 with experimental data is difficult due to the presence of the quantity, $\partial \ln a/\partial P$, in the definition of W_V. Unlike the a parameter itself, neither the sign nor the magnitude of $\partial \ln a/\partial P$ can be estimated with any great degree of confidence at the present time. Consequently, there is no way of establishing whether the value of W_V evaluated from the data represents the actual contribution of the term, $\partial \ln a/\partial P$, or whether it represents imperfections in the theory. It has been argued that a is effectively independent of pressure for aqueous electrolytes (44,58). However, the a parameter includes the effect of any permanently co-ordinated water molecules, as well as the size of the ions. The compressibility of the water in the immediate

vicinity of the ion may be expected to be small (54), so if the "effective hydration number" is independent of pressure, $\partial \ln a/\partial P$ should be small and may be neglected. However, it is not obvious that the "effective hydration number" will be independent of pressure, so the neglect of $\partial \ln a/\partial P$ is open to criticism.

If $\partial \ln a/\partial P$ is assumed to be small, i.e., $|\partial \ln a/\partial P| \ll \beta$, Equation 4.15 becomes independent of the term in W_V for concentrations of the order of a few hundreths molar. Assuming a is effectively independent of pressure has some justification, and in the following discussion, this simplifying assumption will be presumed valid. Neglecting the pressure dependence of a and retaining the terms in Equation 4.15 of order c and lower results in the equation,

$$\phi_V = \phi_V^o + K W^{3/2} c^{\frac{1}{2}} - (3/4) a b K W^{3/2} c , \qquad (4.16)$$

where b is a positive constant for a given electrolyte, solvent, and temperature and is defined by Equation 2.2. Equation 4.16 predicts the first order deviation from the limiting law will be negative and more serious for high valence type electrolytes. It seems likely that the negative deviations observed for strontium chloride are due to the effect of the a parameter.

It is significant to note that Mayer's theory (43), as developed by Poirier (44), also predicts significant negative deviations from the simple limiting law for high valence type

electrolytes. Both Mayer's theory and the Debye-Hückel theory indicate the simple limiting law should be obeyed for 1-1 electrolytes at 0.01 molar, and the limiting law for 3-1 electrolytes should not be obeyed until dilutions of the order of 0.001 molar are reached. For a 3-1 electrolyte with a = 6 Å, both theories predict a deviation from the limiting law of about -0.5 ml./mole at a concentration of 0.01 molar.

Unfortunately, a rigorous quantitative discussion of the effect of the a parameter on apparent molal volumes is impossible until a more reliable method for estimating $\partial \ln a / \partial P$ is found. However, the Owen-Brinkley equation, Equation 4.10, has the correct limiting form, and it probably represents the deviations from the limiting law at low concentrations sufficiently well to be useful as an extrapolation function.

3. Theoretical interpretation of ϕ_v^o

The partial molal volume at infinite dilution, $\bar{V}_2^o$, which is identical to the apparent molal volume at infinite dilution, ϕ_v^o, represents the volume change of a very large quantity of solvent upon addition of one mole of solute. At infinite dilution, it may be assumed that the anion and cation contributions to the partial molal volume are additive, and

$$\bar{V}_2^o = \nu_+ \bar{V}_+^o + \nu_- \bar{V}_-^o , \qquad (4.17)$$

where ν_+ is the number of cations with partial molal volume $\bar{V}_+^o$, and ν_- is the number of anions with partial molal volume, $\bar{V}_-^o$. The partial molal volume of an ion at infinite dilution,

$\bar{V}_i^o$, may be separated into two contributions. One contribution would be a positive term arising from the intrinsic volume of the ion and will be given the sumbol, V*. The other term would represent any change in the volume of the solvent caused by the presence of the ion, which will be symbolized by $\triangle V$. Therefore, the partial molal volume of an ion at infinite dilution may be written as,

$$\bar{V}_i^o = V^* + \triangle V. \tag{4.18}$$

For one mole of spherical ions, Equation 4.18 becomes,

$$\bar{V}_i^o = (4/3)\pi N r^3 + \triangle V, \tag{4.19}$$

where N is Avogadro's number, and r is the radius of the ion in solution. A theoretical discussion of the partial molal volume at infinite dilution will then involve a calculation of $\triangle V$.

An approximate $\triangle V$ may be calculated if it is assumed an ion in solution may be approximated as a rigid charged sphere in a uniform and structureless dielectric medium. Assuming this crude model, the change in Gibbs free energy of the solvent due to the electric field of the ion, F_{el}, may be calculated (59) and expressed in c.g.s. units as,

$$F_{el} = \frac{-z^2e^2N}{2r}(1 - 1/D). \tag{4.20}$$

Using the thermodynamic relation, $\triangle V_{el} = (\partial F_{el}/\partial P)_T$, Equation 4.20 leads to the expression,

$$\triangle V_{el} = -\frac{z^2e^2N}{2\,r\,D} \cdot \partial \ln D/\partial P. \tag{4.21}$$

ΔV_{el} represents the decrease in volume of the dielectric medium resulting from the polarization of the medium by the ion. If ΔV_{el} is identified as ΔV, combination of Equations 4.19 and 4.21 leads to the so called Born approximation for $\bar{V}_i^o$,

$$\bar{V}_i^o = (4/3)\pi N r^3 - \frac{e^2 N}{2D} \cdot (\partial \ln D/\partial P) \cdot z^2/r. \qquad (4.22)$$

Restricting Equation 4.22 to water at 25°C. and using the most recent dielectric constant data (56), the Born approximation becomes,

$$\bar{V}_i^o = 2.52 r_o^3 - 4.18 z^2/r_o , \qquad (4.23)$$

where r_o is the ionic radius in Angstrom units.

It should be noticed that the Born approximation predicts $\bar{V}_i^o$ should increase as the radius of the ion increases and should decrease as the charge on the ion increases. In general, these trends are verified by experimental data (54), but the quantitative agreement is much less satisfactory.

In view of the crude model assumed by the Born approximation, it is not surprising that this theory fails to give a quantitative theoretical expression. The Born approximation assumes the dielectric constant of the solvent is not a function of the distance from the ion. For the extremely high field near an ion, this assumption cannot be valid (54), and will be particularly bad for highly charged ions with small radii. The theory proposed by Padova (54) attempts to correct for this defect in the model by treating the dielectric con-

stant of the solvent as a function of the electrical field intensity of the ion. However, the ionic radii required for Padova's theory to agree with experiment are significantly larger than the corresponding crystal radii. Padova, and also Mukerjee (60), argue that the ionic radii in solution should be significantly larger than the ionic crystal radii. Benson and Copeland (61) disagree and maintain the crystal ionic radius is a good approximation for the ionic radius in solution. According to their interpretation, the difference between the ionic crystal radii and the radii predicted from Padova's theory reflect the failure of a continuum model for the solvent. X-ray diffraction data for aqueous electrolytes (36) and other evidence (62,63) seem to indicate that the conclusions of Benson and Copeland are correct.

Another defect of the Born approximation is that it treats the ion-solvent interaction for both cations and anions in the same way. The theoretical study of Buckingham (64) and the semi-empirical results of Hepler (65) indicate that this defect may be serious.

Desnoyers, Verrall and Conway (66) have recently proposed a method for calculating $\bar{V}_i^o$ that avoids many of the difficulties inherent in a theory based upon the Born approximation. Their theory is based upon a calculation of effective pressure which would, in the absence of the electrical field, cause the same change in volume as the field. This treatment

allows the change in volume of water to be calculated as a function of field intensity. However, the results of their calculations cannot be related directly to experimental data unless some hydration model is assumed.

The Born approximation and the various other theories of $\bar{V}_i^o$ have resulted in a much better understanding of ion-solvent interactions, but a complete quantitative theory is still lacking. It seems obvious that a successful theory must recognize the molecular nature of the solvent, at least in the immediate vicinity of the ion.

B. Experimental

1. Experimental method

The apparent molal volume, ϕ_V, is defined by the equation,

$$\phi_V = \frac{V - n_1 \bar{V}_1^o}{n_2} , \qquad (4.24)$$

where V is the total volume of a solution composed of n_2 moles of solute and n_1 moles of solvent having a molar volume, $\bar{V}_1^o$. If the quantities, $V = (n_1 M_1 + n_2 M_2)/\rho$, $\bar{V}_1^o = M_1/\rho_o$, and $n_1/n_2 = 1000\,\rho/M_1 c - M_2/M_1$, are substituted into Equation 4.24, the apparent molal volume may be written,

$$\phi_V = (1 - \rho/\rho_o)\ 1000/c + M_2/\rho_o , \qquad (4.25)$$

where ρ is the density of the solution, ρ_o is the density of the solvent, c is the molar concentration, M_2 is the molecular weight of the solute, and M_1 is the molecular weight of the solvent. Therefore, experimental data for the specific gravity, ρ/ρ_o, and the molar concentration, c, allow the

apparent molal volume to be calculated. Since the specific gravity of a dilute solution is close to unity, it is obvious that the use of Equation 4.25 for dilute solutions requires extremely accurate specific gravity data. In particular, for a 0.01 molar solution, an uncertainty of only $\pm$ 1x10^{-6} in the specific gravity results in an error of $\pm$ 0.1 ml./mole in the apparent molal volume. Therefore, with this method, meaningful apparent molal volumes below 0.01 molal must be calculated from specific gravity values which have an uncertainty of less than $\pm$ 1x10^{-6}. Direct pyknometry at this level of accuracy is nearly impossible so a more accurate method, such as the magnetic float method, must be used to determine the specific gravity. The magnetic float method will be described in detail later.

Another method of accurately determining apparent molal volumes of dilute solutions was recently proposed (67). This method involves a dilatometric determination of the volume change on isothermally mixing a small volume of relatively concentrated solution with a large volume of pure solvent. Using Equation 4.24, this volume change, ΔV, can be expressed as,

$$\Delta V = n_2 \left[\phi_V(F) - \phi_V(I) \right] , \qquad (4.26)$$

where n_2 is the number of moles of solute involved, $\phi_V(F)$ is the apparent molal volume of the dilute final solution, and $\phi_V(I)$ is the apparent molal volume of the initial concentrated solution. The value of $\phi_V(I)$ can be determined accurately by

conventional pyknometric measurements of the specific gravity and use of Equation 4.25. The apparent molal volume of the dilute solution, $\phi_v(F)$, may then be calculated by using Equation 4.26. This method seems to be capable of very high accuracy.

The apparent molal volumes of the solutes studied in this research were calculated from the experimentally determined specific gravities, ρ/ρ_o, and molar concentrations, c, using Equation 4.25.

The method used for measuring specific gravity was the magnetically controlled float method originated by Lamb and Lee (68) and modified by later workers (7,69,70,71). This method consisted of determining the current in a primary solenoid which was just sufficient to balance a float of known weight in the solution, through the interaction of the field of the solenoid with a permanent magnet in the float. This value of the current, hereafter called the equilibrium current, was converted into weight by using a previously determined calibration factor, Ψ. This factor measured the interaction between the solenoid and the permanent magnet in the float and was given in units of milligrams per milliampere. The float was weighted so it just floats in pure water, and the circuit was designed so that a current through the solenoid would result in a downward force on the float. Small platinum weights, as described by Ayers (7), were added to the float to give an additional force downward when the float was being

balanced in solutions. The equilibrium current was obtained by determining the minimum current necessary to prevent the float from rising.

When the float is balanced in a solution,

$$W + w_s + I^o\Psi = \rho V', \tag{4.27}$$

where W is the weight of the float; w_s is the weight of platinum added to the float, corrected to its weight in solution; I^o is the equilibrium current; Ψ is the calibration factor; ρ is the density of the solution, and V' is the volume of the float. When the float is balanced in pure water, an analogous expression may be written in the form,

$$W + I_o^o\Psi = \rho_o V', \tag{4.28}$$

where I_o^o is the equilibrium current in water, and ρ_o is the density of water. Taking the ratio of Equations 4.27 and 4.28 gives,

$$S = \rho/\rho_o = \frac{W + w_s + I^o\Psi}{W + I_o^o\Psi}, \tag{4.29}$$

for the specific gravity of the solution. The weight of platinum in the solution, w_s, may be calculated from its weight in vacuum, w_v, using the equation,

$$w_s = w_v(1 - \rho/d_{Pt}), \tag{4.30}$$

where ρ and d_{Pt} are the densities of the solution and the platinum, respectively. In practice, w_s may be calculated from Equations 4.29 and 4.30 by successive approximations.

2. Description of apparatus

Schematic diagrams of the apparatus used for measuring specific gravity are given in Figures 1 and 2. A schematic diagram of the electrical circuit is given in Figure 3. Reference to these figures will be designated (i-X), where i refers to the figure and X to the alphabetically labelled part.

The constant temperature bath used in this research was basically that described by Ayers (7), so only a brief description will be given here. The basic component of the constant temperature bath was a 30 gallon stainless steel tank (1-A), which was placed inside an insulated wooden box (1-B). Plexiglass windows (1-C) were fitted into rectangular openings on opposite sides of both the tank and the box. These windows permitted observation of the bath interior with a Gaertner Telemicroscope (1-E). A light (1-D) illuminated the interior of the bath. A mercury thermoregulator (1-F), identical to that used by Ayers, a 250W knife heater (1-G), and an electronic relay were used to control the temperature of the bath. Dry helium gas was passed over the mercury contacts to provide a non-oxidizing atmosphere. Stirring was provided by a large tubular turbine stirrer (1-H), which was mounted on a heavy stand and separated from the bath to minimize vibrations. Cooling water for the system, maintained at 22°C. by an auxillary water bath, was pumped through cooling coils (1-I) by a centrifugal pump.

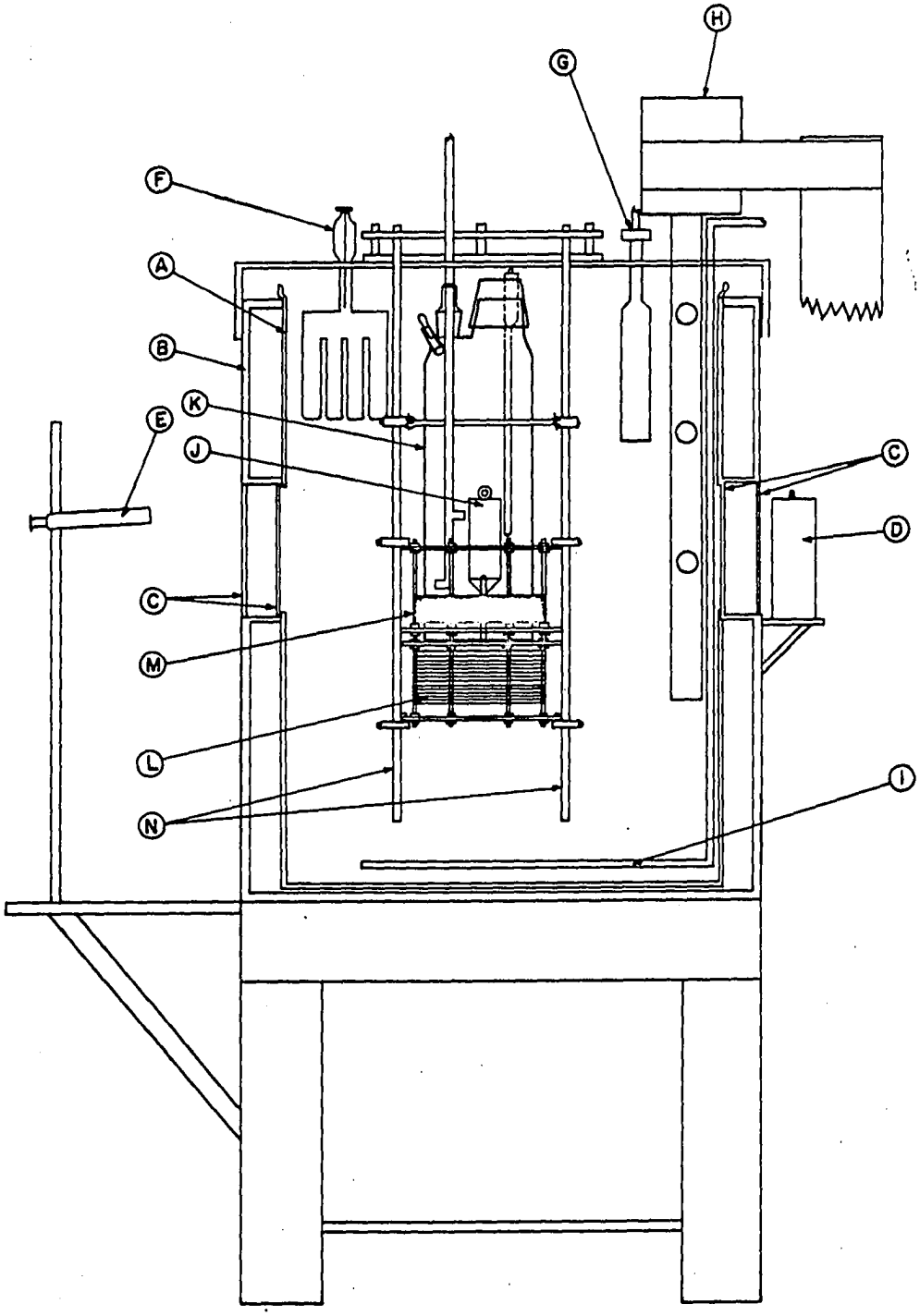

Figure 1. Apparatus for the determination of specific gravity

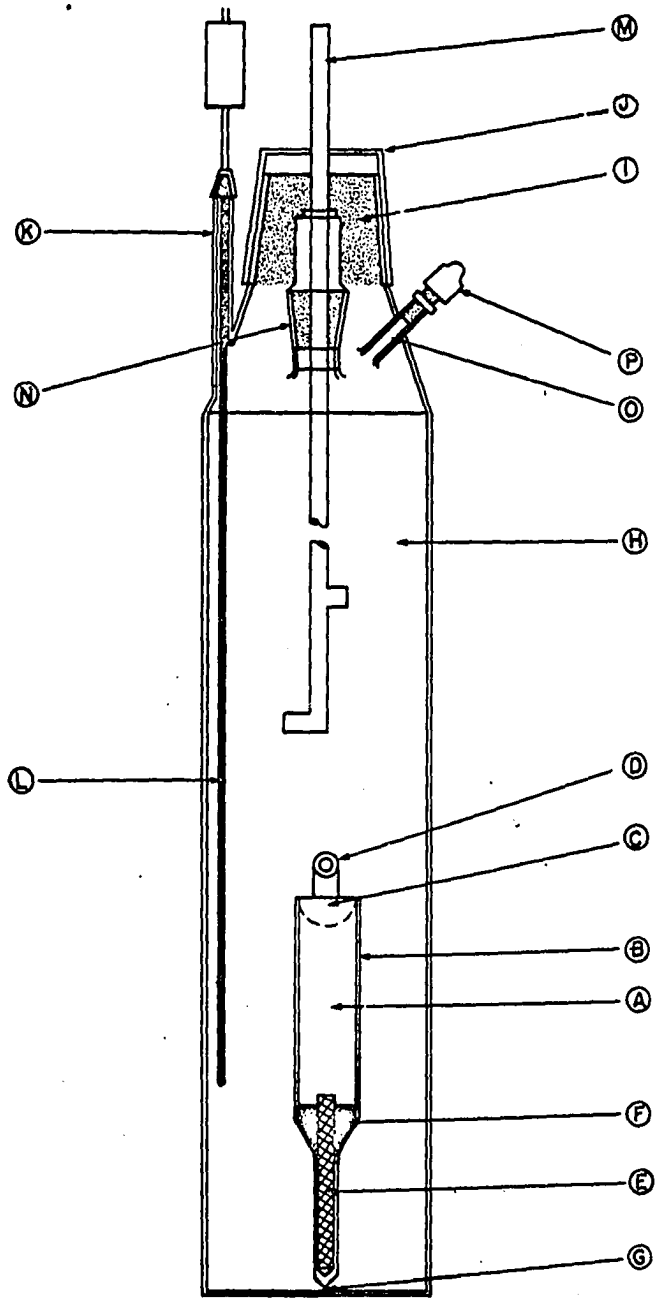

Figure 2. Solution cell and specific gravity float

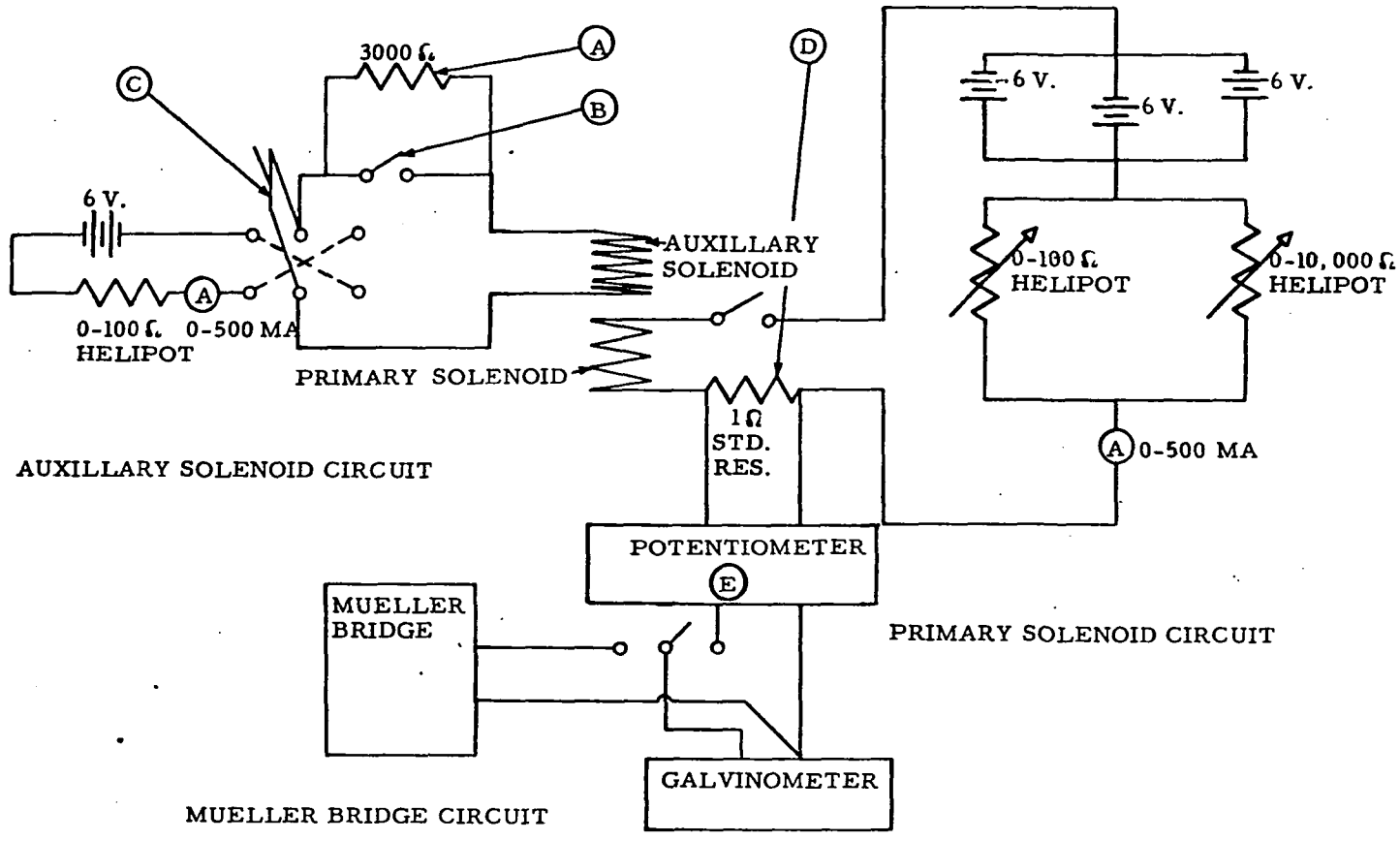

Figure 3. Circuit diagram for specific gravity apparatus

The specific gravity float (1-J)(2-A) was constructed according to the procedure given by Ayers. The float was about 20 cm. long, had a maximum diameter of about 3 cm., and had a total volume of about 100 ml. The shell of the float was constructed from pyrex tubing (2-B) and had a small depression (2-C) to hold platinum weights. A glass loop (2-D) was fashioned from pyrex tubing so the float could be lifted out of the solution. A magnetized Cunife rod (2-E) was placed in the tip of the float, and a ballast of lead shot fixed in place with pyseal (2-F) adjusted the density of the float so it would just float in water at 25°C. A small platinum wire (2-G) was sealed into the pyrex tubing at the tip of the float to minimize the contact area between the float and the solution cell.

The solution cell (1-K)(2-H) was constructed from pyrex tubing and was approximately 50 cm. high and 10 cm. in diameter. To provide access to the interior of the cell, a male 55/50 standard taper (2-I) was attached to the top of the cell. A cap (2-J) for this opening was constructed from the female portion of a 55/50 standard taper. The thermometer shaft (2-K) consisted of a 6 cm. portion of pyrex tubing sealed into the top of the cell. The thermometer shaft terminated with a male 14/35 standard taper that fitted into a female 14/35 standard taper, which was attached with Pyseal to the Leeds and Northrup platinum resistance thermometer (2-L). The

platinum resistance thermometer was used with a Model G-2 Leeds and Northrup Mueller Bridge to measure the temperature of the solution in the cell within $\pm$ 0.001°C. Stirring in the cell was provided by a "True Bore" stirrer (2-M), which consisted of a frosted glass rod that fitted into a 24/40 bearing. A 24/40 female standard taper (2-N) was attached at the top of the cell to match the 24/40 bearing. The stirrer was attached to an adjustable speed electric motor by a flexible coupling of gum rubber tubing. The weight buret shaft (2-O) was constructed from pyrex tubing, which was sealed into the top of the cell. This shaft terminated in a 7/25 female standard taper, which could be sealed with a plug (2-P), made from the male portion of a 7/25 standard taper. The weight buret shaft was used with a 60 ml. weight buret, fitted with an extended tip, when stock solution was added to the cell. The tip of the weight buret was just long enough to rest against the side of the stirring rod when the weight buret was placed into the shaft. The stock solution could then be drained down the stirring rod into the solution in the cell. This procedure eliminated splashing stock solution on the sides of the solution cell.

The primary solenoid (1-L) consisted of 27 turns of #24 insulated copper wire wound on an octagonal shaped frame. The frame was about 6½ inches in diameter and 10 inches high and was constructed from four octagonal Lucite plates and eight threaded 1/4 inch brass rods. The copper wire was

wound on every third thread of the brass rods, and the solenoid was about five inches high.

The auxillary solenoid (1-M) was wound directly above the primary solenoid and consisted of 30 turns of #24 insulated copper wire wound on every thread of the brass rods. The auxillary solenoid was used to pull the float to the bottom of the cell prior to making a determination of the equilibrium current with the primary solenoid.

The entire solenoid unit was fastened to the brass support unit (1-N). The support unit for the solenoids and solution cell was constructed from two 5/8 inch brass rods, 34 inches long, which were attached, at the top, to a triangular brass frame. The three adjustable legs of this frame rested on the flat surface of a similar frame attached to the water bath. Details of the support unit are given by Ayers.

The electrical circuits for the solenoids are shown in Figure 3. The diagram is, for the most part, self-explanatory. However, several features merit further discussion. To minimize induction effects when the auxillary solenoid circuit was broken, a 3000 ohm resistor (3-A) was included in the circuit such that, by using the switch (3-B), it could be placed in the circuit prior to breaking the circuit with the double pole-double throw switch (3-C). The batteries shown in Figure 3 were 6 volt Willard storage batteries. As shown in Figure 3, three of these batteries were connected in

parallel to provide a constant voltage source for the primary solenoid circuit. This arrangement proved to be an excellent constant voltage source. The potential drop across the standard one ohm resistor (3-D) was measured with a Rubicon Type B potentiometer (3-E). Therefore, the potentiometer reading gave the current directly. The standard resistor and the standard cell used with the potentiometer were calibrated by the National Bureau of Standards.

3. Calibration

Several calibrations were necessary before the apparatus could be used for determining the specific gravity of a solution. Ayers (7) noticed that the value of the equilibrium cur-current was strongly dependent on the atmospheric pressure. However, in this research, measurements of the equilibrium current in water at various pressures from 680 mm. Hg to 760 mm. Hg revealed that the effect of pressure on the equilibrium current was negligible for this pressure range. This apparent contradiction of Ayers' observations can be resolved if it is assumed that the volume of the conical shaped float used by Ayers was more dependent upon pressure than was the volume of the cylindrical float used in this research.

It was also necessary to determine the calibration factor, Ψ, so conversion of the equilibrium current to weight could be made. This factor was determined from measurements of the equilibrium current required with various total weights of platinum added to the float. The estimated probable error

in Ψ for a given determination was about $\pm$ 0.0005 mg./ma. It was noticed that, for a given sample of water, the value of the equilibrium current and the Ψ factor changed each time the solution cell was removed and replaced in the support unit. This phenomenon was due to the difficulty in placing the solution cell in exactly the same position within the solenoid each time. The variation in the equilibrium current was often ten or twenty times the experimental error for this quantity, while the variation in Ψ was usually less than three times the estimated probable error for a given Ψ determination. However, since very high accuracy was desired, both the equilibrium current in water, I_o^o, and the calibration factor, Ψ, were determined prior to each run, or series of specific gravity measurements, and the solution cell was not removed from the support unit until after the run had been completed.

4. Experimental procedure

Prior to each specific gravity run, the solution cell and density float were cleaned with alcoholic potassium hydroxide cleaning solution, rinsed with conductivity water and allowed to stand in conductivity water for at least several hours. Next, the solution cell was rinsed with ethanol and dried in a stream of filtered air. The float was dried and placed in a desiccator, which was placed in the balance room. When the float was in thermal equilibrium with the balance room, it was

weighed. When the solution cell was dry, about 1400 grams of conductivity water was weighed into the cell through a long necked funnel, used to eliminate splashing water on the sides of the cell. The funnel was then weighed to determine the weight of water left in the neck. The solution cell was placed in the water bath, and several hours later, the float was placed in the solution cell. To avoid condensation of water on the top of the cell, the apparatus room was maintained at 26°C.

After thermal equilibrium had been reached, the calibration factor, Ψ, was determined. The next morning, the value of the equilibrium current in pure water, I_o^o, was measured. The values of I_o^o obtained were about 400 ma. When an equilibrium current was determined, the current in the primary solenoid was adjusted to a value about 0.5 ma. above the equilibrium current, and the float was brought to the bottom of the cell with the auxillary solenoid. After a pause of several minutes to insure the fluid around the float was motionless, the 3000 ohm resistor was placed in the auxillary solenoid circuit with the switch (3-B). The auxillary solenoid circuit was then broken, and the current through the primary solenoid was decreased in steps of about 0.1 ma. until the float would rise within a time interval of about two minutes. The mean of the "up" and "down" current readings was taken as the equilibrium current for that determination.

At least two equilibrium current determinations were made for each solution and the mean of these determinations was taken as the equilibrium current for that solution. From the reproducibility of the equilibrium current measurements, it was estimated that the probable error in the equilibrium current was about $\pm$ 0.1 ma.

Following the determination of I_o^o, a weighed quantity of the appropriate stock solution was added to the solution cell through the weight buret shaft (2-0), as described earlier. The solution was stirred for several minutes to obtain a homogeneous solution. The float was lifted out of the cell by fitting a long hook into the glass loop of the float, and sufficient platinum weights were added to the float so that the equilibrium current would be as close as possible to the equilibrium current in pure water. Since the effect on the specific gravity of an error in the calibration factor increases in proportion to the difference, $|I^o - I_o^o|$, this procedure was especially important when the specific gravity of a very dilute solution was being measured. Usually it was not difficult to choose the platinum weights so that $|I^o - I_o^o| < 20$ ma. To eliminate formation of air bubbles on the platinum weights, the weights were rinsed in dilute nitric acid and conductivity water, and then heated to a dull red heat in a small gas flame just prior to being added to the float. After the platinum weights had been added to the float, the solution

was stirred until thermal equilibrium had been attained. The equilibrium current was measured, and the solution was stirred again and allowed to stand for about an hour. The equilibrium current was again determined, and if the agreement was within ± 0.2 ma., the results were averaged to obtain the equilibrium current for that solution.

Additional portions of the appropriate stock solutions, sufficient to give solutions of the desired concentrations, were added to the cell. For each solution, the necessary amount of platinum weight was added to the float, and the equilibrium current was determined. About four or five different concentrations were measured during a single run. The temperature control was better than ± 0.001°C. during the entire run. To minimize any time dependent errors in the critical dilute region, the value of I_o^o and the first two dilutions were always measured during a single day.

On completion of a run, the platinum weights were cleaned and weighed on an Ainsworth Type FDJ microbalance, and the specific gravity of each solution was calculated using Equations 4.29 and 4.30.

5. Apparent molal volumes of aqueous potassium chloride solutions

As a final check on the accuracy of the apparatus, apparent molal volumes of aqueous solutions of potassium chloride at 25°C. were measured. The densities and apparent molal volumes obtained for potassium chloride are given in Table 2.

The apparent molal volumes obtained from the measurements in this research were in excellent agreement with those of Geffchen and Price (72), Kruis (57), and Ayers (7).

Table 2. Apparent molal volumes of aqueous KCl solutions at 25°C.

Molarity	Specific gravity	ϕ_v [a]
0.0039999	1.0001910	27.026
0.0093525	1.0004465	27.037
0.014094	1.0006719	27.106
0.031852	1.0015152	27.209
0.055887	1.0026531	27.305
0.097226	1.0046017	27.448
0.14638	1.0069093	27.577
0.20460	1.0096304	27.709

[a]All partial and apparent molal volumes determined in this research are given in milliliters per mole.

6. Treatment of experimental data

As described earlier, the experimental values of the specific gravity and the corresponding experimental apparent molal volumes were calculated by use of Equations 4.29, 4.30, and 4.25. The density of water at 25°C. was taken from the compilation of Dorsey (73), and 21.428 grams per cubic centimeter (74) was used for the density of platinum referred to in Equation 4.30.

The experimental apparent molal volume data for each of the rare-earth salts studied in this research are well repre-

sented by an empirical power series in $m^{\frac{1}{2}}$ of the form,

$$\phi_v = a_o + a_1 m^{\frac{1}{2}} + a_2 m + a_3 m^{3/2} , \qquad (4.31)$$

where m is the molality. For each rare-earth salt, the numerical values of the parameters (a_o, a_1, a_2, a_3) were determined by a least squares analysis of the experimental data, using the inverse square of the probable error in ϕ_v as the weighting factor. An estimation of the probable error in ϕ_v will be discussed later. The partial molal volume is related to the apparent molal volume by Equation 1.3. Therefore, the partial molal volumes for each of the rare-earth salts studied in this research may be calculated from equations of the form,

$$\bar{V}_2 = a_o + \frac{3}{2} a_1 m^{\frac{1}{2}} + 2a_2 m + \frac{5}{2} a_3 m^{3/2} . \qquad (4.32)$$

A primary objective of this research was to obtain accurate values for the partial molal volumes at infinite dilution. Values for $\bar{V}_2^o$ may be obtained by an extrapolation using Equation 4.31. However, it was believed that a more accurate value of $\bar{V}_2^o$ could be obtained if the limiting slope of ϕ_v as a function of $c^{\frac{1}{2}}$ were fixed from theory. Consequently, the Owen-Brinkley equation, Equation 4.10, was used to extrapolate the experimental apparent molal volume data. The justification for this procedure will be discussed in more detail later. For a 3-1 electrolyte, the Owen-Brinkley equation becomes,

$$\phi_v = \phi_v^o + 27.44\, c^{\frac{1}{2}} \tau(\kappa a) + \tfrac{1}{2} W_v \theta(\kappa a) c + \tfrac{1}{2} K_v c , \qquad (4.33)$$

where, $\kappa a = 0.8051 \mathring{a} c^{\frac{1}{2}}$, when the value of a is given in Angstrom units as $\mathring{a}$ (11). The values of $\mathring{a}$ were not evaluated from the apparent molal volume data but were taken from activity coefficient and conductivity data in the literature (22, 23,24,25,75,76). The functions, $\tau(\kappa a)$ and $\theta(\kappa a)$, are easily calculated using the equations and table given by Harned and Owen (11). For a given electrolyte, the values of ϕ_v^o, $\frac{1}{2}W_v$, and $\frac{1}{2}K_v$ were evaluated from the experimental data by means of a least squares analysis of the data, using the inverse square of the probable error in ϕ_v as the weighting factor.

The experimental apparent molal volumes were well represented by Equation 4.33 in all cases studied, except for the $Nd(NO_3)_3$ data of Ayers (7). For $Nd(NO_3)_3$, the parameters in Equation 4.33 could not be adjusted to represent the data within experimental error, so the experimental data for $Nd(NO_3)_3$ was extrapolated using Equation 4.31.

7. Experimental results

The apparent molal volumes of aqueous solutions of $PrCl_3$, $SmCl_3$, $GdCl_3$, $TbCl_3$, $DyCl_3$, $HoCl_3$, and $ErCl_3$ were determined at 25°C. over a concentration range of about 0.0015 molar to 0.18 molar. Ayers also gives apparent molal volume data for $ErCl_3$ over about the same concentration range. However, his data for $ErCl_3$ do not seem to be consistent with the ϕ_v data for the other rare-earth salts, so apparent molal volumes of

$ErCl_3$ were determined as part of this research. The data for $ErCl_3$ obtained in this research are consistent with ϕ_v data for the other rare-earth salts and also show better agreement with the data of Saeger and Spedding (6).

The experimental specific gravities and apparent molal volumes determined during the course of this investigation are given in Table 3. The corresponding concentrations are expressed as $m^{\frac{1}{2}}$ and $c^{\frac{1}{2}}$, where m is the molality and c is the molar concentration. The quantity, Δ, represents the difference, $(\phi_v)_{experimental} - (\phi_v)_{calculated}$, where the calculated value refers to the apparent molal volume calculated from Equation 4.33 with the appropriate parameters. The units of ϕ_v and Δ are ml./mole.

The experimental ϕ_v data for $DyCl_3$ are plotted against $c^{\frac{1}{2}}$ in Figure 4. The value of ϕ_v^o used in constructing Figure 4 was taken from Table 5. The straight line drawn from the intercept refers to the concentration dependence predicted by the theoretical limiting law, Equation 4.6, for a 3-1 electrolyte. The vertical line drawn from the most dilute experimental point represents the error in that ϕ_v value introduced by an error in specific gravity of $\pm 3 \times 10^{-7}$. The data for the other salts in Table 3 show much the same behavior as $DyCl_3$, the only significant difference being in the value of the intercept, ϕ_v^o.

The apparent molal volume data in Table 3 and the data of

Ayers were treated according to the procedure described earlier. The parameters for Equation 4.31 determined by the least squares analysis are given in Table 4 for each of the rare-earth salts studied. The parameters for $ErCl_3$ refer to the data from Table 3. The last column in Table 4 gives, for each salt, the average deviation of the experimental ϕ_v from the corresponding values calculated using the empirical equation. The units are ml./mole. Ayers chose to represent his data in terms of five parameter equations similar to Equation 4.31. However, his data are equally well represented by the simpler four parameter equation, Equation 4.31.

The apparent molal volume data contained in Table 3 and the data of Ayers were extrapolated using the Owen-Brinkley equation in the form of Equation 4.33. The values of ϕ_v^o and the other parameters of Equation 4.33, determined by the least squares treatment, are given in Table 5 for each of the salts studied. The average deviation of the experimental ϕ_v from the values calculated using the Owen-Brinkley equation is given in the last column for each of the salts studied. The units are ml./mole. As previously mentioned, the $Nd(NO_3)_3$ data of Ayers were not consistent with Equation 4.33, and the value of ϕ_v^o given in Table 5 for $Nd(NO_3)_3$ refers to an extrapolation using Equation 4.31. The values of the a parameters used in the extrapolation procedure are also given in Table 5, along with the corresponding literature reference in parenthesis.

It should be mentioned that the experimental ϕ_V values given by Ayers for the 0.026244 molal solution of $YbCl_3$ and the most dilute solution of $Yb(NO_3)_3$ are in obvious error, and these values were not included in the analysis of his data.

Since interionic attraction theory does not predict the value of ϕ_V^o, experimental data is perhaps best compared with theory by comparing the quantity, $d\phi_V/dc^{\frac{1}{2}}$, with the theoretical slope. For this purpose, experimental values of $d\phi_V/dm^{\frac{1}{2}}$ have been computed from Equation 4.31 for each of the rare-earth salts studied, using the appropriate parameters given in Table 4. It may be noticed that the experimental values of the slope were computed on the basis of concentration expressed in molality, m. However, the difference between molality, m, and molar concentration, c, is insignificant for this discussion. Experimental values for the slope, $d\phi_V/dm^{\frac{1}{2}}$, are given in Table 6 at round values of $m^{\frac{1}{2}}$. In Figure 5, the experimental slopes for several of the rare-earth salts are plotted against $m^{\frac{1}{2}}$. The horizontal straight line represents the theoretical limiting slope for a 3-1 salt, 27.44, as calculated from Equation 4.6. The effect of an a parameter of 5.6 $\mathring{A}$ on the theoretical slope is shown by the dashed line, which represents the slope predicted by Equation 4.15 assuming the a parameter is effectively independent of pressure.

Additivity laws, similar to Equations 4.4 and 4.5, may be written for the rare-earth chlorides and nitrates in the form,

$$(\phi_v^o)_{R(NO_3)_3} - (\phi_v^o)_{RCl_3} = 3\left[(\phi_v^o)_{NO_3^-} - (\phi_v^o)_{Cl^-}\right] , \quad (4.34)$$

$$(\phi_v^o)_{R'X_3} - (\phi_v^o)_{RX_3} = (\phi_v^o)_{R'^{+3}} - (\phi_v^o)_{R^{+3}} , \quad (4.35)$$

where R and R' represent the particular rare-earth, and X represents the anion. The differences on the right hand sides of Equations 4.34 and 4.35 were calculated from the values of ϕ_v^o in Table 5, and these differences are given in Table 7. Since the quantity of the right hand side of Equation 4.34 should be independent of the cation, this quantity was also calculated from data on potassium chloride, potassium nitrate, ammonium chloride, and ammonium nitrate. In Table 7, these results are compared with the values calculated from the rare-earth salts. The values of ϕ_v^o used in the calculations were taken directly from the literature for potassium chloride (72), ammonium chloride (77), and ammonium nitrate (72). Apparent molal volumes of potassium nitrate were computed from the data of Gibson and Kincaid (78), and the resulting values were extrapolated using Equation 4.9, which gave a value of 34.4 ml./mole for ϕ_v^o of potassium nitrate.

There is every reason to believe that the additivity laws expressed by Equations 4.34 and 4.35 are valid, so the deviations shown in Table 7 actually reflect the experimental error in ϕ_v^o.

The values of $\bar{V}_2^o$, identical to ϕ_v^o, for the rare-earth chlorides are plotted as a function of ionic radius of the

Table 3. Experimental apparent molal volumes and specific gravities at 25°C.

$c^{\frac{1}{2}}$	$m^{\frac{1}{2}}$	ρ/ρ_o	ϕ_v	Δ
		$PrCl_3$		
0.041633	0.041695	1.0004092	11.92	-0.09
0.068530	0.068634	1.0011053	12.65	+0.04
0.087251	0.087385	1.0017892	12.97	-0.02
0.13551	0.13573	1.0042986	13.91	+0.06
0.16616	0.16644	1.0064508	14.35	-0.03
0.23282	0.23327	1.0126111	15.36	+0.02
0.29549	0.29613	1.020250	16.08	-0.06
0.36348	0.36443	1.030528	16.94	+0.03
0.42226	0.42354	1.041089	17.55	0.00
		$SmCl_3$		
0.045036	0.045103	1.0004971	12.38	+0.13
0.046100	0.046169	1.0005210	12.32	+0.04
0.073046	0.073157	1.0013056	12.78	-0.04
0.095015	0.095162	1.0022054	13.18	-0.04
0.13175	0.13196	1.0042297	13.81	-0.02
0.16024	0.16051	1.0062459	14.23	-0.02
0.22644	0.22687	1.012425	15.15	+0.02
0.28755	0.28817	1.019975	15.89	+0.02
0.35857	0.35949	1.030958	16.68	+0.01
0.41872	0.41998	1.042106	17.32	-0.01
		$GdCl_3$		
0.043430	0.043494	1.0004718	14.25	+0.10
0.057433	0.057520	1.0008245	14.43	-0.02
0.089915	0.090054	1.0020160	15.03	-0.05
0.12314	0.12334	1.0037713	15.67	+0.03
0.15888	0.15915	1.0062666	16.15	-0.04
0.20353	0.20390	1.0102539	16.84	+0.03
0.29340	0.29407	1.021222	17.87	-0.03
0.37085	0.37189	1.033773	18.82	+0.07
0.42181	0.42315	1.043613	19.26	-0.04

Table 3. (Continued)

$c^{\frac{1}{2}}$	$m^{\frac{1}{2}}$	ρ/ρ_o	ϕ_v	Δ
		$TbCl_3$		
0.039062	0.039120	1.0003839	14.46	+0.24
0.070770	0.070878	1.0012586	14.77	-0.12
0.085471	0.085602	1.0018328	15.18	+0.01
0.13862	0.13885	1.0048054	15.99	-0.07
0.16029	0.16056	1.0064137	16.44	+0.06
0.22822	0.22866	1.0129589	17.27	-0.04
0.29238	0.29304	1.021193	18.16	+0.06
0.36527	0.36626	1.032977	18.90	-0.03
0.43056	0.43198	1.045679	19.66	0.00
		$HoCl_3$		
0.045283	0.045306	1.0005306	12.82	-0.03
0.065715	0.065813	1.0011176	13.29	0.00
0.076195	0.076312	1.0015012	13.52	+0.02
0.093206	0.093350	1.0022439	13.80	-0.03
0.11052	0.11069	1.0031499	14.20	+0.05
0.15259	0.15285	1.0059894	14.87	+0.03
0.16191	0.16219	1.0067421	14.92	-0.06
0.19607	0.19642	1.0098644	15.50	+0.02
0.22756	0.22800	1.0132662	15.92	+0.01
0.28329	0.28390	1.020505	16.59	-0.03
0.34586	0.34673	1.030469	17.38	+0.02
0.36281	0.36376	1.033504	17.56	+0.01
0.41869	0.41998	1.044513	18.17	-0.01
		$DyCl_3$		
0.041586	0.041647	1.0004424	13.85	+0.16
0.064935	0.065034	1.0010777	14.07	-0.12
0.086923	0.087057	1.0019267	14.65	+0.04
0.13661	0.13683	1.0047435	15.46	-0.01
0.16315	0.16342	1.0067549	15.88	0.00
0.23848	0.23894	1.0143732	16.92	+0.01
0.27972	0.28032	1.019736	17.42	-0.01
0.35331	0.35425	1.031379	18.28	0.00
0.40290	0.40412	1.040719	18.82	0.00

Table 3. (Continued)

$c^{\frac{1}{2}}$	$m^{\frac{1}{2}}$	ρ/ρ_o	ϕ_v	Δ
		$ErCl_3$		
0.045679	0.045747	1.0005481	11.75	-0.02
0.067254	0.067355	1.0011858	12.27	+0.04
0.091134	0.091274	1.0021743	12.64	-0.06
0.14496	0.14519	1.0054778	13.73	+0.08
0.16076	0.16102	1.0067342	13.86	-0.04
0.23456	0.23500	1.0142755	14.96	+0.02
0.28131	0.28190	1.020492	15.48	-0.05
0.35643	0.35732	1.032779	16.41	+0.02
0.41841	0.41966	1.045059	17.05	0.00

Table 4. Parameters for equation 4.31

Salt	a_0	a_1	a_2	a_3	Avg. dev.
$LaCl_3$	14.38	27.83	-42.02	33.97	0.08
$PrCl_3$	10.96	26.58	-42.55	39.22	0.04
$NdCl_3$	10.48	21.15	-19.28	11.63	0.03
$SmCl_3$	11.42	20.56	-21.81	14.90	0.02
$GdCl_3$	13.30	21.72	-25.94	18.92	0.04
$TbCl_3$	13.51	21.02	-23.02	16.70	0.07
$DyCl_3$	12.82	22.90	-29.97	24.97	0.04
$HoCl_3$	11.83	24.38	-35.72	32.58	0.03
$ErCl_3$	10.69	25.33	-38.86	35.01	0.04
$YbCl_3$	9.22	26.64	-45.10	40.81	0.11
$La(NO_3)_3$	49.08	32.19	-53.01	52.21	0.11
$Nd(NO_3)_3$	44.74	40.42	-54.02	39.39	0.12
$Er(NO_3)_3$	45.59	20.28	-19.95	13.05	0.03
$Yb(NO_3)_3$	43.60	22.31	-25.72	17.62	0.03

Table 5. Parameters for Equation 4.33

Salt	$\phi_V^o (=V_2^o)$	$\frac{1}{2}W_V$	$\frac{1}{2}K_V$	$\overset{o}{a}$	Avg. dev.
$LaCl_3$	14.51	36.33	4.904	5.75 (22)	0.08
$PrCl_3$	10.96	34.47	4.254	5.73 (22)	0.04
$NdCl_3$	10.18	23.82	5.401	5.49 (23)	0.04
$SmCl_3$	11.16	3.83	6.747	5.63 (22)	0.04
$GdCl_3$	13.08	9.56	5.794	5.63 (24)	0.05
$TbCl_3$	13.25	13.00	6.519	5.85 (25)	0.07
$DyCl_3$	12.66	9.53	5.713	5.32 (23)	0.04
$HoCl_3$	11.73	27.45	5.787	6.04 (23)	0.02
$ErCl_3$	10.63	30.92	4.732	5.92 (23)	0.04
$YbCl_3$	9.27	20.07	5.537	5.90 (23)	0.11
$La(NO_3)_3$	49.37	32.82	5.815	4.4 (75)	0.11
$Nd(NO_3)_3$	44.74 - Data did not fit Owen-Brinkley equation				
$Er(NO_3)_3$	45.28	8.29	6.539	5.6 (76)	0.05
$Yb(NO_3)_3$	43.37	32.41	4.821	6.05 (76)	0.03

Table 6. Experimental values of $d\phi_v/dm^{\frac{1}{2}}$ at round $m^{\frac{1}{2}}$

Salt \ $m^{\frac{1}{2}}$	0	0.05	0.10	0.15	0.20	0.25	0.30	0.35	0.40
$LaCl_3$	27.8	23.9	20.5	17.5	15.1	13.2	11.8	10.9	10.5
$PrCl_3$	26.6	22.6	19.2	16.5	14.3	12.7	11.6	11.2	11.4
$NdCl_3$	21.2	19.3	17.6	16.2	14.8	13.7	12.7	11.9	11.3
$SmCl_3$	20.6	18.5	16.7	15.0	13.6	12.4	11.5	10.8	10.3
$GdCl_3$	21.7	19.3	17.1	15.2	13.6	12.3	11.3	10.5	10.1
$TbCl_3$	21.0	18.9	16.9	15.2	13.8	12.6	11.7	11.1	10.6
$DyCl_3$	22.9	20.1	17.7	15.6	13.9	12.6	11.7	11.1	10.9
$HoCl_3$	24.4	21.1	18.2	15.9	14.0	12.6	11.8	11.4	11.4
$ErCl_3$	25.3	21.7	18.6	16.0	14.0	12.5	11.5	11.0	11.0
$YbCl_3$	26.6	22.4	18.8	15.9	13.5	11.7	10.6	10.1	10.1
$La(NO_3)_3$	32.2	27.3	23.2	19.8	17.3	15.5	14.5	14.3	14.9
$Nd(NO_3)_3$	40.4	35.3	30.8	26.9	23.6	20.8	18.7	17.1	16.1
$Er(NO_3)_3$	20.3	18.4	16.7	15.2	13.9	12.8	11.8	11.1	10.6
$Yb(NO_3)_3$	22.3	19.9	17.7	15.8	14.1	12.8	11.6	10.8	10.2

Table 7. Additivity relationships

Cation	$3\left[(\phi_v^o)_{NO_3^-} - (\phi_v^o)_{Cl^-}\right]$	$(\phi_v^o)_{R^{+3}} - (\phi_v^o)_{R'^{+3}}$		Anion	
		R^{+3}	R'^{+3}	Cl^-	NO_3^-
La^{+3}	34.9	La^{+3}	Nd^{+3}	4.3	4.6
Nd^{+3}	34.6	La^{+3}	Er^{+3}	3.9	4.1
Er^{+3}	34.7	La^{+3}	Yb^{+3}	5.2	6.0
Yb^{+3}	34.1	Er^{+3}	Nd^{+3}	0.5	0.5
K^+	34.7	Nd^{+3}	Yb^{+3}	0.9	1.4
NH_4^+	34.2	Er^{+3}	Yb^{+3}	1.4	1.9
mean =	34.5				
Average deviation from mean for rare-earth salts = 0.3		Average deviation from mean of Cl^- and NO_3^- value = 0.2			

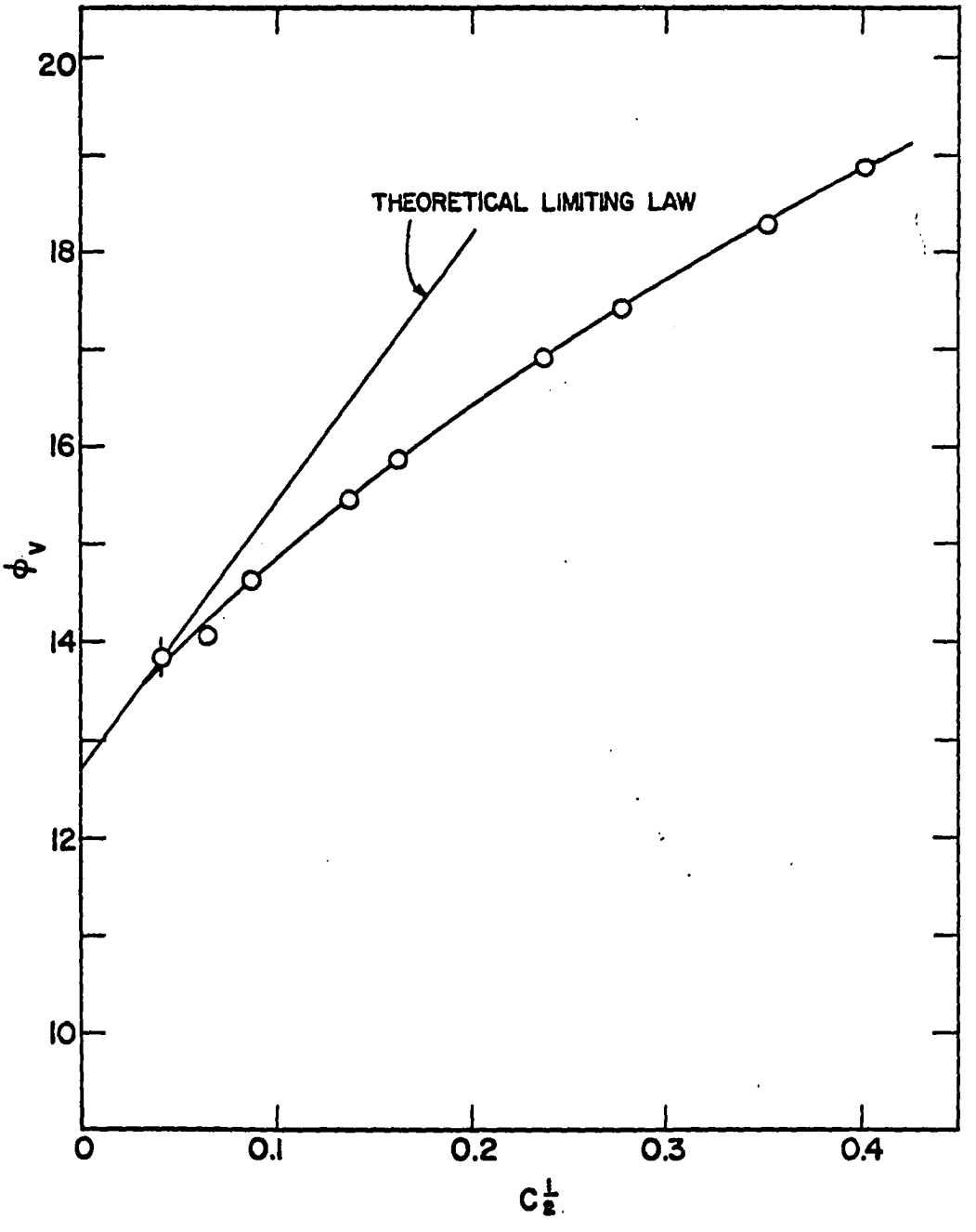

Figure 4. Apparent molal volumes in ml./mole of aqueous solutions of dysprosium chloride at 25°C.

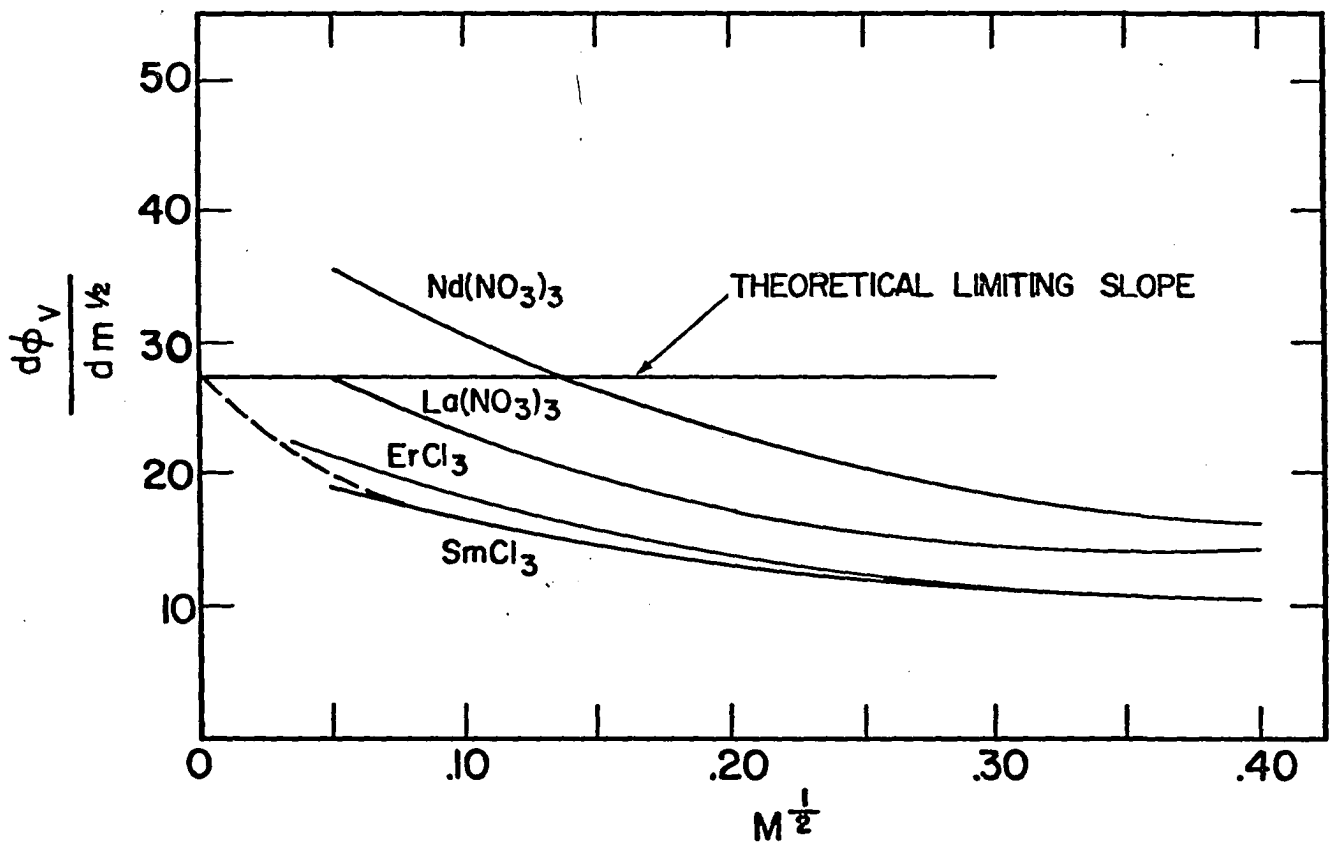

Figure 5. Comparison of experimental values of $d\phi_v/dm^{\frac{1}{2}}$ with theory

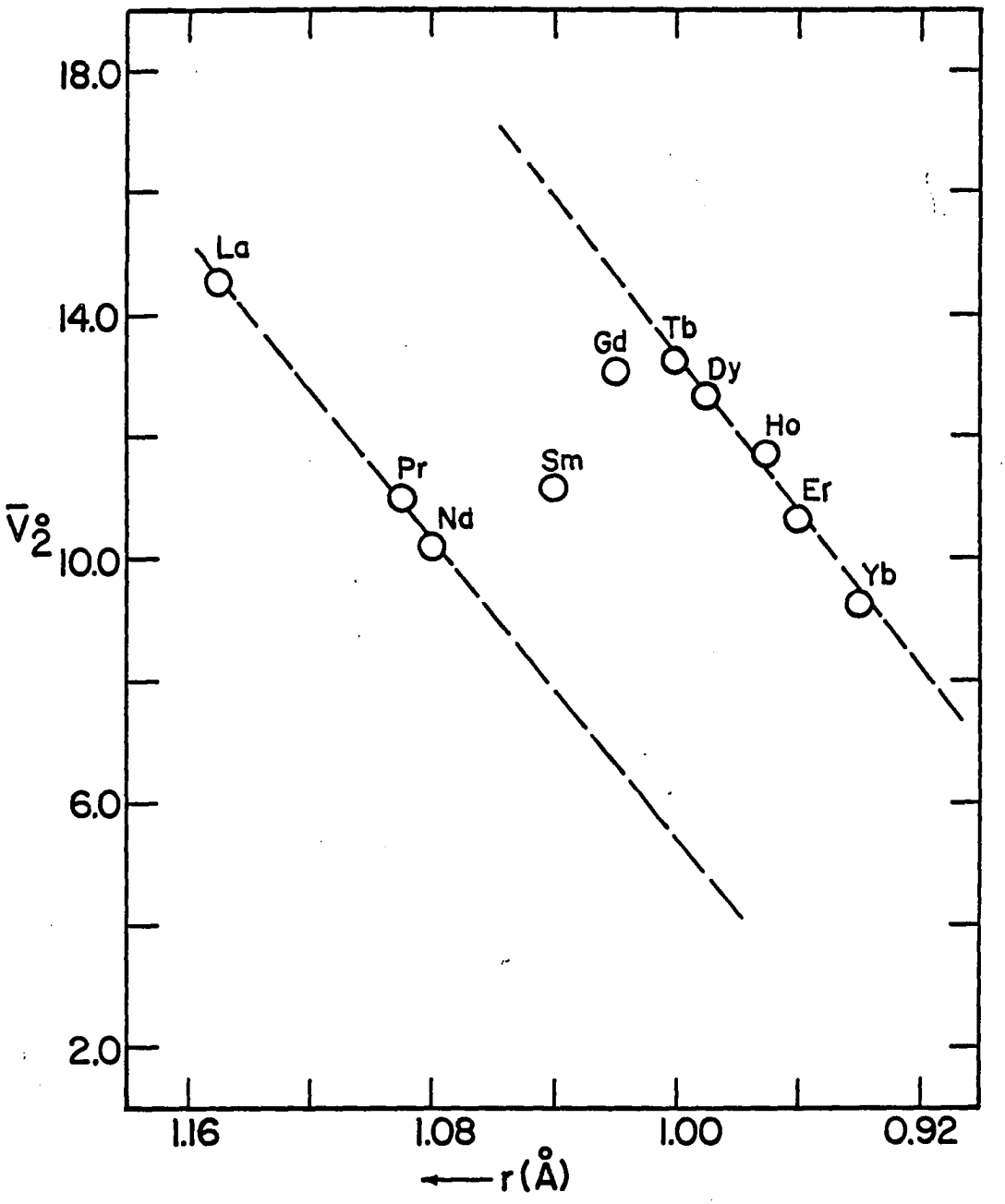

Figure 6. Partial molal volumes at infinite dilution of some rare-earth chlorides as a function of rare-earth ionic radius

rare-earth ion in Figure 6. The values of $\bar{V}_2^o$ were taken from Table 5, and the ionic radii are those of Pauling (79). The dashed lines represent the trends shown by the data.

8. Errors

As previously mentioned, the experimental apparent molal volumes determined in this research were calculated from Equation 4.25,

$$\phi_v = (1 - \rho/\rho_o)1000/c + M_2/\rho_o \qquad (4.25)$$

and the specific gravities were calculated from Equation 4.29,

$$S = \rho/\rho_o = \frac{W + w_s + I^o\Psi}{W + I_o^o\Psi} . \qquad (4.29)$$

Thus, the experimental specific gravities and apparent molal volumes were not directly measured in this research but were calculated from independently measured quantities. When a quantity, U, cannot be directly measured but must be calculated from the mean values of two or more independently measured quantities, $\bar{X}_1$, $\bar{X}_2$, ... $\bar{X}_n$, then the probable error in the mean value of U may be calculated from those of $\bar{X}_1$, $\bar{X}_2$, ... $\bar{X}_n$, using the law of propagation of precision indexes described by Worthing and Geffner (80). According to this method, the probable error of the calculated quantity, $P(\bar{U})$, may be expressed as,

$$P^2(\bar{U}) = \sum_{i=1}^{n} (\partial U/\partial \bar{X}_i)^2 \, P^2(\bar{X}_i) , \qquad (4.36)$$

where $\bar{U}$ is the mean value of the calculated quantity, U; $\bar{X}_i$, the mean value of the directly measured quantity X_i; and $P(\bar{X}_i)$, the probable error in $\bar{X}_i$. Equation 4.36 may be applied to the case of the apparent molal volume to give

$$P^2(\phi_V) = (\partial\phi_V/\partial c)^2 P^2(c) + (\partial\phi_V/\partial S)^2 P^2(S) , \quad (4.37)$$

where the probable error in S is given by,

$$P^2(S) = (\partial S/\partial W)^2 P^2(W) + (\partial S/\partial w_s)^2 P^2(w_s) + (\partial S/\partial I^o)^2 P^2(I^o) + (\partial S/\partial I_o^o)^2 P^2(I_o^o) + (\partial S/\partial \Psi)^2 P^2(\Psi). \quad (4.37a)$$

Calculating the partial derivatives in Equation 4.37 gives the result,

$$P^2(\phi_V) = \left[\frac{1000(S - 1)}{c} \cdot \frac{P(c)}{c}\right]^2 + \left[\frac{100\ P(S)}{c}\right]^2 \quad (4.38)$$

The uncertainty in the concentration, c, was due to the uncertainty in the concentration of the stock solution and to errors introduced in preparing dilutions from a given stock solution. The probable error of the concentration of the stock solution was estimated to be roughly $\pm$ 0.05 percent. The errors introduced in preparing the dilutions would be random errors and were estimated to average about $\pm$ 0.01 percent, so $P(c)/c = \pm 6 \times 10^{-4}$. The quantity, 1000(S - 1)/c, was approximately constant and equal to about 240 for all the solutions studied, so Equation 4.38 becomes,

$$P^2(\phi_V) = (0.14)^2 + \left[1000P(S)/c\right]^2 . \quad (4.39)$$

It should be emphasized that the concentration error of each solution is due mainly to the error in the concentration of the stock solution, and this error will be the same for all solutions prepared from a given stock solution. Therefore, the Δ values given in Table 3 will be much smaller than Equation 4.39 implies if the same stock solution was used to prepare all the dilutions. For $PrCl_3$, $GdCl_3$, and $DyCl_3$, two independently prepared and analyzed stock solutions were used in preparing the dilutions, and for the other rare-earth chlorides, the same stock solution was used to prepare all the dilutions of a given salt.

From Equation 4.39 it is obvious that a given error in specific gravity is much more serious for dilute solutions than for concentrated solutions. For example, an error of $\pm$ 1x10^{-6} in specific gravity results in an error in ϕ_V of $\pm$ 0.01 ml./mole at 0.1 molar, but at 0.002 molar, the same error in specific gravity causes an error in ϕ_V of $\pm$ 0.5 ml./mole. Therefore, an accurate estimate for the probable error in specific gravity is of particular importance for very dilute solutions.

Calculating the partial derivatives appearing in Equation 4.38 from Equation 4.29 and inserting numerical values yields,

$$\partial S/\partial w_s = 1/(W + I_o^o\Psi) \cong 1\text{x}10^{-2}\ (\text{g.})^{-1}, \qquad (4.39)$$

$$\partial S/\partial I^o = \Psi/(W + I_o^o\Psi) \cong 1\text{x}10^{-6}\ (\text{ma.})^{-1}, \qquad (4.40)$$

$$\partial S/\partial I_o^o = \frac{-(W + w_s + I^o\Psi)}{(W + I_o^o\Psi)^2} = 1\times10^{-6}\ (\text{ma.})^{-1}, \qquad (4.41)$$

$$\partial S/\partial \Psi = \frac{I^o}{W + I_o^o\Psi} - \frac{I_o^o(W + w_s + I^o\Psi)}{(W + I_o^o\Psi)^2} \cong \frac{I^o - I_o^o}{W} \cong$$

$$0.2\ \text{ma./g.}, \qquad (4.42)$$

$$\partial S/\partial W = -\frac{\left[(I^o - I_o^o)\Psi + w_s\right]}{(W + I_o^o\Psi)^2} \cong \frac{20\ \text{c g.}}{(W + I_o^o\Psi)^2} \cong$$

$$2\times10^{-3}\ (\text{g.})^{-1}. \qquad (4.43)$$

The weight of platinum on the float was always adjusted to minimize the quantity, $I^o - I_o^o$. Usually this difference was about 20 ma. or less, so a value of $I^o - I_o^o = 20$ ma. was used to obtain the final result for $\partial S/\partial \Psi$. Also, it was observed that the quantity, $(I^o - I_o^o)\Psi + w_s$, was approximately proportional to the molar concentration, c. This fact was used to obtain the final expression for $\partial S/\partial W$.

From the reproducibility of the equilibrium current measurements, it was estimated that, $P(I^o) = P(I_o^o) = \pm 0.1$ ma. Using the approximations given by Equation 4.40 and Equation 4.41, it is possible to write,

$$(\partial S/\partial I^o)^2\, P^2(I^o) + (\partial S/\partial I_o^o)^2\, P^2(I_o^o) \cong 2\times10^{-14}. \qquad (4.44)$$

Reproducibility of the calibration factor, Ψ, for a given position of the solution cell in the solenoid, indicated

that the probable error in Ψ was about $\pm$ 5x10^{-7} g./ma. This estimate and Equation 4.42 leads to the result,

$$(\partial S/\partial \Psi)^2 P^2(\Psi) \cong 1x10^{-14}. \qquad (4.45)$$

The quantity, w_s, was calculated from Equation 4.30, so the error in w_s arises from both uncertainty in w_v and uncertainty in the density of platinum, d_{pt}. The law of propagation of precision indexes may be applied to Equation 4.30 to give

$$P^2(w_s) = P^2(w_v) + w_v^2 P^2(d_{pt})/d_{pt}^4 . \qquad (4.46)$$

A value of 21.428 $\pm$ 0.002 g./cc. for the density of annealed platinum wire (74) was used in all the calculations, so $P(d_{pt})/d_{pt} \cong 1x10^{-4}$. The probable error in the weight of platinum in vacuum, $P(w_v)$, was estimated to be $\pm$ 0.005 mg. or one part in 10^5, whichever is larger. An uncertainty of $\pm$ 0.005 mg. is insignificant compared to the errors expressed by Equations 4.44 and 4.45, but one part in 10^5 becomes significant at higher concentrations where w_v is large. With the above estimates for $P(w_v)$ and $P(d_{pt})$, Equation 4.46 becomes,

$$P^2(w_s) = 1.3\ w_v^2\ x10^{-10}\ (g.)^2. \qquad (4.47)$$

Combining Equation 4.47 and Equation 4.39, and substituting 20c for w_v gives

$$(\partial S/\partial w_s)^2 P^2(w_s) = 5\ c^2\ x10^{-12}. \qquad (4.48)$$

From the accuracy of the weights used with the analytical balance and the reproducibility of the balance, it was estimated that $P(W) = \pm\ 5x10^{-4}$ g. This estimate and Equation 4.43

result in the approximation,

$$(\partial S/\partial W)^2 P^2(W) \cong c^2 \times 10^{-12}. \qquad (4.49)$$

Combination of Equations 4.44, 4.45, 4.48, and 4.49, gives the final expression for the probable error in the specific gravity, which may be expressed as,

$$P(S) = (3\times10^{-14} + 6\ c^2 \times 10^{-12})^{\frac{1}{2}}. \qquad (4.50)$$

Equation 4.50 may then be combined with Equation 4.39 to calculate the probable error in ϕ_V as a function of concentration. The preceeding error analysis for specific gravity and ϕ_V is summarized in Table 8. It should be noticed that the probable error in specific gravity makes an important contribution to the probable error in ϕ_V only for very dilute solutions. In fact, the specific gravity error becomes very serious below 0.002 molar, which is the reason the Δ values in Table 3 are, in general, larger for the most dilute solutions. It is significant to note that if the Δ values in Table 3 for the most dilute solution of a given salt are attributed solely to the specific gravity error, the average specific gravity error is $\pm$ 2x10^{-7}, in perfect agreement with the error analysis.

In addition to the error in ϕ_V caused by an error in the concentration of the stock solution, the values of ϕ_V given in Table 5 also contain a possible extrapolation error. However, it is believed that use of the Owen-Brinkley equation reduced the extrapolation error to less than $\pm$0.1 ml./mole in most

cases. Therefore, it may be expected that the probable error in ϕ_V^o will be about ±0.2 ml./mole. If the deviations given in Table 7 are taken as a measure of the probable error for the difference between two ϕ_V^o values, the predicted probable error for ϕ_V^o is ±0.18 ml./mole, in agreement with the above estimate.

The probable error in the experimental slope, $d\phi_V/dm^{\frac{1}{2}}$, is much more difficult to estimate. However, a crude estimate of the slope may be obtained by a method based upon the use of different empirical equations to represent the ϕ_V data. The values of $d\phi_V/dm^{\frac{1}{2}}$ given in Table 6 were calculated from a power series in $m^{\frac{1}{2}}$ containing four adjustable parameters. However, Ayers (7) chose to represent his data with similar equations but containing five adjustable parameters. Furthermore, it was noticed that, in most cases, the data could be represented by power series in $m^{\frac{1}{2}}$ containing only three adjustable parameters. The three parameter equations did not represent the experimental ϕ_V data as well as either the four or the five parameter equations, but the three parameter equations usually represented the experimental data within the limits of experimental error in ϕ_V.

For each rare-earth salt, $d\phi_V/dm^{\frac{1}{2}}$ was calculated from the corresponding five parameter equation, and also from the corresponding three parameter equation when the three parameter equation represented the data within the limits of experimental error. For a given salt, the values of $d\phi_V/dm^{\frac{1}{2}}$

obtained were compared with those given in Table 6, and the differences observed were taken as a crude estimate of the probable error in the slope, $d\phi_V/dm^{\frac{1}{2}}$. The results of this comparison for $La(NO_3)_3$, $Nd(NO_3)_3$, $SmCl_3$, and $HoCl_3$ are given in Table 9. The deviations shown by $La(NO_3)_3$ were the largest observed for the salts studied, while $Nd(NO_3)_3$, $SmCl_3$, and $HoCl_3$ represent typical examples of the deviations found for the other salts. The three parameter equation for $Nd(NO_3)_3$ did not represent the data so it was not included in the error analysis.

From this "empirical" error analysis, it was concluded that the relative probable error in a given value of $d\phi_V/dm^{\frac{1}{2}}$ from Table 6 is generally about $\pm$ 10 percent at $m^{\frac{1}{2}} = 0.05$ and about $\pm$ 5 percent at higher concentrations. Since the experimental limiting slope involves a possible extrapolation error, in addition to the probable error of about $\pm$ 20 percent indicated by Table 9, all that can be said is that the values of $d\phi_V/dm^{\frac{1}{2}}$ given in Table 6 for $m^{\frac{1}{2}} = 0$ have a probable error of at least $\pm$ 20 percent.

C. Discussion

1. Limiting concentration dependence

The tentative conclusions of Spedding and Ayers (7) indicated that the concentration dependence of the apparent molal volumes of rare-earth salts showed significant deviations from the theoretical limiting law, Equation 4.6, above 0.002 molal,

Table 8. Error analysis for ϕ_v and specific gravity

c	P(S)	$\left\lvert\frac{\partial \phi_v}{\partial S}\right\rvert P(S)$	$\left\lvert\frac{\partial \phi_v}{\partial c}\right\rvert P(c)$	$P(\phi_v)$
0.001	$2 \cdot 10^{-7}$	0.20	0.14	0.22
0.002	$2 \cdot 10^{-7}$	0.10	0.14	0.17
0.004	$2 \cdot 10^{-7}$	0.05	0.14	0.15
0.006	$2 \cdot 10^{-7}$	0.03	0.14	0.14
0.008	$2 \cdot 10^{-7}$	0.03	0.14	0.14
0.01	$2 \cdot 10^{-7}$	0.02	0.14	0.14
0.02	$2 \cdot 10^{-7}$	0.01	0.14	0.14
0.05	$2 \cdot 10^{-7}$	0.00	0.14	0.14
0.10	$3 \cdot 10^{-7}$	0.00	0.14	0.14
0.15	$4 \cdot 10^{-7}$	0.00	0.14	0.14
0.20	$5 \cdot 10^{-7}$	0.00	0.14	0.14

Table 9. Comparison of $d\phi_v/dm^{\frac{1}{2}}$ calculated from different equations

Salt	Slope, $d\phi_v/dm^{\frac{1}{2}}$						
	#par. \ $m^{\frac{1}{2}}$	0	0.05	0.1	0.2	0.3	0.4
$La(NO_3)_3$	3[a]	23.0	21.9	20.7	18.4	16.1	13.8
$La(NO_3)_3$	4[b]	32.2	27.3	23.2	17.3	14.5	14.9
$La(NO_3)_3$	5[c]	53.0	34.6	23.4	15.9	17.4	14.9
$Nd(NO_3)_3$	4[b]	40.4	35.3	30.8	23.6	18.7	16.1
$Nd(NO_3)_3$	5[c]	46.2	37.7	31.2	22.8	18.9	17.2
$SmCl_3$	3[d]	18.4	17.3	16.2	13.9	11.7	9.4
$SmCl_3$	4[b]	20.6	18.5	16.7	13.6	11.5	10.3
$SmCl_3$	5[e]	13.7	16.5	16.8	13.7	10.9	15.0
$HoCl_3$	3[f]	19.7	18.4	17.1	14.6	12.1	9.6
$HoCl_3$	4[b]	24.4	21.1	18.2	14.0	11.8	11.4
$HoCl_3$	5[g]	30.1	33.2	18.4	13.7	12.3	10.6

[a] $\phi_v = 49.59 + 23.00\ m^{\frac{1}{2}} - 11.46m.$

[b] From Table 6.

[c] From Ayers (7).

[d] $\phi_v = 11.54 + 18.44m^{\frac{1}{2}} - 11.26m.$

[e] $\phi_v = 11.65 + 13.74m^{\frac{1}{2}} + 41.90m - 212.6m^{3/2} + 272.8m^2.$

[f] $\phi_v = 12.09 + 19.66m^{\frac{1}{2}} - 12.59m.$

[g] $\phi_v = 11.61 + 30.07m^{\frac{1}{2}} - 81.50m + 174.7m^{3/2} - 149.1m^2.$

and furthermore, that the deviations were more serious for the heavier rare-earths. Before discussing the results obtained in this research, it should be mentioned that their discussion of the limiting behavior assumed the theoretical limiting slope for 3-1 salts was 37, as given by Harned and Owen (11). As previously mentioned, the more recent study of Redlich and Mayer (50) shows the correct value to be 27.44.

Since interionic attraction theory predicts only the slope of a ϕ_V vs. $c^{\frac{1}{2}}$ curve, it was decided that a consistent comparison of apparent molal volume data with interionic attraction theory would best be made by comparing the experimental slopes with the slope predicted by interionic attraction theory. However, as revealed in the error analysis, the experimental slopes in dilute solution may be subject to large errors, and a theoretical discussion of the experimental slopes must recognize this limitation.

From Table 6, the average experimental limiting slope for the 3-1 salts studied was calculated to be 25. In view of the possible errors introduced by extrapolation, the value agrees remarkably well with the theoretical value of 27. For the most part, the limiting slopes given in Table 6 are less than the theoretical limiting value. This trend is most likely due to an extrapolation error introduced by the use of empirical equations to represent the data.

It is perhaps more meaningful to discuss the slopes at

experimental concentrations. At experimental concentrations (above 0.002 molar) the experimental slopes are observed to be less than the theoretical limiting slope, with the exception of $Nd(NO_3)_3$. Examples of this negative deviation are shown graphically in Figure 4 and Figure 5. It is important to note that significant negative deviations from the simple limiting law above 0.002 molar are consistent with interionic attraction theory and require no special explanation other than including the effect of the a parameter. The theoretical first order deviations from the limiting law were expressed earlier by Equation 4.16.

Figure 5 shows $d\phi_V/dm^{\frac{1}{2}}$ for several rare-earth salts as a function of $m^{\frac{1}{2}}$. The theoretical limiting slope is given by the horizontal line, and the theoretical slope at non-zero concentrations is given by the dashed line. As mentioned earlier, the theoretical slope was calculated from Equation 4.15 for a 5.6 Å, neglecting the W_V term. From Figure 5 it is evident that, within experimental error, the experimental slopes of $ErCl_3$ and $SmCl_3$, which are typical of most of the salts studied, are in agreement with the theoretical slope, at least below about 0.01 molar. The slope of $Nd(NO_3)_3$ shows positive deviations from the theoretical limiting slope at low concentrations. From the error analysis, it seems certain that these positive deviations are real and represent a true anomaly. However, the seemingly anomalous behavior shown by $La(NO_3)_3$ may be due to the unusually large experimental error

in the slope for this salt. The values of $d\phi_v/dm^{\frac{1}{2}}$ for the other rare-earth salts in Table 6 exhibit much the same behavior as shown in Figure 5 for $SmCl_3$ and $ErCl_3$. In fact, except for $Nd(NO_3)_3$ and possibly $La(NO_3)_3$, the experimental values of $d\phi_v/dm^{\frac{1}{2}}$ at low concentrations are represented by the theoretical curve within the limits of experimental error.

The success of Equation 4.15 with the a parameter assumed independent of pressure, in predicting the observed values of $d\phi_v/dm^{\frac{1}{2}}$ implies the quantity, $\phi_v - 27.44\ c^{\frac{1}{2}}\tau(\kappa a)$, should be nearly constant in dilute solution. Indeed, this phenomenon was observed for all the rare-earth salts studied, except $Nd(NO_3)_3$. In fact, it is this behavior that makes the Owen-Brinkley equation an ideal extrapolation function for the rare-earth salts. The observed slight increase in the quantity, $\phi_v - 27.44\ c^{\frac{1}{2}}\tau(\kappa a)$, as the concentration increased was probably due to imperfections in the theory as well as the influence of $\partial \ln a/\partial P$.

In summary, it may be concluded that significant deviations from the simple limiting law do occur at experimental concentrations for the rare-earth salts, but that these deviations are consistent with interionic attraction theory for all the salts studied except $Nd(NO_3)_3$. The tentative conclusion of Spedding and Ayers that the heavier rare-earth salts show greater deviations from the limiting law is not supported.

The behavior of $Nd(NO_3)_3$ is anomalous, and some special

explanation is needed to resolve this problem. Spedding and Ayers suggested that the unusually large slope for $Nd(NO_3)_3$ could be explained if it were assumed the nitrate ion could displace a water molecule from the co-ordination sphere of Nd^{+3}. In view of the postulated change in co-ordination number with ionic radius starting near Nd^{+3} (6), this interpretation seems reasonable. Furthermore, if this interpretation is correct, one might also expect to find unusually large slopes for $Sm(NO_3)_3$ and $Pr(NO_3)_3$.

2. Partial molal volumes at infinite dilution

Values of $\bar{V}_2^o$ for ten rare-earth chlorides are shown in Figure 6 as a function of ionic radius. It should be noticed that $\bar{V}_2^o$ decreases with decreasing ionic radius from La to Nd and from Tb to Yb. However, in the region from Nd to Tb, $\bar{V}_2^o$ increases with decreasing ionic radius. The more accurate values of $\bar{V}_2^o$ obtained in this research differ somewhat in magnitude from those determined by Saeger and Spedding (6), since their data was obtained by extrapolating from considerably higher concentrations, but the variation of $\bar{V}_2^o$ with ionic radius is essentially the same.

In Equation 4.18, the partial molal volume at infinite dilution of an ion was written in the form,

$$\bar{V}_i^o = V^* + \triangle V, \qquad (4.18)$$

where V^* is the intrinsic volume of the ion and $\triangle V$ represents the change in volume of the solvent, which is water in

the present discussion. Due to the strong ion-dipole forces between a rare-earth ion and water molecules, one may speak of a $R^{+3} \cdot XH_2O$ species in solution, where R^{+3} is a rare-earth ion, and X is the number of water molecules co-ordinated to the ion. For a given co-ordination number, V* and $\triangle V$ should decrease smoothly with decreasing ionic radius, while a change in co-ordination number may result in sharp changes in both quantities with the major change occurring in the negative term, $\triangle V$. Since the effective volume of a water molecule in the co-ordination sphere should be less than the corresponding volume outside this co-ordination sphere, a shift to a lower co-ordination number should decrease the absolute magnitude of $\triangle V$ and therefore increase the value of $\bar{V}_2^o$.

According to the original proposal of Spedding and Ayers (7) and the later modification given by Saeger and Spedding (6), a rare-earth ion in water may exist in an equilibrium between two possible co-ordination numbers. Furthermore, this equilibrium may be sharply displaced toward a lower co-ordination number below a critical radius, due to the influence of dipole-dipole repulsions and short range repulsive forces between the water molecules in the co-ordination sphere. On the basis of this simple model, the $\bar{V}_2^o$ data may be qualitatively explained. According to this postulate, the equilibrium between the possible co-ordination numbers favors the higher co-ordination number for the rare-earth ions between La and

Nd. After Nd, a displacement of this equilibrium toward the lower co-ordination number begins to take place that results in the lower co-ordination number becoming increasingly more favorable for the rare-earth ions from Nd to around Tb. The smooth decrease of $\bar{V}_2^o$ from Tb to Yb indicates the shift toward the lower co-ordination number terminates around Tb, and the rare-earth ions from around Tb to Yb have essentially the same co-ordination number.

Numerous other recent investigations indicate a possible change in water co-ordination number for the rare-earth ions (4,5,81, 82, 83). In particular, Morgan (81) suggested that the principle co-ordination number for the $R^{+3} \cdot XH_2O$ species in solution may vary across the lanthanide series. He suggested a co-ordination number of nine at the beginning of the series and a co-ordination number of six at the end, including Er^{+3} among the latter. From proton relaxation data on dilute (0.0003-0.02 molar) aqueous gadolinium perchlorate solutions, he concluded that either co-ordination number eight or nine is acceptable for Gd^{+3}.

Morgan's conclusions do not agree with the interpretation given the partial molal volume data since a co-ordination number of six for Er^{+3} would require the major change in co-ordination number to take place between Gd^{+3} and Er^{+3}. The partial molal volume data was interpreted as showing the change in co-ordination number takes place between Nd and Tb.

However, Morgan's conclusions are based upon the x-ray diffraction work of Brady (36) on aqueous solutions of $ErCl_3$ and ErI_3. According to Brady, the principle solution species are $Er(H_2O)_6Cl_2^+$ and $Er(H_2O)_6I_2^+$ in concentrated (greater than 0.9 molar) solutions of $ErCl_3$ and ErI_3, respectively. However, at infinite dilution, it seems quite likely that water molecules would replace the halide ions in the co-ordination complex, giving the species, $Er(H_2O)_8^{+3}$. Co-ordination numbers of nine for the rare-earth ions from La^{+3} to Nd^{+3} and of eight for Gd^{+3} and Er^{+3} would qualitatively agree with the $\bar{V}_2^o$ data.

It would be interesting to determine whether or not a change in co-ordination number of nine to eight would agree quantitatively with the $\bar{V}_2^o$ data. For this purpose, let it be assumed that the dashed line drawn through the $\bar{V}_2^o$ values for $LaCl_3$, $PrCl_3$, and $NdCl_3$ in Figure 6 represents $\bar{V}_2^o$ as a function of ionic radius from Nd to Tb had no change in co-ordination number occurred. The difference between the actual value of $\bar{V}_2^o$ for $TbCl_3$ and the value predicted by the dashed line is 8 ml./mole. According to the model, this difference represents the "experimental" value of the change in volume, δV, of the reaction,

$$Tb\cdot 9H_2O^{+3} \longrightarrow Tb\cdot 8H_2O^{+3} + H_2O \ , \qquad (4.51)$$

where δV is given by,

$$\delta V = \bar{V}^o(Tb\cdot 8H_2O^{+3}) - \bar{V}^o(Tb\cdot 9H_2O^{+3}) + V_{H_2O} \ . \qquad (4.52)$$

The quantities, $\bar{V}^o(Tb\cdot 8H_2O^{+3})$ and $\bar{V}^o(Tb\cdot 9H_2O^{+3})$, represent

the partial molal volumes at infinite dilution of the co-ordinated ions, and $\bar{V}_{H_2O}$ is the molar volume of the water released from the co-ordination sphere. It will be assumed that $\bar{V}_{H_2O}$ is approximately given by the molar volume of pure water, 18 ml./mole. Furthermore, since the effective radii of the eight and nine co-ordinated terbium ions, r_8 and r_9 respectively, may be expected to be about 4 Å, there is some justification for using Equation 4.23 to calculate the difference in partial molal volume between the eight and nine co-ordinated species. Using Equation 4.23 to calculate the difference between the first two terms in Equation 4.52 and assuming $\bar{V}_{H_2O}$ = 18 ml./mole allows Equation 4.52 to be written as,

$$\delta V = 2.52(r_8^3 - r_9^3) - 37.6(1/r_8 - 1/r_9) + 18. \qquad (4.53)$$

The effective radii, r_8 and r_9, must be calculated from some co-ordination model. It will be assumed that the effective radii are approximately given by the average Tb^{+3}-OH_2 distance calculated from the co-ordination model plus the radius of a water molecule. X-ray diffraction data for erbium ethylsulfate (84) shows nine water molecules about the erbium ion at an average distance of 2.42 Å. If the radius of the water molecule is taken as, $r_{H_2O} \cong r_{O^=} = 1.40$ Å (79), the effective radius of a nine co-ordinated erbium ion is 3.82 Å. Correcting for the difference in ionic radii (79) between Tb^{+3} and Er^{+3}, the model gives, $r_9 = 3.86$ Å. The crystal structure of $GdCl_3 \cdot 6H_2O$ (85) will be taken as the model for an eight

co-ordinated rare-earth ion. Here, six water molecules, at an average distance of 2.41 Å, and two chloride ions, at a distance of 2.77 Å, are co-ordinated to the gadolinium ion. Assuming water molecules occupy the chloride positions and correcting for the difference in radii gives 2.40 Å for the average Gd^{+3}-OH_2 distance for the solution species. Adding the radius of a water molecule to the average Gd^{3}-OH_2 distance and subtracting the difference in radii of 0.02 Å (79) between Gd^{+3} and Tb^{+3}, the effective radius of $Tb \cdot 8H_2O^{+3}$ is calculated to be, $r_8 = 3.78$ Å.

Substituting 3.78 Å for r_8 and 3.86 Å for r_9, Equation 4.53 gives, $\delta V = 9$ ml./mole, which is in excellent agreement with the "experimental" value of 8 ml./mole. In fact, the near perfect agreement is perhaps fortuitous since the exact theoretical value of δV is quite sensitive to the choice of co-ordination model. Furthermore, the above calculation does not prove that a change of co-ordination number from nine to eight does actually occur. However, the calculation does show that a change in co-ordination number from nine to eight for the rare-earths is compatible with the $\bar{V}_2^o$ data.

V. VISCOSITIES

A. Historical

1. Experimental methods-capillary viscometry

The viscosity of a Newtonian fluid was defined by Equation 1.4,

$$\eta = S/(dv/dx) , \qquad (1.4)$$

where S is the shearing force and dv/dx is the velocity gradient in the fluid. Equation 1.4 and classical hydrodynamic theory provide the basis for most experimental methods for measuring the viscosity of a Newtonian fluid. Generally, an apparatus designed to determine the viscosity of a fluid is called a viscometer. Equation 1.4 states that the shearing force is directly proportional to the velocity gradient, the constant of proportionality being the viscosity. It should be mentioned that some fluids do not obey the simple relationship between shearing force and velocity gradient given by Equation 1.4. These fluids are called non-Newtonian fluids and are discussed by Van Wazer, Lyons, Kim, and Colwell (86). However, there are no known exceptions to Equation 1.4 for aqueous electrolytes composed of ions of molecular dimensions, as long as turbulent flow is avoided, so this discussion will be confined to the viscosity of Newtonian fluids.

A variety of experimental methods exist which allow the viscosity of a Newtonian fluid to be measured. When a cylinder is rotated in a viscous fluid, a retarding force acts upon

it as a consequence of the viscous resistance in the fluid. This retarding force may be used to determine the viscosity of the fluid. Another method for measuring the viscosity consists of measuring the velocity of a sphere falling through the fluid. Perhaps the most accurate and widely used method is the capillary method. In this method, a given volume of liquid in a reservoir is forced through a capillary tube by either an externally applied pressure or the hydrostatic pressure head of the fluid, and the viscosity of the fluid is determined from the measured volumetric flow rate, pressure, and capillary dimensions. Most of the available experimental methods for measuring viscosity and a number of commercially available viscometers are discussed by Van Wazer, Lyons, Kim, and Colwell (86). Nearly all of the viscosity studies on electrolytes have employed some type of capillary viscometer to measure the viscosity of the solutions studied, and in most cases, the pressure forcing the liquid through the capillary was the hydrostatic head of the solution. The popularity of these "gravity-flow" capillary viscometers is probably due to the simplicity of operation and the high level of accuracy that can be attained. The following discussion will consider the measurement of viscosity using the "gravity-flow" capillary method.

It might be said that capillary viscometry was born in 1840 with the work of Poiseuille (87). Experiments on the flow of water through fine tubes led Poiseuille to empirically

discover the relationship between the volumetric flow rate, Q; the pressure difference between the ends of the tube, P; the radius of the tube, r; and the length of the tube, L. His results may be summarized by the equation,

$$Q = k\, P\, r^4/L\ , \qquad (5.1)$$

where k is a constant characteristic of the fluid and temperature. Poiseuille's empirical equation may also be deduced from theory. Using Equation 1.4 and hydrodynamics, Barr (88) gives a theoretical derivation of Equation 5.1. His result may be written as,

$$Q = \frac{\pi r^4 P}{8\eta L}\ . \qquad (5.2)$$

Therefore, the constant, k, in Poiseuille's empirical equation is equal to $\pi/8\eta$. If a volume, V, flows through the capillary tube in time, t, Q is given by, $Q = V/t$. Furthermore, if the hydrostatic pressure head of the fluid is the driving force, $P = h\rho g$. Here, h is the mean pressure head, ρ is the density of the fluid, and g is the gravitational constant. Making the above substitutions for P and Q, Equation 5.2 may be written in the form,

$$\eta = \left[\frac{\pi r^4 hg}{8VL}\right] \rho\, t\ , \qquad (5.3)$$

where the quantity in brackets is a constant for a given viscometer and temperature. Equation 5.3 is often referred to as Poiseuille's law and has been the equation employed to obtain much of the viscosity data on electrolytes.

The theoretical derivation of Poiseuille's law assumes the only work expended when the fluid flows through the capillary is that due to the viscous resistance in the capillary. However, in an actual viscometer the fluid in the reservoir is accelerated at the entrance of the capillary and attains a certain kinetic energy. Consequently, part of the work expended per second is expended in giving the fluid kinetic energy. This effect and its correction, termed the kinetic energy correction, is discussed in detail by Barr (88). Briefly, the result of the kinetic energy effect is that only part of the hydrostatic pressure head is effective in overcoming viscous resistance. Equation 5.3 may be modified to correct for the kinetic energy effect by replacing the value of h by the pressure head effective in overcoming viscous resistance, h', where,

$$h' = h - m\, V^2/\pi^2 g r^4 t^2 \,. \qquad (5.4)$$

The quantity, m, is a coefficient which depends, in part, on the geometry of the capillary ends. Various experimental and theoretical estimates of m are discussed in detail by Barr. Generally, the estimates summarized by Barr indicate m is about unity for the viscometers and flow rates studied.

In a capillary viscometer, a liquid in a wide reservoir enters into the capillary tube in a converging stream and exits either into open air or into another reservoir in a diverging stream. Any differences in velocity between adjacent lines of flow in these streams will require the expen-

diture of work in overcoming viscous resistance. This additional resistance, which is not included in the derivation of Poiseuille's law, is usually corrected for by a hypothetical addition to the capillary length (88) and involves replacing L in Equation 5.3 by L', where

$$L' = L + n\,r\,. \qquad (5.5)$$

In Equation 5.5, r is the radius of the capillary, and n is a coefficient which is normally assumed to be a constant for a given viscometer. The exact value of n depends upon the geometry of the capillary ends, but the various estimates of this coefficient, as discussed by Barr, indicate that n is a constant for a particular viscometer and is approximately equal to unity. This correction involving n is usually called the Couette correction.

Correcting Equation 5.3 for the kinetic energy effect and the Couette effect gives

$$\eta = \left[\frac{\pi r^4 h g}{8V(L + n r)}\right] \rho t - \left[\frac{m V}{8\pi(L + n r)}\right] \rho/t\,. \qquad (5.6)$$

It should be noticed that for long flow times with a viscometer having a small value of r/L, Equation 5.6 reduces to Poiseuille's law.

In an absolute measurement of viscosity, the dimensions of the viscometer must be known with high accuracy and the values of m and n must be estimated as accurately as possible. Because of these problems and several other difficulties (88, 89), absolute measurements of viscosity are very difficult.

However, if m and m are assumed constant over the viscosity range of interest, Equation 5.6 may be written in the form,

$$\eta/\rho = C\,t - K'/t, \qquad (5.7)$$

where C and K′ are constants for a given viscometer and temperature. The second term in Equation 5.7, $-K'/t$, is normally called the kinetic energy correction. These constants may be determined by a calibration procedure using fluids of known viscosity. For long flow times, Equation 5.7 reduces to the simple expression,

$$\eta/\rho = C\,t. \qquad (5.8)$$

Using special viscometers designed to magnify the kinetic energy term, Cannon, Manning, and Bell (90) have shown that the value of K′ in Equation 5.7 is not independent of flow time. Their treatment defined K′ by,

$$K' = t(C\,t - \eta/\rho), \qquad (5.9)$$

where C is a true constant. The value of C for a given viscometer was determined by a calibration using a viscosity standard which allowed Equation 5.8 to be employed. The flow times of less viscous fluids of known viscosity and density were then measured, and the values of K′ were calculated from Equation 5.9. Their study shows that K′ may be expressed empirically in terms of the Reynolds number, Re, defined by

$$Re = v\,r\,\rho/\eta\ , \qquad (5.10)$$

where v is the velocity of the fluid in the capillary. The other symbols have their usual meanings. According to their results, for trumpet shaped capillary ends, K′ is given by,

$$K' = 0.037(Re)^{\frac{1}{2}}\ V/8\pi L\ , \qquad (5.11)$$

over the Reynolds number range of practical interest. Cannon, Manning, and Bell then derive the expression,

$$\eta/\rho = C\ t - E/t^2\ , \qquad (5.12)$$

where C and E are true constants for a given viscometer and temperature. The constant, E, may be approximately calculated from Equation 5.13.

$$E = \frac{1.66\ V^{3/2}}{L(C\ 2r)^{\frac{1}{2}}}\ , \qquad (5.13)$$

where V is the efflux volume, L and r are the length and radius of the capillary, respectively.

Cannon, Manning, and Bell attribute the observed variation of K' with Reynolds number to the increase of the kinetic energy coefficient, m, with increasing Reynolds number and do not mention the Couette correction coefficient, n. However, their observed variation of K' with Reynolds number would also include any variation of n with flow time since their experimental procedure determined all deviations from Equation 5.8, whatever their cause. It is significant to note that the final equation of Cannon and co-workers, Equation 5.12, reduces to Equation 5.8 for long flow times.

A number of viscometer designs, experimental procedures, and sources of error in practical viscometry have been well summarized in the literature (86,88,91,92,93,94,95), so only a brief discussion of practical viscometry will be given here.

Many of the "gravity-flow" capillary viscometers in common use today are modifications of the simple Ostwald viscometer, which consists of two glass reservoir bulbs separated by a glass capillary in a U-tube arrangement. With viscometers of the Ostwald type, the viscometer is charged with a given volume of liquid and placed in a constant temperature bath to attain the desired temperature. The liquid is then raised into the upper bulb, normally by suction, and then allowed to flow back through the capillary into the lower bulb. The time is measured for the volume of fluid in the upper bulb to flow through the capillary. The viscosity of the fluid is then calculated using Equation 5.8, provided the flow time is sufficiently long to neglect the kinetic energy correction.

In order to obtain an accurate result, the hydrostatic head must be the same for the calibration and all subsequent measurements. This requires, for many viscometers, the volume of the liquid in the viscometer to be the same for the calibration and all viscosity measurements. If this condition is not satisfied, but is necessary, the viscometer constant must be corrected for the difference in volume between the calibration volume and the test volume (86).

In capillary viscometers of the "gravity-flow" type, the driving force is due to the hydrostatic pressure head of the fluid. Surface tension between a liquid meniscus and the surface of the glass bulb will alter the pressure head slightly if the upper and lower bulbs differ in diameter.

If the surface tension of the calibrating fluid differs greatly from that of the test fluid and if the bulb diameters above and below the capillary differ considerably, the surface tension correction may be significant for some viscometers. The surface tension error and its correction is discussed in detail by Barr (88).

Another source of error is the "alignment error". The hydrostatic pressure head will change as the orientation of the viscometer changes from the vertical position. Consequently, precautions must be taken to insure that the viscometer is aligned in the same vertical position each time the instrument is used. This "alignment error" is more serious for viscometers where the upper and lower bulbs do not lie on the same vertical axis (91).

One novel viscometer that minimizes many of the sources of error in viscometry was proposed by Ubbelohde (92,93,94). In the Ubbelohde viscometer, a tube connects the bulb beneath the capillary (the lower bulb) with the atmosphere so that the pressure above the liquid in the upper bulb is the same as the pressure in the lower bulb. This feature results in an air gap between the bottom of the capillary and the level of liquid in the lower bulb, thus forming a suspended level. Therefore, the liquid is induced to flow only down the walls of the bulb below the capillary in the form of a hollow hemisphere. The suspended level assures that the lower liquid level is automatically fixed and coincides with the

lower end of the capillary, so that it is not necessary to use a constant volume of liquid. For the same reason, the viscometer constant is nearly independent of temperature. The only temperature dependence would be a result of the expansion of the glass, which would change C only by about 0.1 percent for a 100°C. change in temperature. Perhaps even more important, the suspended level principle allows the surface tension at the upper bulb to be balanced by the surface tension of the hemispherical layer of liquid at the lower bulb. Therefore, surface tension corrections need not be applied when using a viscometer of the Ubbelohde design (94).

2. Experimental observations

Poiseuille, in 1847 (96), was perhaps the first to investigate viscosity behavior of electrolytes. Poiseuille found that addition of some salts to water increased the viscosity, while for others, the viscosity of the resulting solution was less than that of pure water. Arrhenius (97) observed that, in many cases, the difference between the viscosity of a solution and that of water was roughly proportional to the concentration for dilute solutions but increased more rapidly with increasing concentration at higher concentrations. Arrhenius proposed an empirical equation to represent the concentration dependence of the relative viscosity which may be written as,

$$\ln \eta_r = K_o\, c \,, \qquad (5.14)$$

where K_o is a constant for a given salt and temperature. The more accurate measurements of Grüneisen (98) and Applebey (99) showed that the Arrhenius equation was not obeyed by electrolytes, particularly in very dilute solution. Instead of the relative viscosity varying linearly with the concentration in very dilute solutions, plots of $(\eta_r - 1)/c$ against molar concentration, c, exhibited pronounced negative curvature in very dilute solutions, suggesting the relative viscosity of an electrolyte varies with some fractional power of the concentration in very dilute solution.

In 1929, reasoning from the Debye Hückel theory (1), Jones and Dole (100) suggested that the relative viscosity might be expected to vary as the square root of the molar concentration in very dilute solution. They proposed Equation 5.15 to represent the concentration dependence of the relative viscosity in dilute solution,

$$1/\eta_r = 1 - A\, c^{\frac{1}{2}} - B'\, c\,, \qquad (5.15)$$

where A and B' are constants for a given electrolyte and temperature. The value of A was predicted to be positive. Jones and Dole showed that the viscosity data for a number of dilute electrolytes were well represented by Equation 5.15. The values of A determined were positive and were of the order of magnitude of 0.01, the exact value depending upon the electrolyte and temperature under consideration. The values of B' were either positive or negative, depending on the electrolyte and temperature, and the absolute value of B' was of the

order of magnitude of 0.2. For non-electrolytes, A was always zero, and B' was positive.

For dilute solutions, Equation 5.15 may be rearranged to give,

$$\eta_r = 1 + A c^{\frac{1}{2}} + B c . \qquad (5.16)$$

Later investigations by Jones and co-workers (101,102,103) and by others (104,105) have established that Equation 5.16, generally called the Jones-Dole equation, accurately represents the viscosity data for many dilute electrolytes. In the past 30 years, the viscosity behavior of a large number of dilute electrolytes have been analyzed in terms of the Jones-Dole equation, and experimental values for A and B have been tabulated for a number of electrolytes at various temperatures (8,9,11,104).

The experimental values of A are positive in all known cases and are larger for higher valence type electrolytes. Furthermore, the values of A always increase with increasing temperature for the cases where accurate data are available at a number of temperatures.

The experimental values of B are highly specific with respect to the electrolyte and the temperature. In most cases, the value of B is positive, but a number of aqueous electrolytes have negative B coefficients and at moderate concentrations, have a viscosity less than that of pure water. The B coefficients have been shown to be an additive property of the individual ions (8,104), and additivity laws similar

to those written for the apparent molal volumes at infinite dilution may be written for the B coefficients. However, since the ionic B coefficients, B_i, are not directly measured, any division of the B coefficient of a given electrolyte into ionic contributions must be somewhat arbitrary, at least at the present time. This problem is similar to the problem encountered when attempting to divide the values of ϕ_v^o into ionic contributions. Based upon various theoretical considerations, a number of different methods of assigning values of B_i have been proposed (8,9,104). It is encouraging to note that the various methods of dividing the B coefficients into ionic contributions lead to values of B_i that do not depend greatly on the method used to accomplish the division. Some examples of B_i at 25°C., as given by Kaminsky (8), are: $B_{Ce^{+3}} = 0.577$, $B_{Li^+} = 0.150$, $B_{Cs^+} = -0.045$, $B_{Cl^-} = -0.007$.

In general, for a given ionic radius and temperature, values of B_i increase as the charge on the ion increases. For a given valence and temperature, the values of B_i generally decrease as the size of the ion increases, and large monovalent ions usually have negative B coefficients. One group of electrolytes that do not obey the preceding generalization are the tetraalkylammonium ions, where the B coefficients increase as the size of the ion increases. For ions with large positive B coefficients, the magnitude of the B coefficient generally decreases with increasing temperature, but for ions with negative B coefficients, the B coefficients

generally increase with increasing temperature and become positive at higher temperatures. Thus, the phenomena of "negative viscosity", or a value of the relative viscosity less than unity, usually disappears at higher temperatures.

At moderate to high concentrations the Jones-Dole equation is no longer obeyed, and the relative viscosity increases very rapidly as the concentration increases (106,107,108,109), suggesting some form of exponential dependence on the concentration. For those electrolytes having negative B coefficients, the relative viscosity increases with increasing concentration at higher concentrations, and eventually the phenomena of "negative viscosity" disappears. In the case of aqueous CsCl (8,106) at 25°C., the relative viscosity is less than unity only between about 0.01 molar and 3.5 molar and increases to a value of about 1.3 at 10 molar. In general, the same trends in relative viscosity with ion size, valence, and temperature as shown in moderate concentrations seem to be followed in concentrated solutions as well.

3. Theoretical

Shortly after Jones and Dole showed experimentally that the relative viscosity of an electrolyte varied as the square root of the concentration in very dilute solutions, Falkenhagen and co-workers (110,111) mathematically derived the theoretical limiting expression for the concentration dependence of the relative viscosity. Their derivation was based upon the "ionic atmosphere" concept advanced by Debye and

Hückel (1) and led to the equation,

$$\eta_r = 1 + A\, c^{\frac{1}{2}} , \qquad (5.17)$$

valid for extremely dilute solutions. The theoretical value for A is a positive constant which depends upon the electrolyte, temperature, and solvent under consideration. It has been shown to be in excellent agreement with experimental values of A for a large number of electrolytes at various temperatures (11). The general theoretical expression for A is a complex function of fundamental constants, temperature, properties of the solvent, and equivalent conductances of the ions. The general form for A was derived by Falkenhagen and Vernon (111) and is given by Harned and Owen (11). For the special case of a symmetrical electrolyte with equal ionic equivalent conductances, the theoretical expression for A may be written as,

$$A = \frac{b\, F|z|\, e\, 10^8}{480\pi\, \eta_o\, c\, \lambda^o} , \qquad (5.18)$$

where b was defined by Equation 2.2, F is Faraday's constant, c is the speed of light and λ^o is the equivalent conductance of the ion at infinite dilution. The other symbols have their usual meanings.

In attempts to theoretically calculate the B coefficient, Falkenhagen and Kelbg (112), and also Pitts (113), have extended the earlier theory of Falkenhagen and co-workers to include the effect of the a parameter. From these studies, it was concluded that the a parameter has only a minor effect

on the viscosity, and the major contributions to the B coefficient must result from other effects. In particular, the results of Pitts may be written in the form,

$$\eta_r = 1 + A\, c^{\frac{1}{2}} \,(1 + P(\kappa a)\,), \qquad (5.19)$$

where the function $P(\kappa a)$ is defined by,

$$P(x) = \frac{\frac{1}{2}x^2}{(1 + x)(1 + x + x^2/3)} \,. \qquad (5.20)$$

Retaining only terms of order $c^{3/2}$ and lower, Equation 5.19 may be written as,

$$\eta_r - 1 - A\, c^{\frac{1}{2}} = \tfrac{1}{2}A(b\, a)^2 c^{3/2}, \qquad (5.21)$$

where b is positive and is defined by Equation 2.2. Thus, the deviation from the simple limiting law, Equation 5.17, is predicted to be always positive and to vary as $c^{3/2}$, clearly not in agreement with experiment.

Aqueous solutions of large non-electrolyte molecules such as sucrose (11) have large positive B coefficients and therefore behave much like moderately concentrated electrolyte solutions containing highly charged ions. Consequently, it is of interest to briefly examine the theory of viscosity for solutions composed of large neutral solute particles. The increase in viscosity of a non-electrolyte solution with increasing concentration of large solute particles was explained by Einstein (114) as due to interference of the particles with the stream lines in the liquid. Treating the liquid as a viscous continuum containing a suspension of

rigid spherical obstructions at the surface of which the liquid is at rest, Einstein employed classical hydrodynamic methods and obtained a result valid at low concentrations which may be written as,

$$\eta_r = 1 + 2.5\ \bar{v}\ c\ , \qquad (5.22)$$

where $\bar{v}$ is the molar volume of the spherical obstruction and c is the molar concentration. If Equation 5.22 is assumed to apply for electrolytes at moderate concentrations where the effect of the term in $c^{\frac{1}{2}}$ is small, the B coefficient may be interpreted as, $B_i = 2.5\ \bar{v}_i$, where $\bar{v}_i$ is the "effective" molar volume of the hydrated ion. This interpretation seems to be reasonable for ions that may be expected to be highly hydrated (10,38), but it fails completely for large monovalent ions with negative B coefficients.

Vand (115) has extended Einsteins theory to higher concentrations giving,

$$\ln \eta_r = \frac{k_1\ \bar{v}\ c + r_2(k_2 - k_1)\ \bar{v}^2\ c^2 + \cdots}{1 - Q\ \bar{v}\ c}\ , \qquad (5.23)$$

where k_1 is the "shape factor" for single solute particles, k_2 is the "shape factor" for collision doublets, r_2 is the collision time constant, and Q is a hydrodynamic interaction constant. For rigid, non-solvated spheres without Brownian motion, the following values were derived by Vand: $k_1 = 2.5$; $k_2 = 3.175$; $r_2 = 4$; and $Q = 0.60937$. Vand has shown that his theory is in agreement with experiment (116,117).

Vand's theory may not be expected to apply rigorously to electrolytes. However, it is interesting and perhaps significant to note that a slight modification of Vand's equation in the form,

$$\ln \eta_r = A_3 \, c/(1 - Q'c) \, , \qquad (5.24)$$

where A_3 and Q' are adjustable parameters, gives an excellent representation of the viscosities of many strongly hydrated electrolyte solutions in the region of moderate to high concentration (10,38). This success of Equation 5.24 suggests that the major contribution to the viscosity of a "highly hydrated" electrolyte at moderate to high concentrations arises from the "obstruction effect" of large hydrated ions (10,38).

At the present time, no successful quantitative theory of the B coefficient has been presented. However, its qualitative interpretation has been discussed at great length by Kaminsky (8) and by Gurney (9). The B coefficient is generally regarded as being a measure of ion-solvent interactions and effectively independent of ion-ion interactions. Kaminsky divides the ion-solvent interactions into the following types of interactions:

1. The co-ordination of solvent molecules with the ion forming a relatively stable complex; this effect would cause an increase in viscosity.

2. The effect of the field of the ion in producing long-

range order of the solvent molecules; this effect would cause an increase in viscosity.

3. Destruction of the structure of water by the ionic field; this effect would cause a decrease in viscosity.

4. Steric effects.

It seems reasonable to expect that the "co-ordination effect" would cause an increase in viscosity similar to that expressed by Equation 5.22, the Einstein equation. The "co-ordination effect" and the "long-range ordering effect" have their greatest effect for ions of high surface charge density and are the dominant effects for this class of ions (8). Consequently, the B coefficients of highly charged ions and of small ions are positive, and the B coefficient increases as the charge on the ion increases and decreases as the size of the ion increases. For large monovalent ions, the dominant effect is a destruction of the water structure (8). Therefore, the B coefficient of large monovalent ions are negative in aqueous media.

As the temperature increases, it is reasonable to assume that the water structure is broken down due to thermal agitation. The viscosity changes which are due to structure breaking of the ions therefore diminishes in importance relative to the effect of thermal agitation (8). Therefore, the B coefficients of "structure breaking" ions increase with increasing temperature. According to Kaminsky (8), the effect

of long-range ordering, which is important for ions of high surface charge density, decreases at higher temperatures because of increasing thermal agitation. Consequently, the B coefficients for this class of ions decrease as the temperature increases.

The B coefficients for the ammonium ion are very nearly zero over a considerable temperature range, and Kaminsky interprets this behavior in terms of special steric effects.

Gurney's discussion of the B coefficient differs slightly from that of Kaminsky in point of view but seems to be equivalent. Gurney shows that the B coefficients are strongly correlated with the partial molal entropies. If the ionic B coefficients for a number of monoatomic ions are plotted against the corresponding ionic partial molal entropies (based on $\bar{S}_{H^+} = -5.5$ eu.) a straight line with a negative slope results. Thus, according to Gurney, a large positive B coefficient corresponds to a high degree of order in the solution and therefore to a small ionic partial molal entropy.

According to Gurney's interpretation, when an ion is introduced into water, the order due to the water structure is partially destroyed, which raises the entropy of the system. However, if the ion becomes appreciably hydrated, the ordering effect of hydration lowers the entropy. For strongly hydrated ions, the net effect lowers the entropy of the system, and a positive B coefficient results. For weakly hydrated ions,

the net effect raises the entropy of the system, and a negative B coefficient results. The characteristic trends shown by the B coefficients are then explained by examining the effects of ionic charge, ion size, and temperature on the entropy of the water surrounding the ion, using arguments similar to those employed by Kaminsky.

The tetraalkylammonium ions exhibit a somewhat anomalous behavior. For these ions, the B coefficients are positive and increase as the size of the ion increases, becoming quite large. Nightingale (105) interprets this behavior by assuming the tetraalkylammonium ions increase the viscosity of water by increasing the "ice-like" structure of water around the ions.

In summary, the B coefficient of an ion in aqueous solution is generally attributed to the effects of ion-solvent interactions, and ions are classified as either "structure-formers", giving positive ionic B coefficients, or "structure-breakers", giving negative B coefficients. Ions with a high surface charge density may be expected to be "structure-formers", due to strong hydration effects. Large monovalent ions may generally be expected to be "structure-breakers" because of the lack of appreciable hydration to compensate for the partial destruction of the water structure.

B. Experimental

1. Method

The "gravity-flow" capillary method was used to measure the viscosities determined in this research. The viscometers

used were Cannon-Ubbelohde Filter Stick viscometers, modified to eliminate solvent evaporation, and were obtained from the Cannon Instrument Company. These viscometers were of the suspended-level Ubbelohde design and have all the advantages of the Ubbelohde viscometer, but are more durable and are designed to allow use of Equation 5.8 for flow times in excess of about 300 seconds. In order to use flow times between 5 minutes and 30 minutes, four viscometers, size 25, having viscometer constants of about 2×10^{-3} and two viscometers, size 75, having viscometer constants of about 8×10^{-3} were purchased. The size 25 viscometers were used for the rare-earth chloride solutions below about 1.5 molal, and the size 75 viscometers were used for the more concentrated solutions. Equation 5.8 was then used to determine the viscosities.

2. Description of apparatus

Two seven jewel Sargent stopwatches, readable to $\pm$ 0.02 second, were used to measure the flow times. These stopwatches were calibrated against an electronic timer to within $\pm$ 0.01 percent. The electronic timer had previously been calibrated against the National Bureau of Standards station WWV, and found to be accurate to better than $\pm$ 0.01 second.

Schematic diagrams of the apparatus used for measuring the viscosities are given in Figures 7, 8, 9, and 10. Reference to these figures will be designated (i-X), where i refers to the figure and X to the alphabetically labelled part.

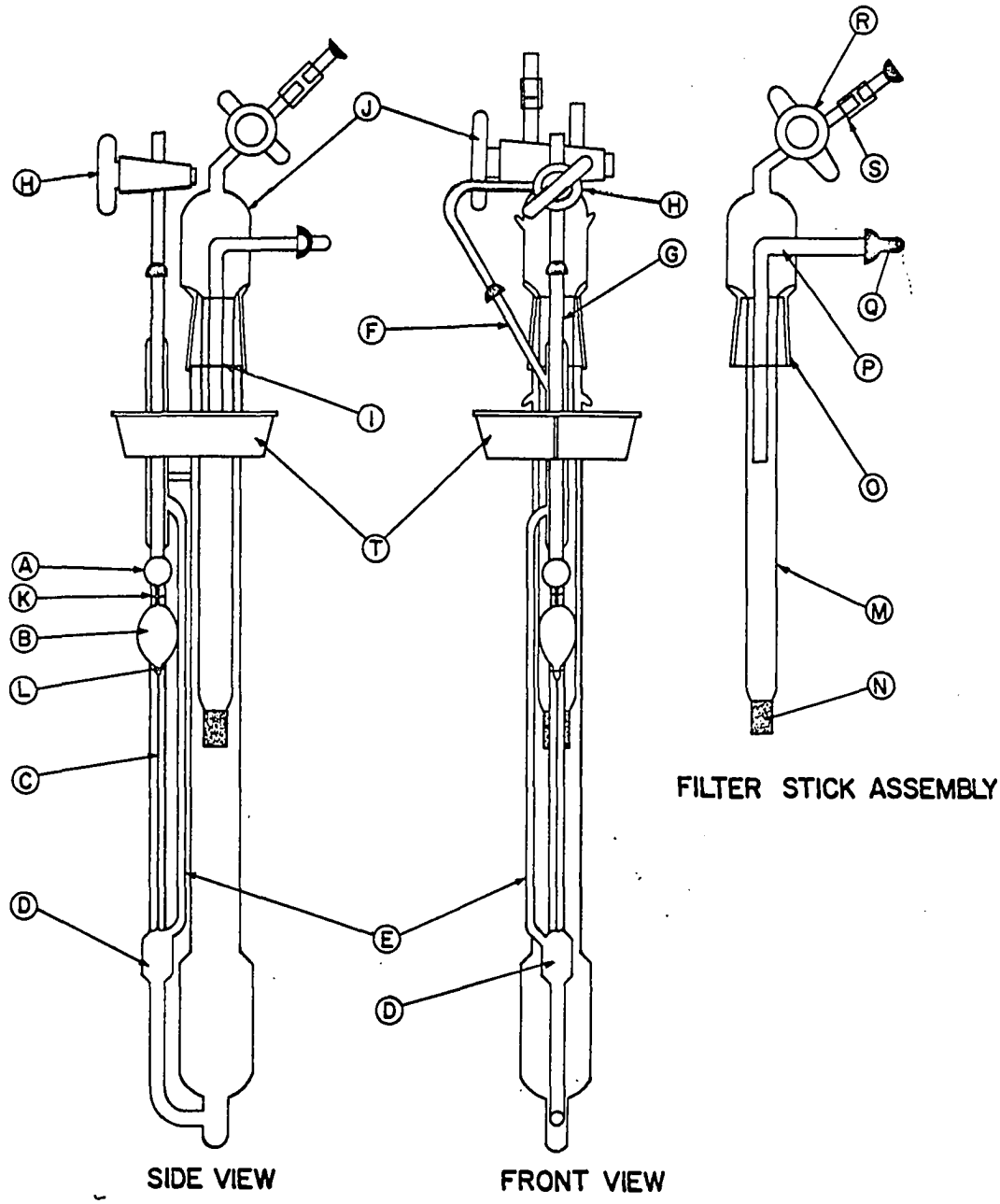

Figure 7. Modified Cannon-Ubbelohde Filter Stick viscometer

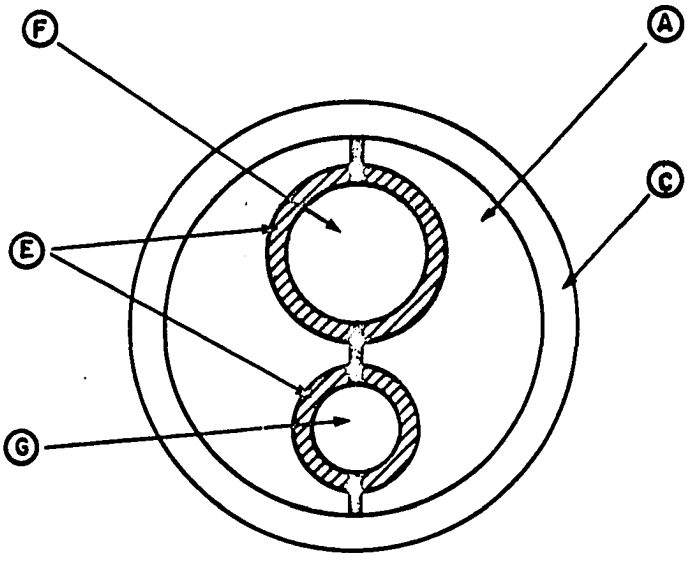

TOP VIEW

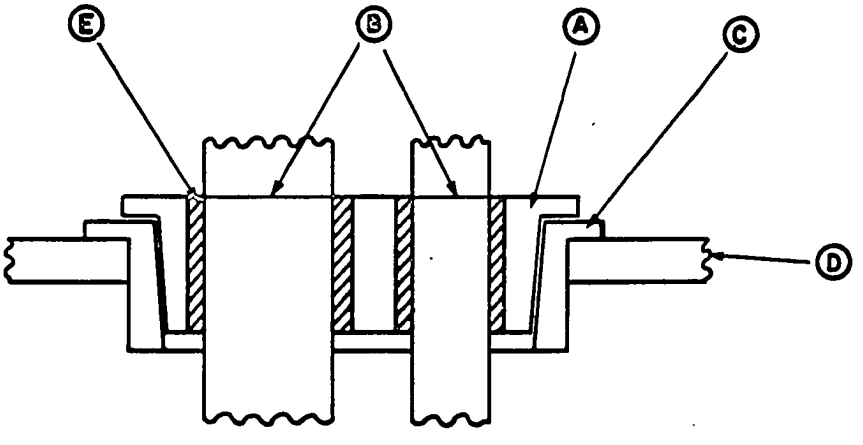

CROSS SECTION SIDE VIEW

Figure 8. Viscometer holders

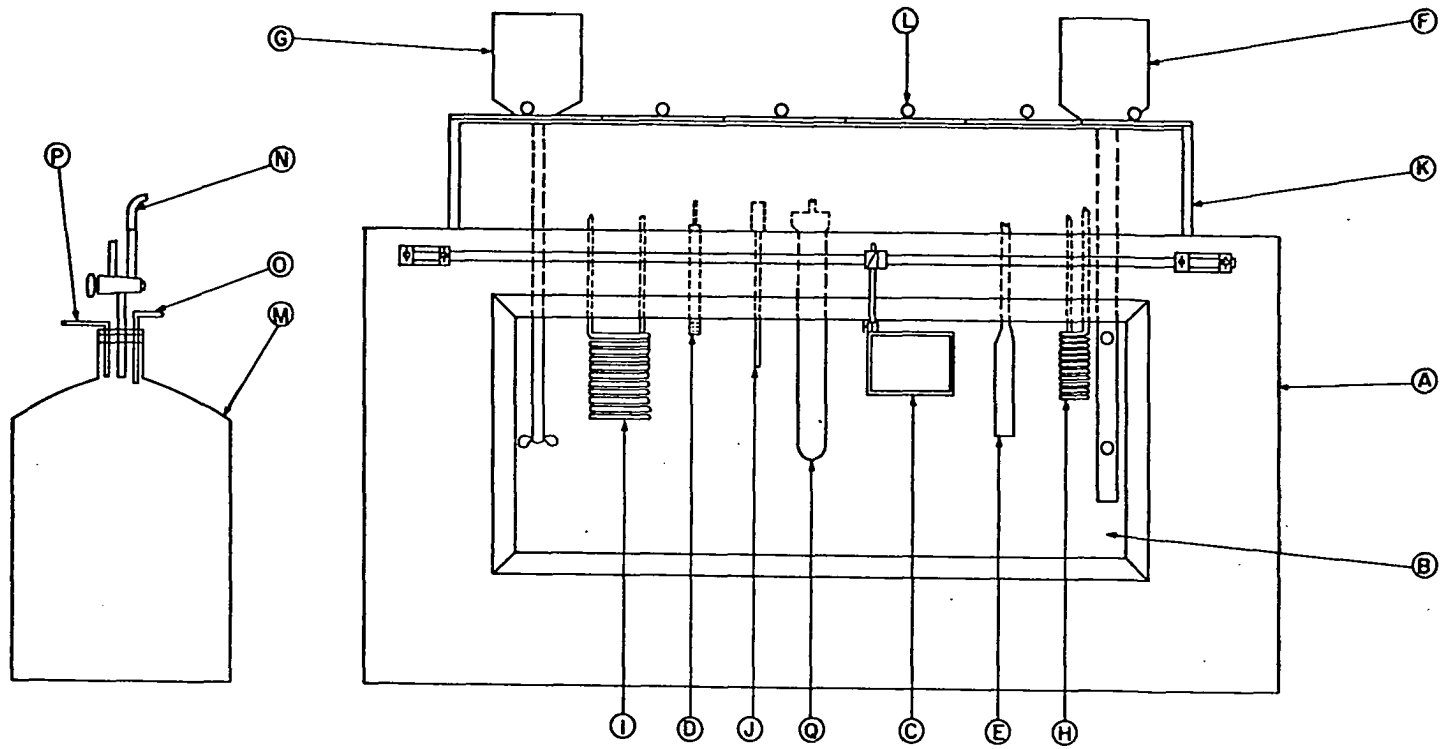

Figure 9. Constant temperature bath and accessories for viscosity measurements

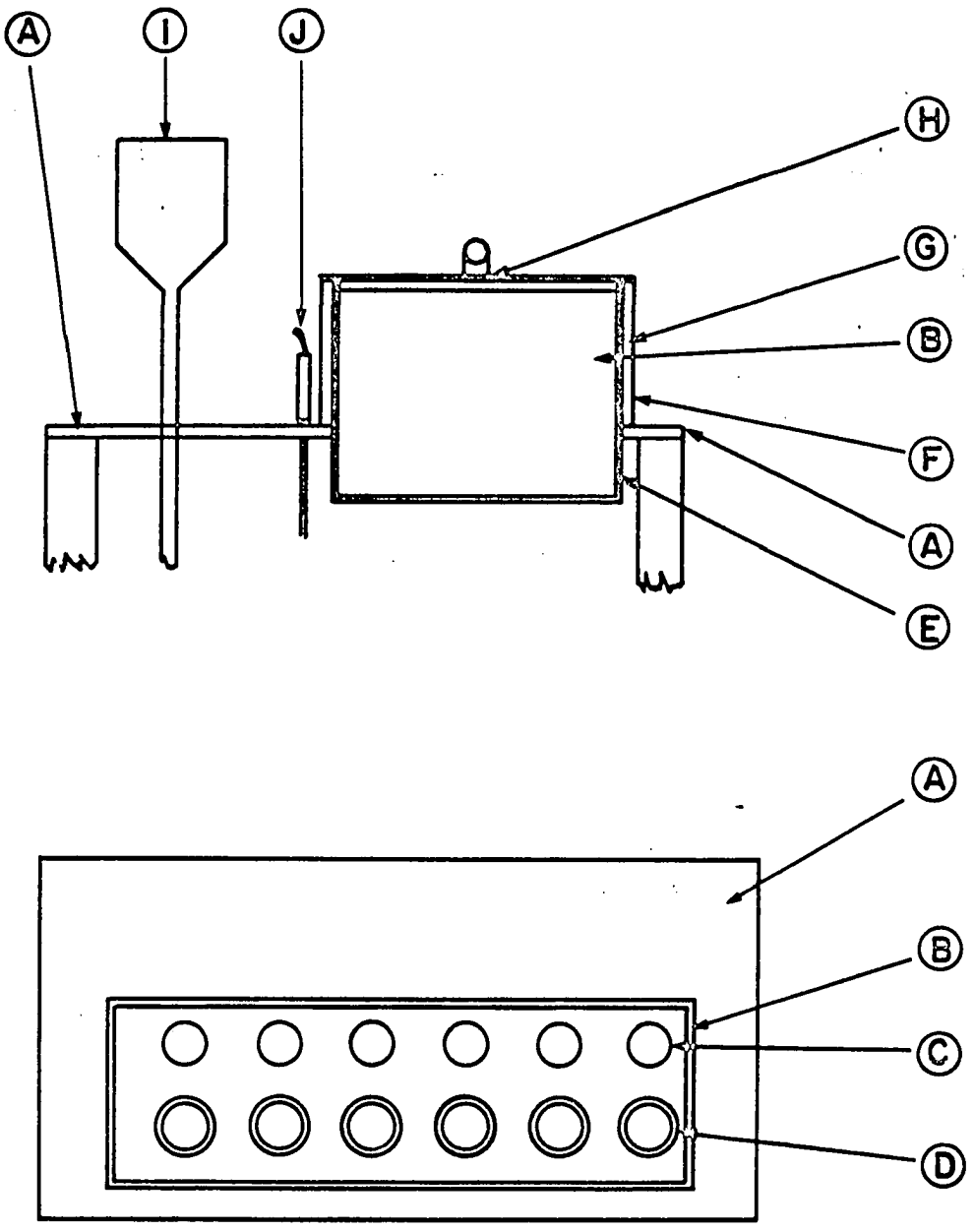

Figure 10. Constant temperature bath-viscometer "box"

Schematic diagrams of the modified Cannon-Ubbelohde Filter Stick viscometer used in this research are shown in Figure 7. In operation, liquid in the viscometer is forced up through the capillary (7-C), filling the upper bulb (7-B) and part of the overflow bulb (7-A). The liquid is then allowed to flow back through the capillary, and the efflux time is measured as the time required for the liquid to flow between timing mark (7-K) and timing mark (7-L). The essential feature of a suspended level viscometer is the tube (7-E), which connects the lower bulb (7-D) with either the atmosphere or the overflow bulb (7-A). This feature results in an air gap between the bottom of the capillary and the level of fluid in bulb (7-D), thus forming a suspended level. The liquid then flows down the walls of the lower bulb (7-D). To eliminate solvent evaporation, a T-stopcock (7-H) was fitted to tube (7-F) and tube (7-G) with ball joints. This stopcock allowed the lower bulb to be connected with the overflow bulb, resulting in a suspended level yet sealing the system from the atmosphere.

The filter stick of the original Cannon-Ubbelohde Filter Stick viscometer was modified slightly to allow the system to be sealed off from the atmosphere. The resulting filter stick assembly (7-J) consisted of a glass tube (7-M), at the end of which was a sintered glass filter (7-N). The upper end of this tube was attached to a female 24/25 standard

taper (7-O), which fitted over the male 24/25 standard taper (7-I) on the viscometer itself. A glass tube (7-P), placed inside of tube (7-M), was sealed into the side of the filter stick assembly. The liquid was added to the viscometer through this tube, which could then be sealed off from the atmosphere by a cap (7-Q) constructed from a female ball joint. A "two-way" stopcock (7-R) was sealed into the top of the filter stick assembly to enable the system to be sealed off from the atmosphere. One of the tubes (7-S) leading from this stopcock was attached to a female ball joint with Tygon tubing. The purpose of this feature will be described later. The inner portion of the viscometer holder (7-T) is also shown in Figure 7.

The viscometer holder, made from plexiglass, is shown in actual size by Figure 8. The inner portion of the viscometer holder (7-T)(8-A) was permanently attached to the two tubes of the viscometer (8-B), while the outer portion (8-C)(10-D) was permanently attached to the bottom of the viscometer "box" (8-D). The viscometer "box" formed part of the top of the constant temperature bath and will be described later. The inner portion of the viscometer holder (7-T)(8-A) was fashioned from 3/4 inch plexiglass to the form of a plug with tapered sides. Two holes (8-F)(8-G) were then drilled in the plug, and the plug was cut into two equal halves. The holes were lined with rubber (8-E), fixed in place with glue. The two halves were then glued to the viscometer as shown in

Figures 7 and 8. The outer portion of the viscometer holder was fashioned from 3/4 inch plexiglass to the form of a short cylinder, with the interior walls tapered to match the taper of the inner portion of the viscometer holder. The outer portion of the viscometer holder was then glued to the bottom of the viscometer "box". The viscometer holder allowed the viscometer to be placed in the same vertical alignment each time the viscometer was placed into the water bath.

The main constant temperature bath (9-A) consisted of an insulated wooden box, lined with galvanized iron, with a plexiglass window (9-B) in the front of the bath. The bath was about 42 inches long, 24 inches wide, and 21 inches deep. A magnifying glass (9-C) used to observe the viscometers was attached to the bath in such a way as to allow it to be adjusted to any desired position. A thermistor (9-D) and a 250W knife heater (9-E) were used in conjunction with a Sargent Model S Thermonitor to control the temperature of the main bath. Stirring was provided by two stirrers (9-F)(9-G) situated at opposite ends of the bath. Auxiliary heaters, not shown in the figures, were placed at the back of the bath for use at higher temperatures. Cooling water for the system was maintained at a temperature about 3°C. lower than the temperature of the main bath by an auxiliary water bath and was pumped through cooling coils (9-H)(9-I) by a centrifugal pump. When the constant temperature bath was being maintained at 5°C. during the calibration of the viscometers, the tempera-

ture of the auxiliary bath was maintained at 0°C. by a Blue-M Constant Flow portable cooling unit. The temperature in the main constant temperature bath was measured using a Leeds and Northrup Model 8160-B platinum resistance thermometer (9-J) in conjunction with a Honeywell Model 1551 Mueller Bridge. Temperature control in the main bath was better than ± 0.01 °C., and the measured temperature was estimated to be accurate to within about ± 0.01°C. A 40W showcase light (9-Q) was used to illuminate the interior of the bath.

Prior to measuring the flow time for a given liquid, the liquid must be forced up through the capillary tube into the upper reservoir bulb. For this purpose, a pressure of about 100 mm. Hg was maintained in a "ballast tank" (9-M), which could be released through the stopcock tube (9-N) to force the liquid in the viscometer into the upper reservoir bulb. The air pressure in the "ballast tank" was raised to the desired pressure by passing compressed air from an air line through air purifiers and into the "ballast tank" through the tube (9-P). The pressure in the tank was read from a manometer which was connected to the tank by tube (9-O).

Part of the top of the main constant temperature bath consisted of a plexiglass "box" (9-K)(10-B) having removable lids (9-L)(10-H) that provided access to the interior of the "box". This "box" is shown in more detail in Figure 10, where the top diagram represents a cross-section side view, and the bottom diagram represents a top view. Most of the bath top

was covered with 3/4 inch plywood (10-A), but near the front of the bath a large rectangular hole was cut in the plywood. The "box" fitted into this hole. The plexiglass "box" was constructed from 1/4 inch plexiglass plates (10-E) and 1/16 inch plexiglass plates (10-F) with an air gap (10-G) between the plates for insulation. Six holes to accomodate the outer portions of the viscometer holders (8-C)(10-D) were drilled in the bottom of the "box", and the outer portions of the viscometer holders were glued to the bottom of the "box". Six other holes (10-C) were drilled in the bottom of the "box" so small flasks of the solution could be brought to the bath temperature before the solution was introduced into the viscometer. This feature was included for viscosity measurements at temperatures other than 25°C., and in this research was used only for the calibrations. The purpose of designing this insulated "box", in which the viscometers were enclosed, was to minimize temperature gradients between the tops of the viscometers and the remaining portions in the water bath. Although this feature was not necessary when working at 25°C., it was included in the apparatus so possible future studies of the viscosity as a function of temperature could make use of the present apparatus. In Figure 10, a stirrer (10-I) and the platinum resistance thermometer (10-J) are also shown in the top diagram.

3. Calibration

The size 25 viscometers were calibrated using conductivity water at 20°C. as the calibration fluid. The efflux times were in excess of 600 seconds so no kinetic energy correction was necessary. The absolute viscosity of water at 20°C. is 1.002 centipoise (89), and the density of water at 20°C. is 0.99823 g./ml. (73), so Equation 5.8 may be rearrange to give

$$C = 1.0038/t_o \ , \qquad (5.25)$$

where t_o is the efflux time, in seconds, of water at 20°C. The values of C for viscometers Z62, Z63, Z64, and Z65 were 1.4813×10^{-3}, 1.4901×10^{-3}, 1.5353×10^{-3}, and 1.5948×10^{-3}, respectively. For each viscometer, the value of C was the result of at least four independent determinations, the viscometer being cleaned after each determination. For each determination, the efflux time was measured five times, and the mean value was used to calculate C for that determination. The calibration data for the size 25 viscometers are given in more detail in Table 10.

The viscosities of water at 5°C., 25°C., and 45°C. were determined using the size 25 viscometers and Equation 5.8. The densities of water at these temperatures were taken from the compilation of Dorsey (73). The viscosities obtained in this research are compared, in Table 11, with the corresponding data given by Hardy and Cottington (118). With the exception of the viscosity at 45°C., the agreement is excellent.

Table 10. Calibration data for size 25 viscometers

Determination	$Cx10^3$	Determination	$Cx10^3$
viscometer Z62		viscometer Z64	
1	1.4828	1	1.5345
2	1.4804	2	1.5349
3	1.4805	3	1.5350
4	1.4813	4	1.5368
		5	1.5365
mean	1.4813	6	1.5333
		7	1.5362
		mean	1.5353
viscometer Z63		viscometer Z65	
1	1.4899	1	1.5948
2	1.4909	2	1.5945
3	1.4896	3	1.5936
4	1.4904	4	1.5962
5	1.4898	5	1.5940
mean	1.4901	mean	1.5948

Table 11. Viscosity of water at 5°C., 25°C., and 45°C., in centipoise

Source of data \ t °C.	5	25	45
Viscometer Z62	1.5155	0.8899	0.5952
Viscometer Z63	1.5178	0.8909	0.5954
Viscometer Z64	1.5197	0.8901	0.5949
Viscometer Z65	1.5182	0.8900	0.5952
Mean of viscometers Z62, Z63, Z64, and Z65	1.5179	0.8903	0.5952
Hardy and Cottington	1.5184	0.8899	0.5969

However, the uncertainty in the data of Hardy and Cottington is given as ± 0.25 percent, so even for the value at 45°C., the agreement is with experimental error.

The size 75 viscometers were calibrated using conductivity water at 5°C., 20°C., 25°C., and 45°C., using Equation 5.12. Equation 5.12 may be rearranged to give

$$\eta/(\rho t) \equiv C^* = C - E/t^3 , \qquad (5.26)$$

where t is the efflux time of water for a particular viscometer and temperature. Therefore, measurement of t at various temperatures gave C* as a linear function of $1/t^3$. The values of C* for viscometers Z111 and Z112 are given in Table 12 along with the corresponding values of t. For this calibration, the viscosities of water at 5°C., 20°C., 25°C., and 45°C. were taken as 1.5179, 1.002, 0.8903, and 0.5952 centipoise, respectively. Except for the standard value of 1.002 centipoise, these values are the viscosities determined in this research and are given in the fifth row in Table 11.

Table 12. Calibration data for size 75 viscometers

t°C.	$C^* \times 10^3$	t(sec.)	t°C.	$C^* \times 10^3$	t(sec.)
	viscometer Z111			viscometer Z112	
5	6.742	225.15	5	6.164	246.27
20	6.736	149.02	20	6.161	162.93
25	6.741	132.46	25	6.155	145.06
45	6.724	89.40	45	6.139	97.91

Using the data in Table 12, the constants, C and E, of Equation 5.26 were determined by the method of least squares. For viscometer Z111, C is 6.741×10^{-3}, and E is 12. For viscometer Z112, C is 6.166×10^{-3}, and E is 25. The values of E calculated from Equation 5.13 were about 10 for both viscometers. Considering the approximate nature of Equation 5.13 and the large experimental error in E, the agreement is satisfactory.

For each viscometer, the efflux time for water at 25°C. was checked periodically throughout the course of this research and found to remain constant.

As a further check on the accuracy of the method used, the relative viscosities of several aqueous electrolytes were determined and compared with the corresponding literature values. The results of these comparisons are summarized in Table 13. The literature references are given in parenthesis in the first column. Since a concentration error of only $\pm$ 0.05 percent could account for the difference between the relative viscosities determined in this research and the corresponding literature values, the agreement is quite satisfactory.

4. Experimental procedure

Prior to each viscosity determination, each viscometer was filled with filtered chromic acid cleaning solution, placed in a water bath maintained at 55°C., and allowed to remain in this water bath for about two hours. The viscom-

eters were then thoroughly rinsed with filtered tap distilled water and conductivity water and allowed to soak in filtered conductivity water for at least two hours. Next, the viscometers were drained, rinsed with filtered acetone, and dried with a stream of filtered nitrogen or helium. When thoroughly dried, the viscometers were charged with about 10 ml. of solution through tube (7-P) shown in Figure 7. The viscometers were then placed in the constant temperature bath.

Table 13. Relative viscosities at 25°C. determined in this research compared to the literature values

Salt(ref.)	Molality	Density	η_r (this research)	η_r (literature)
K_2CrO_4(103)	2.910	1.3443	1.757	1.758
$LiNO_3$(108)	12.90	1.341	4.247	4.254
LiCl(106)	19.19	1.289	15.78	15.73

After thermal equilibrium had been attained (about ½ hour), the tube (7-S) shown in Figure 7 was connected to the "ballast tank" (9-M) shown in Figure 9, and the solution was forced up through the capillary tube until the overflow bulb (7-A) was partially filled. During this operation, the T-stopcock (7-H) was adjusted so that tube (7-F) was sealed and tube (7-G) was open to the atmosphere. The pressure in the viscometer was then released by adjusting stopcock (7-R), and the T-stopcock plug was rotated 360°, thus allowing the suspended level to be formed. The T-stopcock was then adjusted

so tube (7-F) and tube (7-G) were connected, and the viscometer was sealed off from the atmosphere. The time was then measured for the liquid to flow between timing mark (7-K) and timing mark (7-L). The efflux time was measured at least twice for each viscosity determination and the viscosity was calculated using Equation 5.8. The densities of the rare-earth chloride solutions were interpolated from the data of Saeger and Spedding (6) and that of Spedding, Brown, and Gray[1]. The relative viscosity was calculated using 0.8903 centipoise for the viscosity of water at 25°C., as given in Table 11. Two independent relative viscosity determinations, using different viscometers, were made for each solution, and the mean of the two results was taken as the relative viscosity of that solution.

5. Treatment of data

The viscosity B coefficients are usually obtained by evaluating both A and B from the experimental data. However, the theoretical expression for A has been well verified for a number of electrolytes and temperatures (11). In particular, the relative viscosity data of Jones and Stauffer (102) for $LaCl_3$ and that of Kaminsky (119) for $CeCl_3$ show that the Jones-Dole equation, Equation 5.16, is obeyed for these salts up to 0.1 molar and that the experimental values of A are in

[1]Spedding, F. H., Brown, M., and Gray, K., Ames Laboratory of the A.E.C., Ames, Iowa. Apparent molal volumes of some aqueous rare-earth chloride solutions. Private communication. 1964.

excellent agreement with the theoretical values. Consequently, it was felt that more accurate B coefficients could be obtained from the relative viscosity data obtained in this research if the values of A were calculated from theory, and only the B coefficients were determined from the data. The B coefficients obtained in this research were calculated using the equations,

$$B_k = \frac{(\eta_r)_k - A\, c_k^{\frac{1}{2}} - 1}{c_k} \qquad (5.27)$$

and

$$B = \left(\sum_k w_k B_k \right) / \left(\sum_k w_k \right) , \qquad (5.28)$$

where B_k is the B coefficient calculated from the relative viscosity of a given solution, $(\eta_r)_k$, of molar concentration, c_k. The B coefficient, B , for a given rare-earth chloride was taken to be the weighted mean of the B_k values for each of the solutions studied having a concentration less than about 0.1 molar, as indicated by Equation 5.28. The weighting factor, w_k, was taken to be the inverse square of the probable error in B_k, calculated assuming a probable error in $(\eta_r)_k$ of $\pm$ 0.05 percent. The theoretical values for A were calculated using the conductivity data given by Spedding and Atkinson (3) and the equations and tables given by Harned and Owen (11). The relative viscosity data reported in this thesis are given at the experimental molalities, m. To calculate B_k from Equation 5.27, the molality was converted to the molar concentration, c, using the equation,

$$c = \rho m/(1 + 10^{-3} m M_2) , \qquad (5.29)$$

where ρ is the density of the solution, and M_2 is the molecular weight of the solute.

One of the objectives of this research was to compare the viscosities of rare-earth chloride solutions at "iso-molalities". For this purpose, some form of empirical equation representing the experimental relative viscosities as a function of molality was needed. The relative viscosities of the rare-earth chloride solutions studied in this research changed by roughly a factor of 20 over the concentration range studied. Furthermore, the relative viscosities were not a simple function of molality. Therefore, a simple representation of the relative viscosities in terms of a power series in m or $m^{\frac{1}{2}}$ containing a reasonable number of adjustable parameters was not possible.

The assumptions made by Vand in deriving Equation 5.23 and the assumptions made by Pitts in deriving Equation 5.19 are certainly not valid for concentrated solutions of electrolytes. However, the exponential form of the Vand equation predicts a rapid change in viscosity with concentration in concentrated solutions, which was observed for the rare-earth chloride solutions. Also, while the Pitts equation did not succeed in theoretically calculating the B coefficient of the Jones-Dole equation, which is normally attributed to ion-solvent interactions, the Pitts equation might be expected to

give a good approximation for the electrical contribution to the viscosity in dilute solutions. Therefore, it seemed likely that a crude approximation to the relative viscosity might be given by a combination of Equations 5.19 and 5.23 in the form,

$$\eta_r \cong Am^{\frac{1}{2}}(1 + P(4.831m^{\frac{1}{2}})\ ) + \exp\left(\frac{2.5\ \bar{v}\ m}{1 - 0.60937\ \bar{v}\ m}\right), \quad (5.30)$$

where the function P(x) is defined by Equation 5.20, and as discussed earlier, $\bar{v}$ is the molar volume of the spherical obstructions. In the case of a solution containing large uncharged solute particles, $\bar{v}$ represents the molar volume of the solute in solution. Equation 5.30 states that the relative viscosity of an electrolyte solution is approximately given by the sum of the "electrical contribution" calculated by Pitts and the "obstruction effect" calculated by Vand for the simplest case, where the molality, m, has replaced the molar concentration, c, and the higher order terms in the numerator of Equation 5.23 have been omitted. As mentioned earlier, the argument of the Pitts function, P(x), is κa, where a is the a parameter of the Debye-Hückel theory, and κ was defined by Equation 2.2. The numerical factor, 4.831, appearing in the argument of the Pitts function, is a result of assuming an a parameter of 6 Å for an aqueous 3-1 salt at 25°C. and replacing the molar concentration by the molality.

If we define the "electrical contribution" by,

$$El = Am^{\frac{1}{2}}(1 + P(4.831m^{\frac{1}{2}})\ ), \quad (5.31)$$

Equation 5.30 may be rearranged to give,

$$\left\{ m\left[1/\ln(\eta_r - El) + 0.24375\right] \right\}^{-1} \cong 2.5\ \bar{v} \ . \qquad (5.32)$$

For convenience, the left hand side of Equation 5.32 will be defined by,

$$Y \equiv \left\{ m\left[1/\ln(\eta_r - El) + 0.24375\right] \right\}^{-1} \ . \qquad (5.32a)$$

If Equation 5.30 were exact, values of the defined quantity, Y, which may be calculated from the experimental data and the theoretical value of A, would be independent of molality, since according to the Vand theory $\bar{v}$ should be a constant. Actually, the values of Y calculated from the experimental data are about 0.5 and change by about 20 percent over the concentration range studied. However, it was possible to accurately express the concentration dependence of Y by empirical power series in molality of the form,

$$Y = b_o + b_1 m + b_2 m^2 + b_3 m^3 \ , \qquad (5.33)$$

where the coefficients were determined by the method of least squares. The "experimental" values of Y were weighted using the inverse of the square of the probable error in Y as the weighting factor. The probable error in Y was computed by an application of the law of propagation of precision indexes, as expressed by Equation 4.36, assuming the probable error in both the molality and the relative viscosity were $\pm$ 0.05 percent.

Using the definitions of Y and El given by Equations 5.31 and 5.32a, the relative viscosity may be written empirically as,

$$\eta_r = Am^{\frac{1}{2}}(1 + P(4.831m^{\frac{1}{2}})) + \exp\left(\frac{Y\,m}{1 - 0.24375\,Y\,m}\right), \quad (5.34)$$

From Equation 5.33, Y may be conveniently written as,

$$Y = B_0(1 + B_1m + B_2m^2 + B_3m^3). \quad (5.35)$$

In all cases, Equation 5.34 with Y given by Equation 5.35 represents the experimental relative viscosity data determined in this research within the limits of experimental error over the entire concentration range studied. For $DyCl_3$, the experimental data is best represented if B_3 is zero. For the other salts studied, four adjustable parameters were needed to give the best representation of the data. Numerical values of the function, P(x), defined by Equation 5.20, are given in Table 14 for various values of the argument, x.

Table 14. Numerical values of P(x), defined by Equation 5.20

x	P(x)	x	P(x)
0.0	0.0	1.4	0.1337
0.1	0.0041	1.6	0.1426
0.2	0.0137	1.8	0.1491
0.3	0.0260	2.0	0.1538
0.4	0.0393	2.5	0.1599
0.5	0.0526	3.0	0.1607
0.6	0.0654	4.0	0.1548
0.7	0.0774	5.0	0.1453
0.8	0.0883	6.0	0.1353
0.9	0.0982	7.0	0.1259
1.0	0.1071	8.0	0.1172
1.2	0.1221	9.0	0.1095
1.4	0.1337	10.0	0.1025

6. Experimental results

The relative viscosities of aqueous solutions of $LaCl_3$, $NdCl_3$, $SmCl_3$, $TbCl_3$, $DyCl_3$, $HoCl_3$, and $ErCl_3$ were determined at 25°C. over a concentration range of about 0.05 molal to saturation at 25°C. The relative viscosities of three dilute $PrCl_3$ solutions were determined to allow the B coefficient for $PrCl_3$ to be calculated. The experimental relative viscosities, η_r, determined during the course of this investigation are given in Table 15. The corresponding concentrations are expressed in terms of molality, m, and the corresponding densities, d, are listed. The quantity, Δ, represents the relative difference, $\left[(\eta_r)\text{experimental} - (\eta_r)\text{calculated}\right] \times 10^2/(\eta_r)\text{calculated}$, where except for $PrCl_3$, the calculated value refers to the relative viscosity calculated from Equations 5.34 and 5.35 with the appropriate parameters. For $PrCl_3$, the calculated relative viscosities were obtained from the Jones-Dole equation for this salt.

Jones and Stauffer (102) determined relative viscosities of aqueous $LaCl_3$ solutions up to a maximum concentration of about one molar. Their results are somewhat higher than the relative viscosities determined in this research, and the deviations become larger as the concentration increases, becoming about 0.35 percent at one molar. These deviations are most likely due to the fact that the $LaCl_3$ solutions investigated in this research were at the equivalence pH,

whereas those investigated by Jones and Stauffer were at a pH of about 6 and might be expected to contain certain basic species, such as hydrolysis products, oxychloride, and colloidal oxide, therefore having higher viscosities.

The experimental relative viscosity data for $LaCl_3$ are shown in Figure 11 as a function of molality. The data for the other salts in Table 15 show somewhat similar behavior, although significant differences do exist between the various rare-earth chlorides studied. However, these differences are not well illustrated by small scale relative viscosity-molality graphs like Figure 11.

The relative viscosity data in Table 15 were treated according to the procedure described earlier. The B coefficients, the values of A, and the parameters for the empirical viscosity equation,

$$\eta_r = Am^{\frac{1}{2}}(1 + P(4.831m^{\frac{1}{2}})) + \exp\left(\frac{Y\,m}{1 - 0.24375\,Y\,m}\right), \quad (5.34)$$

where

$$Y = B_0(1 + B_1m + B_2m^2 + B_3m^3), \quad (5.35)$$

are given in Table 16 for each of the salts studied. As previously mentioned, for each salt the appropriate value of A appearing in the Jones-Dole equation and in Equation 5.34 was calculated from theory. The limited amount of data for $PrCl_3$ were not analyzed in terms of Equations 5.34 and 5.35, so only the theoretical value of A and the B coefficient are given for this salt. Using Equations 5.34 and 5.35 and the appropriate

parameters, relative viscosities at 0.2 molal intervals from 0.2 to 3.6 molal were calculated for each of the rare-earth chlorides studied. The results of these calculations are given in Table 17.

It was previously mentioned that the differences in viscosity between the rare-earth chlorides could not be illustrated by a small scale relative viscosity-molality graph. For the purpose of illustrating these differences on small scale graphs, the ratio of the viscosity of a rare-earth chloride solution to the viscosity of a $LaCl_3$ solution of the same molality, $(\eta)_{RCl_3}/(\eta)_{LaCl_3}$, was calculated. Values of this ratio are given in Table 18 at selected even molalities and are plotted as a function of molality in Figure 12.

Viscosity B coefficients, taken from Table 16, are plotted as a function of ionic radius of the rare-earth ion in Figure 13. The ionic radii are those of Pauling (79). The size of the circles indicate the estimated probable error in the B coefficient.

Figures 14, 15, and 16 show values of the ratio, $(\eta)_{RCl_3}/(\eta)_{LaCl_3}$, at selected molalities plotted as a function of ionic radius of the rare-earth ion.

7. Errors

From the estimated probable error of about $\pm$ 0.04 percent in the efflux time, the estimated probable error of about $\pm$ 0.05 percent in the viscometer constant, C, and the fact that each value of the relative viscosity given in Table 15

Table 15. Experimental relative viscosities at 25°C.

m	d	η_r	Δ%	m	d	η_r	Δ%
	$LaCl_3$				$NdCl_3$		
0.01104	0.9996	1.0085	-0.04	0.05293	1.0096	1.0361	+0.04
0.01606	1.0007	1.0108	-0.15	0.06613	1.0126	1.0449	+0.11
0.04665	1.0076	1.0324	+0.08	0.09959	1.0204	1.0636	-0.08
0.08038	1.0151	1.0523	0.00	0.25320	1.0556	1.1639	+0.13
0.09821	1.0191	1.0626	-0.06	0.49269	1.1094	1.3342	-0.02
0.10213	1.0199	1.0658	+0.02	0.64067	1.1420	1.4541	-0.13
0.20139	1.0418	1.1286	+0.07	1.0058	1.2200	1.8219	+0.01
0.49440	1.1047	1.3316	-0.14	1.4553	1.3118	2.4548	+0.11
0.64686	1.1365	1.4584	+0.04	1.7024	1.3603	2.9180	-0.07
1.0076	1.2094	1.8153	+0.02	1.9480	1.4071	3.503	-0.04
1.4108	1.2875	2.3563	+0.07	2.2566	1.4641	4.466	-0.01
1.6927	1.3395	2.8530	-0.08	2.5524	1.5167	5.713	-0.04
1.9750	1.3901	3.498	+0.03	2.8974	1.5758	7.765	-0.03
2.2517	1.4382	4.305	-0.05	3.2499	1.6336	10.867	+0.03
2.5649	1.4907	5.520	-0.02	3.5901	1.6870	15.352	+0.10
2.8324	1.5340	6.900	-0.04	3.9292	1.7379	22.07	-0.04
3.2896	1.6050	10.391	+0.11				
3.6003	1.6512	14.012	+0.15				
3.8959	1.6943	18.91	-0.05				
	$SmCl_3$				$TbCl_3$		
0.04717	1.0085	1.0341	+0.09	0.04788	1.0089	1.0361	0.00
0.07660	1.0154	1.0525	+0.03	0.08136	1.0171	1.0592	-0.01
0.09712	1.0203	1.0651	-0.01	0.10090	1.0218	1.0736	+0.06
0.26869	1.0605	1.1795	+0.03	0.25812	1.0597	1.1871	+0.04
0.51578	1.1172	1.3655	0.00	0.49015	1.1144	1.3764	-0.05
0.85276	1.1921	1.6781	-0.04	0.73211	1.1700	1.6131	-0.02
1.0625	1.2376	1.9176	-0.08	1.0005	1.2301	1.9327	-0.05
1.4371	1.3161	2.4689	+0.12	1.3007	1.2951	2.3868	+0.04
1.6664	1.3623	2.8988	0.00	1.6309	1.3643	3.039	+0.07
1.9453	1.4176	3.562	-0.01	1.8759	1.4140	3.657	-0.02
2.1161	1.4504	4.061	-0.04	2.1862	1.4751	4.671	-0.07
2.5233	1.5260	5.652	-0.09	2.4998	1.5347	6.052	-0.05
2.8645	1.5864	7.606	-0.04	2.7954	1.5910	7.820	+0.08
3.1788	1.6398	10.165	+0.07	3.1003	1.6432	10.287	-0.02
3.5070	1.6934	13.995	+0.33	3.3803	1.6911	13.403	-0.05
3.6401	1.7144	15.883	-0.29	3.5735	1.7234	16.226	+0.04

Table 15. (Continued)

m	d	η_r	Δ%	m	d	η_r	Δ%
	$DyCl_3$				$HoCl_3$		
0.05554	1.0111	1.0412	-0.08	0.04955	1.0097	1.0376	-0.01
0.07650	1.0163	1.0574	+0.06	0.07894	1.0171	1.0597	+0.12
0.09742	1.0214	1.0713	-0.01	0.10195	1.0229	1.0759	+0.11
0.24914	1.0586	1.1808	-0.14	0.25290	1.0604	1.1851	-0.06
0.49471	1.1175	1.3866	-0.02	0.49457	1.1192	1.3881	-0.08
0.64312	1.1523	1.5278	-0.14	0.74130	1.1777	1.6391	-0.05
1.0055	1.2352	1.9624	+0.18	1.0021	1.2379	1.9680	+0.09
1.4371	1.3297	2.6737	0.00	1.2884	1.3020	2.4175	-0.06
1.6767	1.3803	3.208	+0.09	1.5907	1.3675	3.042	+0.08
1.9529	1.4369	3.980	-0.05	1.8945	1.4313	3.860	-0.07
2.2620	1.4983	5.122	-0.14	2.2007	1.4934	4.971	-0.06
2.5342	1.5506	6.462	-0.11	2.4903	1.5501	6.384	-0.03
2.8530	1.6098	8.583	-0.14	2.6713	1.5847	7.507	-0.01
3.1478	1.6626	11.313	+0.14	2.7907	1.6071	8.382	+0.07
3.6310	1.7451	18.14	+0.18	3.0919	1.6623	11.157	+0.06
				3.3877	1.7146	15.000	-0.02
				3.6942	1.7670	20.81	-0.04
	$ErCl_3$				$PrCl_3$		
0.05533	1.0114	1.0415	-0.06	0.05011	1.0087	1.0332	-0.13
0.07409	1.0161	1.0555	+0.01	0.07986	1.0155	1.0526	-0.01
0.10483	1.0239	1.0778	+0.04	0.10083	1.0203	1.0661	+0.07
0.25090	1.0607	1.1857	+0.02				
0.49531	1.1209	1.3927	-0.05				
0.77238	1.1874	1.6815	-0.02				
1.0096	1.2427	1.9889	+0.07				
1.4609	1.3443	2.7770	0.00				
1.7153	1.3994	3.388	-0.02				
1.9944	1.4582	4.255	-0.02				
2.2695	1.5143	5.379	-0.04				
2.5878	1.5772	7.154	-0.01				
2.9182	1.6401	9.789	+0.08				
3.2497	1.7010	13.660	+0.08				
3.5379	1.7520	18.57	-0.03				
3.7821	1.7939	24.50	-0.05				

Table 16. Parameters for viscosity equations

Salt	A	B	B_o	$B_1 \times 10^3$	$B_2 \times 10^3$	$B_3 \times 10^3$
$LaCl_3$	0.0285	0.554	0.52145	-31.635	-4.7569	0.64282
$PrCl_3$	0.0285	0.562	---	---	---	---
$NdCl_3$	0.0286	0.557	0.52479	-35.168	0.70453	-0.29122
$SmCl_3$	0.0288	0.584	0.54687	-56.684	5.4394	-0.74824
$TbCl_3$	0.0293	0.633	0.59406	-66.423	-0.16163	0.44780
$DyCl_3$	0.0297	0.639	0.60165	-68.006	1.7828	0.0
$HoCl_3$	0.0295	0.650	0.60210	-55.522	-4.6225	1.0342
$ErCl_3$	0.0296	0.646	0.60731	-58.876	-2.4475	0.73771

Table 17. Relative viscosities at 25°C. calculated at even molalities

m \ salt	$LaCl_3$	$NdCl_3$	$SmCl_3$	$TbCl_3$	$DyCl_3$	$HoCl_3$	$ErCl_3$
0.2	1.127	1.128	1.132	1.143	1.145	1.146	1.147
0.4	1.263	1.265	1.274	1.299	1.304	1.305	1.308
0.6	1.418	1.421	1.437	1.479	1.487	1.490	1.495
0.8	1.598	1.603	1.624	1.688	1.700	1.707	1.714
1.0	1.806	1.815	1.843	1.933	1.951	1.963	1.974
1.2	2.051	2.065	2.100	2.221	2.248	2.267	2.282
1.4	2.338	2.361	2.404	2.562	2.601	2.629	2.651
1.6	2.677	2.713	2.764	2.968	3.022	3.061	3.093
1.8	3.080	3.136	3.196	3.451	3.527	3.581	3.628
2.0	3.562	3.646	3.714	4.030	4.135	4.209	4.276
2.2	4.139	4.266	4.341	4.726	4.870	4.971	5.066
2.4	4.836	5.023	5.104	5.569	5.764	5.900	6.037
2.6	5.682	5.955	6.037	6.593	6.855	7.040	7.236
2.8	6.715	7.108	7.184	7.845	8.192	8.449	8.727
3.0	7.984	8.544	8.602	9.385	9.837	10.20	10.60
3.2	9.556	10.35	10.36	11.29	11.87	12.40	12.97
3.4	11.52	12.62	12.56	13.67	14.40	15.20	15.99
3.6	13.99	15.50	15.30	16.66	17.55	18.78	19.91

Table 18. $\eta_{RCl_3}/\eta_{LaCl_3}$ at 25°C. calculated at even molalities

m \ salt	$NdCl_3$	$SmCl_3$	$TbCl_3$	$DyCl_3$	$HoCl_3$	$ErCl_3$
0.4	1.001	1.009	1.029	1.032	1.034	1.036
0.8	1.003	1.017	1.057	1.064	1.069	1.073
1.2	1.007	1.024	1.083	1.096	1.106	1.113
1.6	1.013	1.033	1.108	1.129	1.143	1.155
2.0	1.024	1.043	1.131	1.161	1.182	1.200
2.4	1.039	1.055	1.152	1.192	1.220	1.248
2.8	1.059	1.070	1.168	1.220	1.258	1.300
3.2	1.083	1.084	1.182	1.242	1.298	1.357
3.6	1.108	1.094	1.191	1.255	1.343	1.423

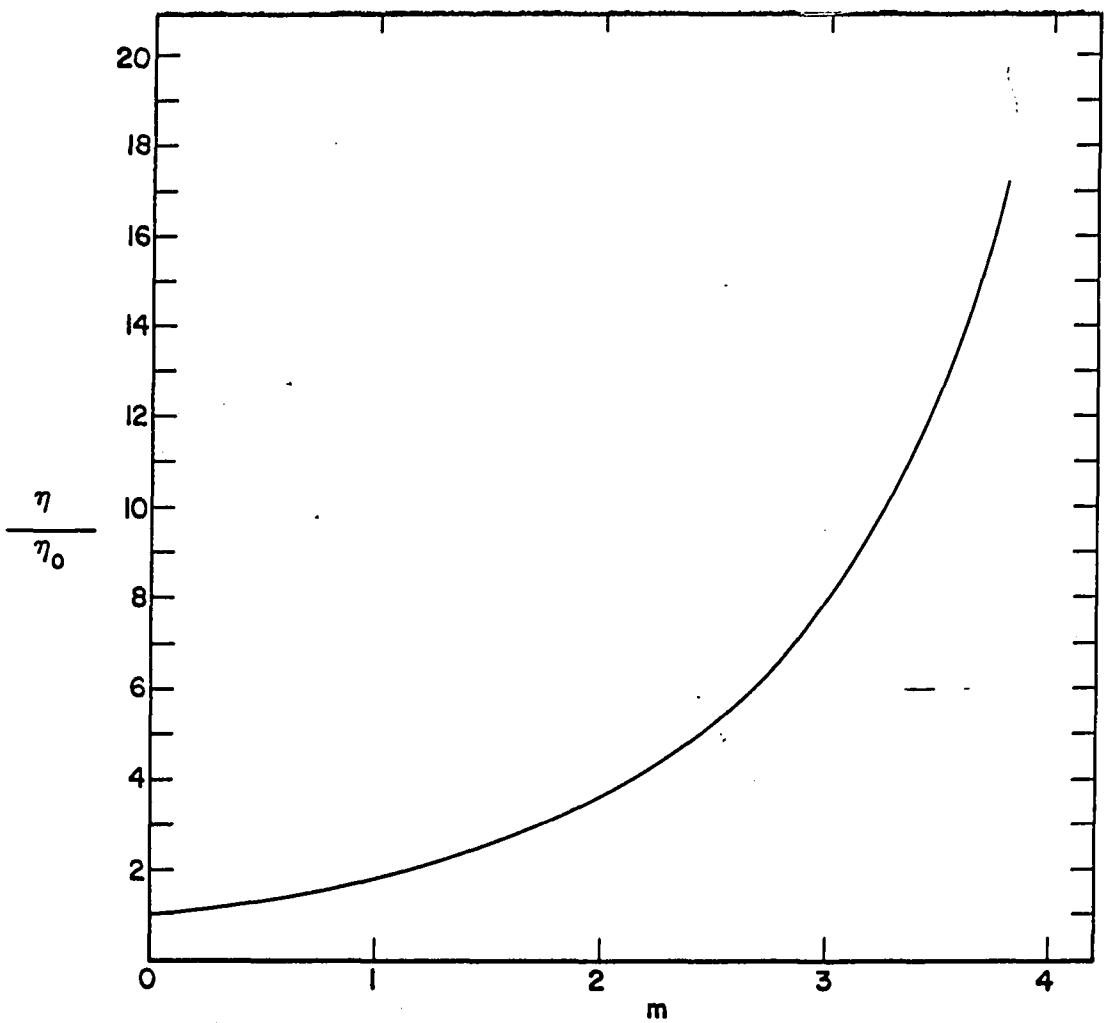

Figure 11. Relative viscosity of aqueous $LaCl_3$ at 25°C. as a function of molality

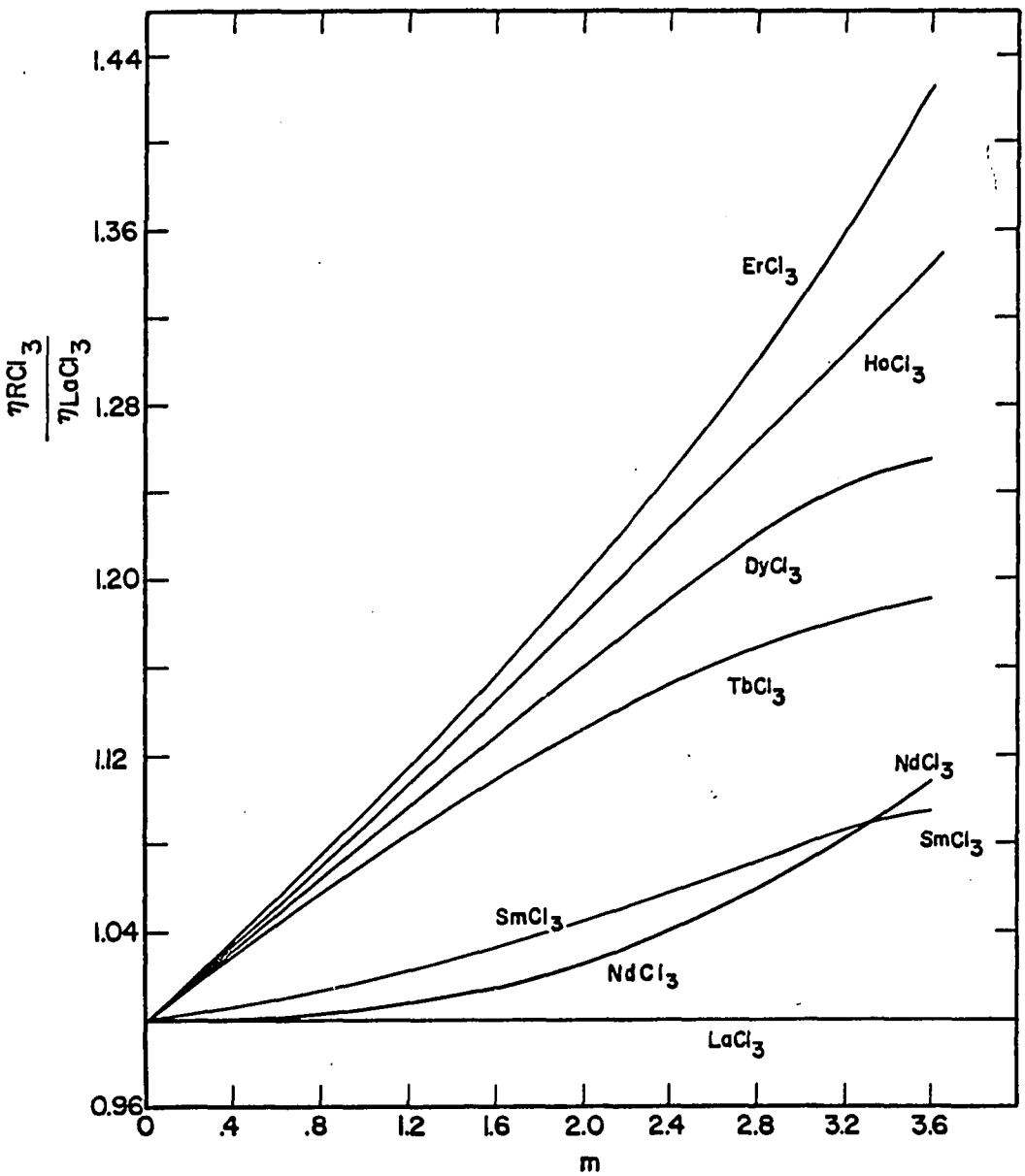

Figure 12. $(\eta)_{RCl_3}/(\eta)_{LaCl_3}$ for some aqueous rare-earth chloride solutions at 25°C. as a function of molality

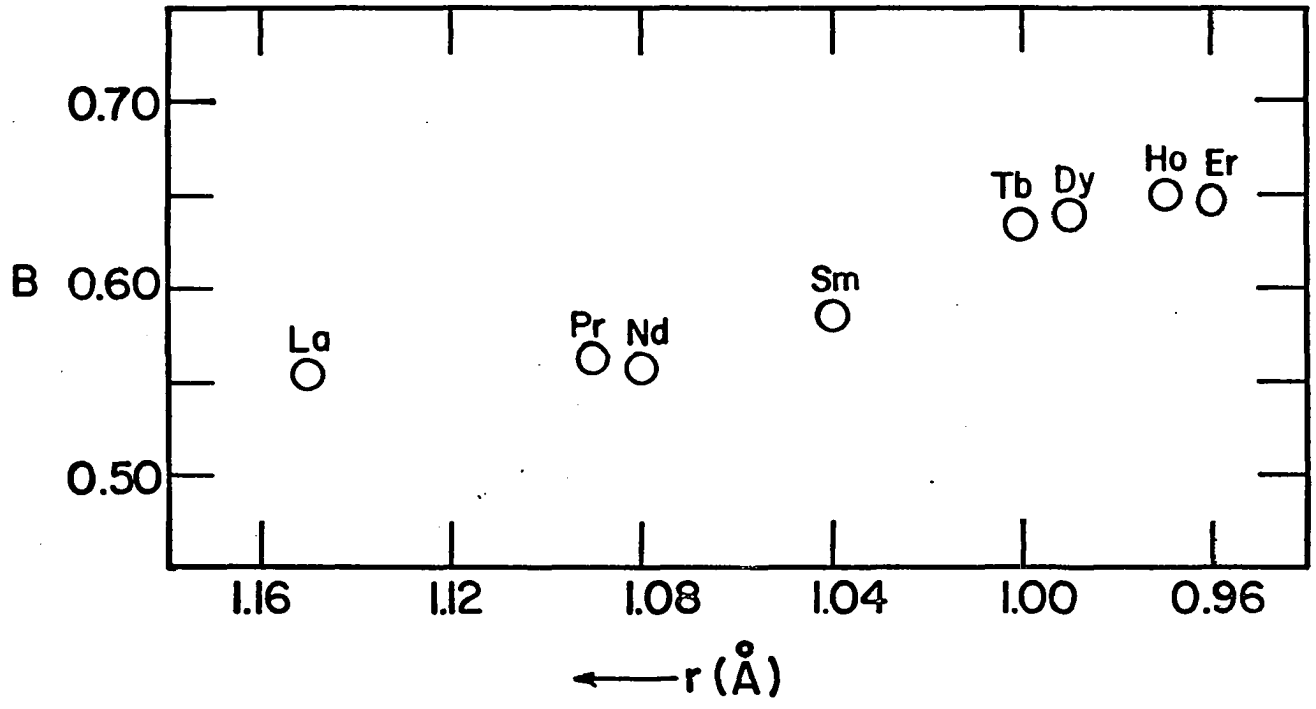

Figure 13. Viscosity B coefficient at 25°C. as a function of ionic radius for some aqueous rare-earth chloride solutions

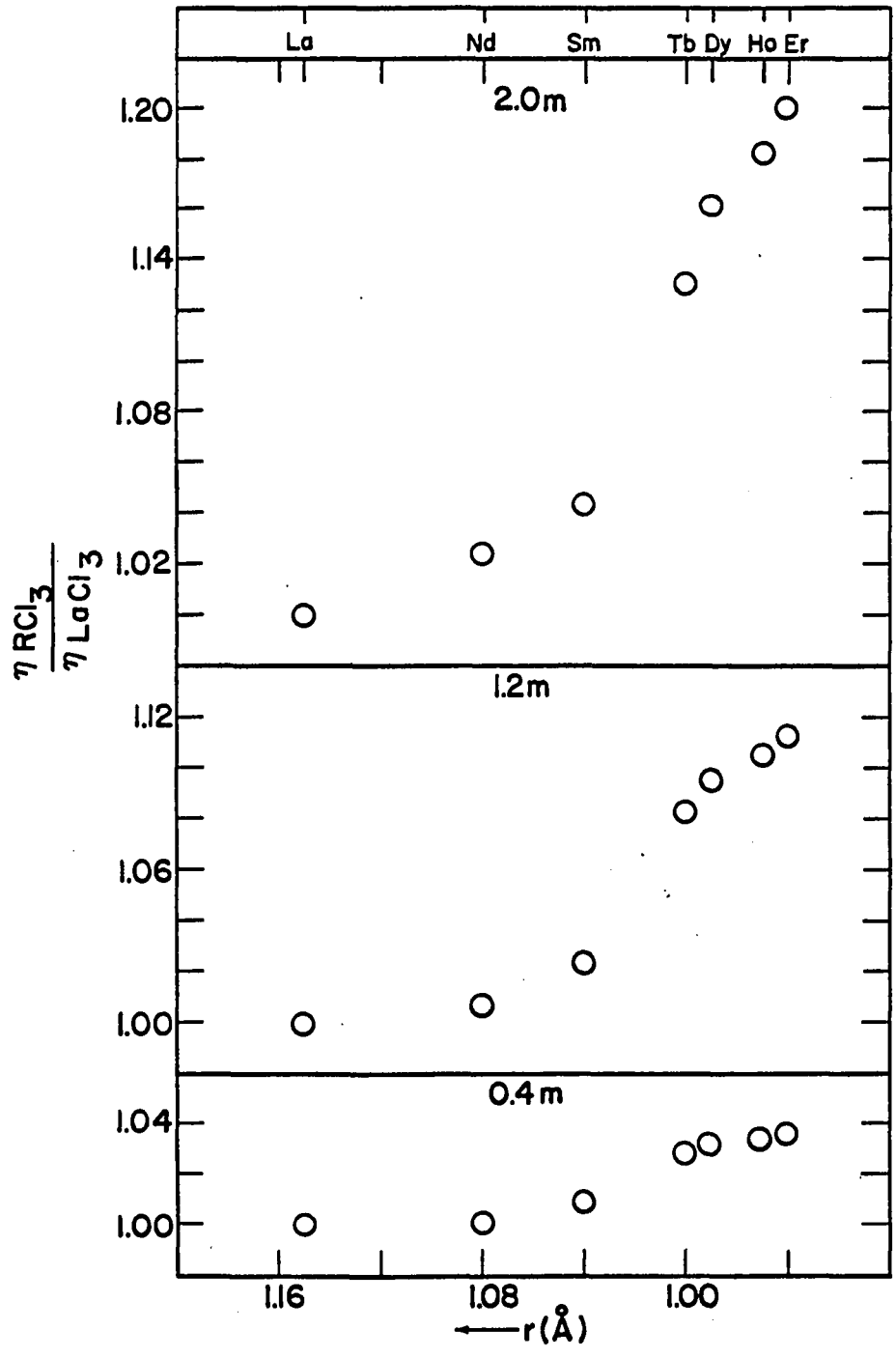

Figure 14. $(\eta)_{RCl_3}/(\eta)_{LaCl_3}$ for some aqueous rare-earth chlorides at 25°C. as a function of ionic radius at 0.4, 1.2, and 2.0 molal

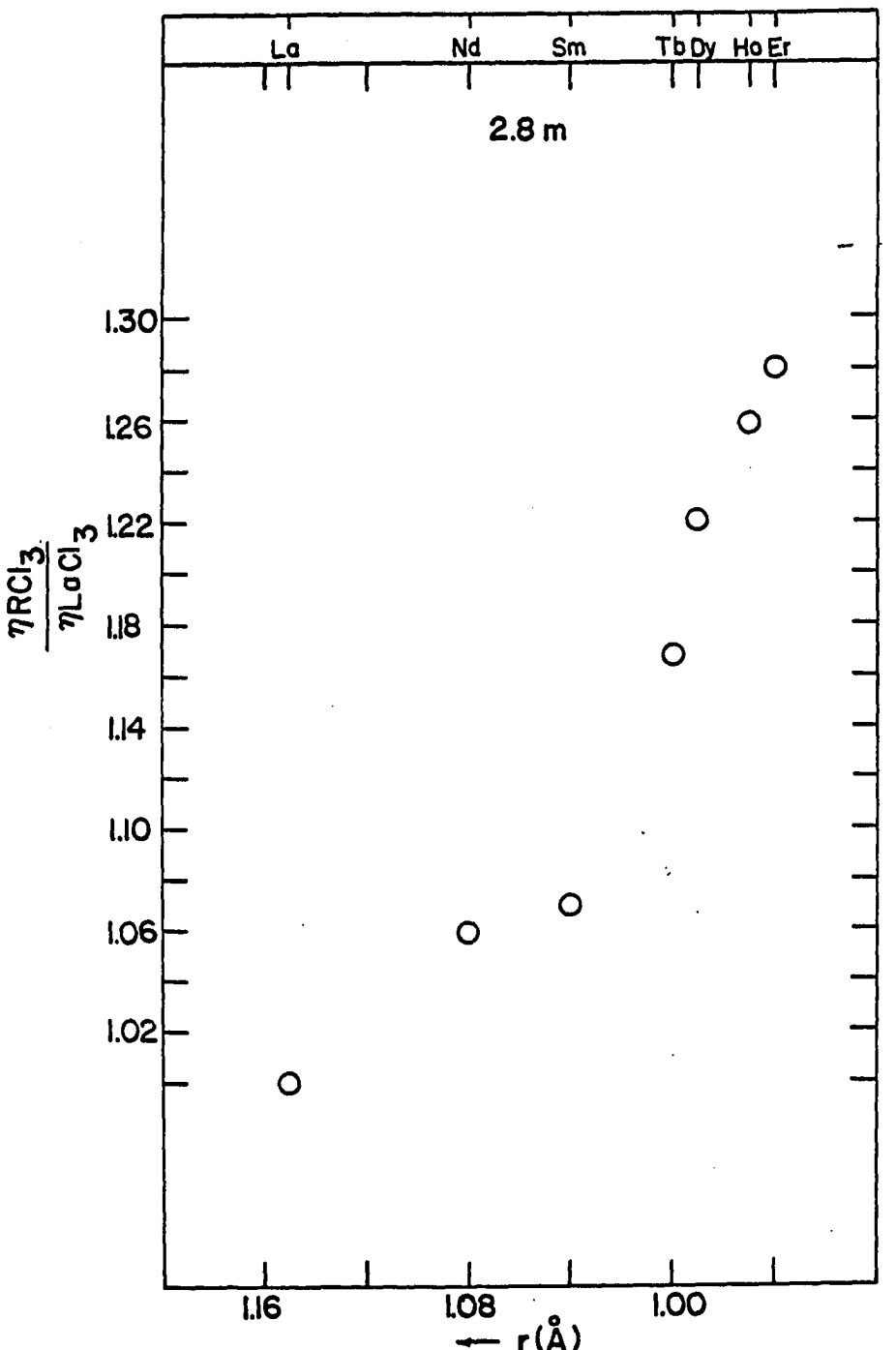

Figure 15. $(\eta)_{RCl_3}/(\eta)_{LaCl_3}$ for some aqueous rare-earth chlorides at 25°C. as a function of ionic radius at 2.8 molal

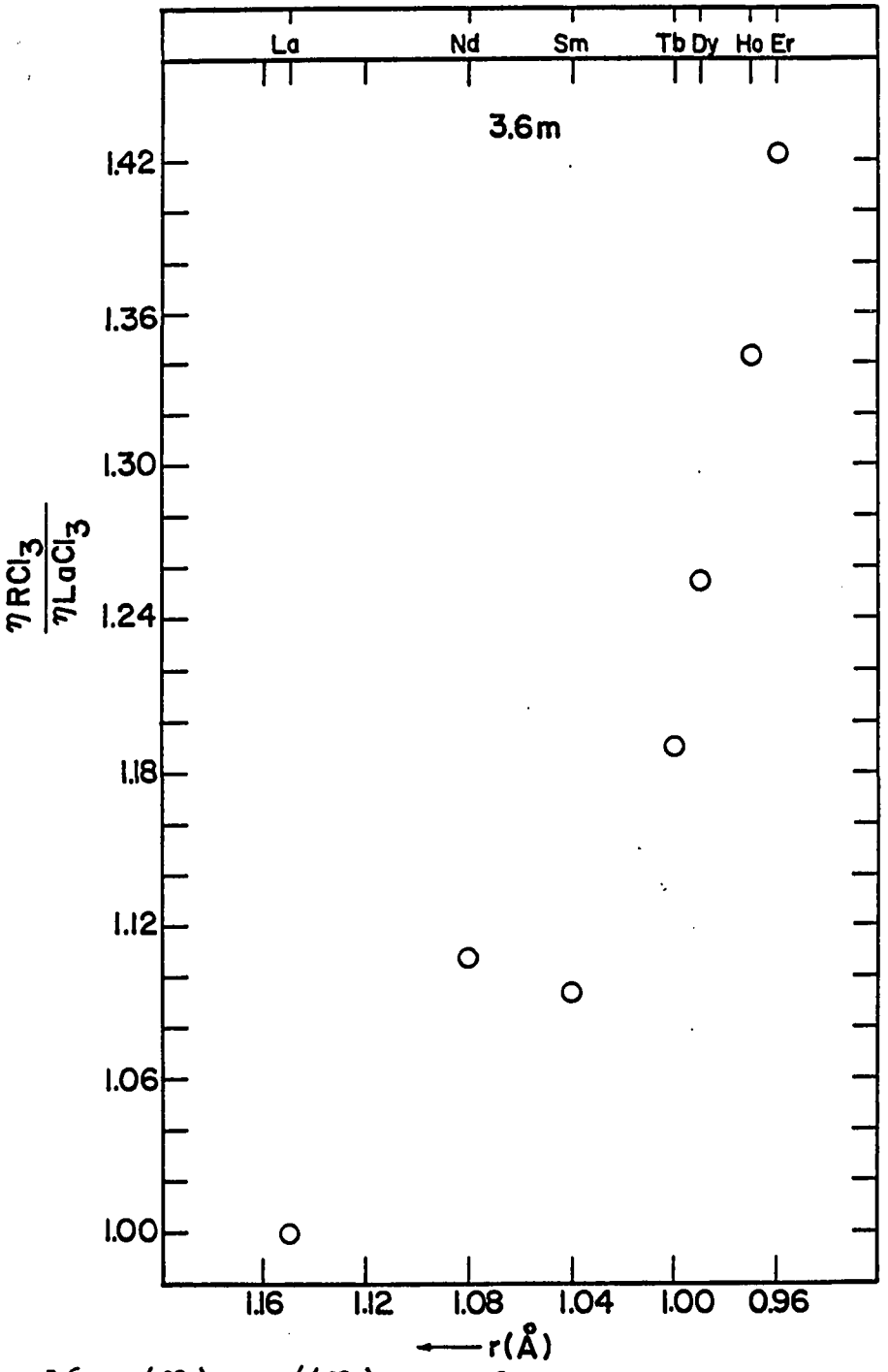

Figure 16. $(\eta)_{RCl_3}/(\eta)_{LaCl_3}$ for some aqueous rare-earth chlorides at 25°C. as a function of ionic radius at 3.6 molal

is the mean of two independent determinations, it is estimated that the probable error in the relative viscosity of a given solution if about ± 0.05 percent.

The B coefficients of the Jones-Dole equation were calculated from Equations 5.27 and 5.28, normally from experimental relative viscosities at about 0.05, 0.08, and 0.1 molar. If the law of propagation of precision indexes, expressed by Equation 4.36, is applied to Equation 5.28, the probable error in the B coefficient, P(B), may be expressed in terms of the probable error in B_k, $P(B_k)$, in the form,

$$P^2(B) = \sum_k (\partial B/\partial B_k)^2 \, P^2(B_k) \, . \qquad (5.36)$$

However, $\partial B/\partial B_k$ is given by the quantity, $w_k/(\sum_k w_k)$, and $P^2(B_k) = 1/w_k$, so Equation 5.36 becomes,

$$P^2(B) = 1/(\sum_k w_k) \, . \qquad (5.37)$$

Assuming a probable error of ± 0.05 percent in the relative viscosity, $P(B_k) = \pm 5 \times 10^{-4}/c_k$ and $\sum_k w_k = \sum_k c_k^2/25 \times 10^{-8}$. For values of c_k of 0.05, 0.08, and 0.1 molar, the calculated probable error in the B coefficient is ± 0.004. Thus, it is estimated that the probable error in the B coefficient of a rare-earth chloride given in Table 16 is about ± 0.004.

It was stated earlier that the estimated probable error in the relative viscosity of a given solution was ± 0.05 percent. However, the uncertainty in the concentration of the solution must also be considered when the viscosities of

different solutions are being compared. Since the concentration of the solution must be specified before the comparison can be made, an uncertainty in the concentration of the solution has the same effect as an uncertainty in viscosity. This error is not serious in the lower concentration region where the viscosity does not change rapidly with concentration. However, above two molal this type of error, which results from an inability to specify the concentration exactly, becomes quite significant. For the rare-earth chlorides studied in this research, a probable error in concentration of $\pm$ 0.05 percent has the same effect as a probable error in viscosity of about $\pm$ 0.1 percent at two molal, $\pm$ 0.2 percent at three molal, and $\pm$ 0.4 percent at four molal. Consequently, this "effective" viscosity uncertainty due to a concentration error must be considered when examining the viscosity data presented in this thesis. It should be emphasized that the concentration error of each solution is due mainly to the error in concentration of the stock solution, and this error will be the same for all solutions prepared from a given stock solution. Thus, the concentration error is mostly a systematic error, and therefore, the $\triangle$ values in Table 15 are smaller than the errors quoted above.

C. Discussion of Results

The relative viscosity data given in Table 15 and the $LaCl_3$ data illustrated in Figure 11 show that the relative

viscosities of rare-earth chloride solutions increase slowly with increasing concentration at low concentrations, but above about 2 molal, increase very rapidly as the concentration increases. It was noted earlier that the relative viscosities of many electrolytes containing highly hydrated ions are well represented by a slight modification of the Vand equation, Equation 5.23, of the form,

$$\ln \eta_r = A_3 c/(1 - Q'c) , \qquad (5.24)$$

where A_3 and Q' are adjustable parameters. This success of Equation 5.24 was interpreted by Stokes (10) and by Robinson and Stokes (38) as indicating the major contribution to the viscosity of "highly hydrated" electrolytes is the "obstruction" effect, due to the interference of large hydrated ions with the stream lines in the solvent.

The relative viscosities of the rare-earth chloride solutions investigated in this research may be represented by Equation 5.24 within about $\pm$ one percent over the entire concentration range studied, provided A_3 and Q' are suitably adjusted. The values of A_3 and Q' evaluated from the data are about 0.5 and 0.1, respectively, the exact values depending upon the particular rare-earth chloride under consideration. If the "obstruction" effect is the dominant contribution to the viscosity of a rare-earth chloride solution, comparison of the Vand equation, Equation 5.23, with Equation 5.24 indicates A_3 should be approximately equal to 2.5 $\bar{v}$, where $\bar{v}$ represents the molar volume of the hydrated ions, and the ratio, Q'/A_3,

should be approximately given by, $Q/2.5 = 0.24$. The quantity, Q, is the hydrodynamic interaction constant, which was theoretically calculated by Vand to be 0.60937 for the simplest case. The experimental ratios, Q'/A_3, are about 0.2 and therefore are in good agreement with what one would expect on the basis of the Vand theory. The experimental values of $\bar{v}$ are about 0.2 liter. If it is assumed the chloride ions are unhydrated and have a radius of 1.8 Å, and that the hydrated rare-earth ion is spherical, a value of 0.2 liter for $\bar{v}$ implies the radius of the hydrated rare-earth ion is about 4 Å. This result is in good agreement with what one would expect if the rare-earth ion were firmly co-ordinated with one row of water molecules.

The success of Equation 5.24 in approximately representing the relative viscosity data for the rare-earth chlorides with reasonable values for A_3 and Q' suggests that the major contribution to the viscosity of a rare-earth chloride solution arises from the "obstruction" effect. It should be emphasized that the preceding statement does not imply the "obstruction" effect is the only significant factor in determining the viscosity of a rare-earth chloride solution, but states only that the largest effect is probably the "obstruction" effect.

Although the viscosities of the rare-earth chloride solutions at a given concentration are somewhat similar, significant differences do exist. These differences are illustrated graphically by Figures 12, 13, 14, 15, and 16. In Figure 12,

these viscosity differences are illustrated as a function of molality, where values of the viscosity ratio, $\eta_{RCl_3}/\eta_{LaCl_3}$, are plotted as a function of molality for each of the rare-earth chlorides studied. As mentioned earlier, the reason for plotting this ratio instead of the relative viscosity was only to enable the differences in viscosity to be illustrated on a small scale graph. From Figure 12, it should be noticed that the viscosities of the rare-earth chlorides increase as the atomic number of the rare-earth ion increases at all concentrations below about 3.3 molal. However, above 3.3 molal $NdCl_3$ solutions have viscosities greater than $SmCl_3$ solutions of the same concentration. This "cross-over" will be briefly discussed later.

In Figure 13 the B coefficients of the Jones-Dole equation, Equation 5.16, are plotted as a function of ionic radius of the rare-earth ion. The B coefficients for $LaCl_3$, $PrCl_3$, and $NdCl_3$ are equal within experimental error. However, the B coefficient of $SmCl_3$ is slightly greater, and the B coefficients for the rare-earth chlorides from Tb to Er are about 15 percent greater than those of $LaCl_3$, $PrCl_3$, and $NdCl_3$. The B coefficients from Tb to Er exhibit a slight increase with decreasing rare-earth ionic radius. The theoretical interpretation of the B coefficient has been discussed in detail by Kaminsky (8) and by Gurney (9), and a summary of these discussions was given earlier in this thesis. Briefly, the B coefficient is an addi-

tive property of the ions, and it is considered to be a function only of ion-solvent interactions. Furthermore, the ionic B coefficient is normally interpreted as a measure of the order the ion introduces in the solvent surrounding the ion, a larger B coefficient indicating a higher degree of order.

According to the interpretation given the apparent molal volumes at infinite dilution, as discussed earlier in this thesis, the rare-earth ion in water exists in an equilibrium between two possible water co-ordination numbers. For the rare-earth ions from La^{+3} to Nd^{+3}, this equilibrium favors the higher co-ordination number. After Nd^{+3}, a displacement of this equilibrium toward the lower co-ordination number begins to take place that results in the lower co-ordination number becoming increasingly more favorable for the rare-earth ions from Nd^{+3} to around Tb^{+3}. This shift toward the lower co-ordination number terminates around Tb^{+3}, and the remaining rare-earth ions have essentially the same co-ordination number. The B coefficients may be discussed in terms of this model.

For a given co-ordination number, the B coefficients may be expected to increase slightly with decreasing ionic radius, due to the increasing effect of the field of the ion in producing order in the water surrounding the co-ordination complex. For small changes in ionic radii, this effect should be small. This phenomena is observed for the rare-earth chlorides from La to Nd and from Tb to Er. However, a shift

to a lower co-ordination number occurring in the region from Nd to Tb might be expected to result in an irregularity in a plot of B coefficients as a function of ionic radius, as indeed is observed. The B coefficients for the rare-earth chlorides from Tb to Er are significantly larger than those from La to Nd, indicating the shift to a lower co-ordination number has the effect of increasing the order in the water surrounding the ion.

According to the theory of the B coefficient as presented by Kaminsky (8), a shift to a lower co-ordination number might be expected to affect the viscosity, and therefore the B coefficient, in the following ways:

1. The effect of the water molecules directly co-ordinated to the ion in increasing the viscosity is greater the greater the co-ordination number. Therefore, a change to a lower co-ordination number would reduce this effect and decrease the B coefficient.

2. The effective radius of the rare-earth-water co-ordination complex might be expected to be less, and the ordering effect of the ion on the water molecules outside of this complex would therefore increase. This effect would increase the B coefficient.

3. Special steric effects may not be the same for both co-ordination complexes. These effects might include the geometry of the co-ordination complex and the effect of

hydrogen bonding between the water molecules co-ordinated to the ion and those outside the co-ordination complex. This effect may either increase or decrease the B coefficient.

Consequently, because of the various possible interactions contributing to the B coefficient, it is difficult to predict from theory how the net effect of a change in co-ordination number would affect the B coefficient. However, since the effect of a change in co-ordination number may either increase or decrease the B coefficient, the trends shown by the B coefficients of the rare-earth chlorides seem to be consistent with the proposed change in co-ordination number. From the above discussion, it seems likely that the observed differences between the rare-earth chloride B coefficients are due to phenomena involving water molecules outside the co-ordination complex.

The viscosity of a rare-earth chloride solution cannot be interpreted in terms of ion size and ion-solvent interactions alone. However, it seems reasonable to expect that the effects of ion-ion interactions would be a smooth function of rare-earth ionic radius for the rare-earth chlorides. Thus, any irregularities in the viscosity as a function of ionic radius of the rare-earth ion are probably the result of ion-water interactions.

Figures 14, 15, and 16 show values of the viscosity ratio, $\eta_{RCl_3}/\eta_{LaCl_3}$, as a function of ionic radius of the rare-earth

ion at various concentrations. It should be noticed that the effect of the ionic radius on the viscosity at 0.4 and 1.2 molal is much the same as the effect on the B coefficient, and the variation of the viscosity ratio with ionic radius at these concentrations may be interpreted using basically the same model and arguments presented when discussing the B coefficients.

However, at higher concentrations the general shape of the viscosity ratio-ionic radius curve begins to change, and at 3.6 molal it appears as though two distinct series exist, $LaCl_3$ and $NdCl_3$ forming one series and the rare-earth chlorides from Sm through Er forming the other series. Figure 16 may also be interpreted as indicating the viscosity of $NdCl_3$ is anomalously high, and the viscosities of the other rare-earth chlorides form just one series. Viscosity data for concentrated solutions of $CeCl_3$ or $PrCl_3$ are needed before it can be proven which interpretation is correct. It is the opinion of this author that the "two series" interpretation is probably correct and that the irregularity between $NdCl_3$ and $SmCl_3$ is a result of a change to a lower water co-ordination number. Thus, the decrease in viscosity from $NdCl_3$ to $SmCl_3$ could be interpreted as a result of Sm^{+3} having a lower co-ordination number than Nd^{+3}. When a water molecule is displaced from the co-ordination sphere of an ion in concentrated solution, the net result would seem to be a smaller co-ordination complex

moving in a significantly greater quantity of "free" solvent, which might be expected to lower the viscosity. This interpretation does qualitatively explain the data. However, this interpretation is little more than an educated guess, and a more complete discussion of the viscosity results shown in Figures 15 and 16 should be attempted when viscosity data for concentrated $PrCl_3$ and $CeCl_3$ solutions become available.

VI. SUMMARY

The specific gravities and apparent molal volumes of aqueous solutions of $PrCl_3$, $SmCl_3$, $GdCl_3$, $TbCl_3$, $DyCl_3$, $HoCl_3$, and $ErCl_3$ were determined over a concentration range of about 0.0015 molar to 0.18 molar. A magnetically controlled float apparatus was used to determine the specific gravities. The apparent molal volume data obtained in this research and existing apparent molal volume data for several other rare-earth salts were extrapolated to zero concentration to obtain partial molal volumes at infinite dilution. The concentration dependence of the apparent molal volumes of these salts was examined and found to show significant deviations from the simple limiting law at low concentrations. However, it was shown that, except for $Nd(NO_3)_3$, these deviations are consistent with interionic attraction theory if the effect of the distance of closest approach parameter, a, is recognized. The partial molal volumes at infinite dilution, $\bar{V}_2^o$, do not decrease smoothly as the ionic radius of the cation decreases. The $\bar{V}_2^o$ values decrease smoothly with decreasing ionic radius from La to Nd and from Tb to Yb, but from Nd to Tb the $\bar{V}_2^o$ values increase with decreasing ionic radius. This irregular behavior was discussed in terms of a gradual change in preferred water co-ordination number of the rare-earth ion occurring over the rare-earth ions from Nd^{+3} to Tb^{+3}, this change resulting in the rare-earth ions from Tb^{+3} to Yb^{+3} having a lower co-ordin-

ation number than the rare-earth ions from La^{+3} to Nd^{+3}.

The relative viscosities of aqueous solutions of $LaCl_3$, $NdCl_3$, $SmCl_3$, $TbCl_3$, $DyCl_3$, $HoCl_3$ and $ErCl_3$ were determined at 25°C. over a concentration range of about 0.05 molal to saturation at 25°C. The B coefficients of the Jones-Dole equation were determined for these salts. The relative viscosities of several dilute $PrCl_3$ solutions were also measured to allow the B coefficient for this salt to be determined. The concentration dependence of the relative viscosity of a rare-earth chloride solution was discussed in terms of the Vand theory for large non-electrolyte molecules. It was suggested that the major contribution to the viscosity of a rare-earth chloride solution arises from the effect considered by the Vand theory, which is the interference of the species in solution with the stream lines in the solvent. The B coefficients and the relative viscosities at "iso-molalities" were studied as a function of the ionic radius of the rare-earth ion, and irregularities were noted near the middle of the rare-earth series. These irregularities were discussed in terms of a change in preferred water co-ordination number of the rare-earth ion.

VII. BIBLIOGRAPHY

1. Debye, P. and Hückel, E., Physik. Z., 24, 185 (1923).

2. Kavanau, J. L., "Water and Solute-Water Interactions", Holden-Day Inc., San Francisco, California, 1964.

3. Spedding, F. H. and Atkinson, G., "Properties of Rare Earth Salts in Electrolytic Solutions". In Hamer, Walter J., ed., "The Structure of Electrolytic Solutions", pp. 319-339, John Wiley and Sons Inc., New York, New York, 1959.

4. Dekock, Carroll W., "Heats of Dilution of Some Aqueous Rare-Earth Chloride Solutions at 25°C", Unpublished Ph.D. thesis, Library, Iowa State University of Science and Technology, Ames, Iowa, 1965.

5. Jones, Kenneth C., "Partial Molal Heat Capacities of Some Aqueous Rare-Earth Chloride Solutions at 25°C.", Unpublished Ph.D. thesis, Library, Iowa State University of Science and Technology, Ames, Iowa, 1965.

6. Saeger, V. W. and Spedding, F. H., U.S. Atomic Energy Commission Report IS-338, [Iowa State University of Science and Technology, Ames, Iowa, Inst. for Atomic Research] (1960).

7. Ayers, Buell O., "Apparent and Partial Molal Volumes of Some Rare-Earth Salts in Aqueous Solution", Unpublished Ph.D. thesis, Library, Iowa State University of Science and Technology, Ames, Iowa, 1954.

8. Kaminsky, M., Discussions Faraday Soc., 24, 171 (1957).

9. Gurney, R. W., "Ionic Processes in Solution", McGraw-Hill Book Company, Inc., New York, New York, 1953.

10. Stokes, R. H., "Mobilities of Ions and Uncharged Molecules in Relation to Viscosity: a Classical Viewpoint". In Hamer, Walter J., ed., "The Structure of Electrolytic Solutions", pp. 298-307, John Wiley and Sons, Inc., New York, New York, 1959.

11. Harned, H. S. and Owen, B. B., "The Physical Chemistry of Electrolytic Solutions", 3rd ed., Reinhold Publishing Corporation, New York, New York, 1958.

12. Fuoss, R. M. and Accascina, F., "Electrolytic Conductance", Interscience Publishers, Inc., New York, New

York, 1959.

13. Arrhenius, S., Z. physik. Chem., 1, 631 (1887).

14. Falkenhagen, H., "Electrolytes", Oxford University Press, London, England, 1934.

15. van Laar, J. J., Z. physik. Chem., 15, 457 (1894).

16. Bjerrum, N., D. Kgl. Danske Vidensk. Selsk. Skrifter (7), 4, 1 (1906). Original available but not translated; cited in Harned, H. S. and Owen, B. B., "The Physical Chemistry of Electrolytic Solutions", 3rd ed., p. 42, Reinhold Publishing Corporation, New York, New York, 1958.

17. Sutherland, W., Phil. Mag., Ser. 6, 3, 161 (1902).

18. Noyes, A. A., Congress Arts Sci., St. Louis Exposition, 4, 317 (1904).

19. Milner, R., Phil. Mag., Ser. 6, 23, 551 (1912).

20. Fowler, R., and Guggenheim, E., "Statistical Thermodynamics", Cambridge University Press, Cambridge, England, 1960.

21. Kramers, H., Proc. Royal Acad. Sci. Amsterdam, 30, 145 (1927).

22. Spedding, F. H., Porter, P. E., and Wright, J. M., J. Am. Chem. Soc., 74, 2781 (1952).

23. Spedding, F. H. and Dye, J. L., J. Am. Chem. Soc., 76, 879 (1954).

24. Spedding, F. H. and Yaffe, I. S., J. Am. Chem. Soc., 74 4751 (1952).

25. Nelson, Robert, "Some Thermodynamic Properties of Aqueous Solutions of Terbium", Unpublished M.S. thesis, Library, Iowa State University of Science and Technology, Ames, Iowa, 1960.

26. Kirkwood, J. G. and Poirier, J. C., J. Phys. Chem., 58, 591 (1954).

27. Onsager, L., Chem. Rev., 13, 73 (1933).

28. Bjerrum, N., Kgl. Danske Vidensk., 7, No. 9 (1926). Original available but not translated; cited in Harned, H. S. and Owen, B. B., "The Physical Chemistry of

Electrolytic Solutions", 3rd ed., p. 70, Reinhold Publishing Corporation, New York, New York, 1958.

29. Gronwall, T. H., La Mer, V. K., and Sandved, K., Physik. Z., 29, 358 (1928).

30. Fuoss, R. M. and Onsager, L., Proc. Natl. Acad. Sci. U.S., 47, 818 (1961).

31. Fowler, R., Trans. Faraday Soc., 23, 434 (1927).

32. Debye, P. and Pauling, L., J. Am. Chem. Soc., 47, 2129 (1925).

33. Glueckauf, E., Trans. Faraday Soc., 60, 776 (1964).

34. Kirkwood, J., J. Chem. Phys., 2, 767 (1934).

35. Alei, M. and Jackson, J., J. Chem. Phys., 41, 3402 (1964).

36. Brady, G., J. Chem. Phys., 33, 1079 (1960).

37. Bernal, J. and Fowler, R., J. Chem. Phys., 1, 515 (1933).

38. Robinson, R. and Stokes, R., "Electrolyte Solutions", 2nd ed., Butterworth's Scientific Publications, London, England, 1959.

39. Scatchard, G. and Kirkwood, J., Physik. Z., 33, 297 (1932).

40. Scatchard, G., Physik. Z., 33, 22 (1932).

41. Scatchard, G., Chem. Rev., 19, 309 (1936).

42. Frank, H. and Thompson, P., J. Chem. Phys., 31, 1086 (1959).

43. Mayer, J., J. Chem. Phys., 18, 1426 (1950).

44. Poirier, J., J. Chem. Phys., 21, 965 (1953).

45. Friedman, Harold L., "Ionic Solution Theory", Interscience Publishers, Inc., New York, New York, 1962.

46. Masson, D. O., Phil. Mag., Ser. 7, 8, 218 (1929).

47. Geffchen, W., Z. physik. Chem., A155, 1 (1931).

48. Scott, A. F., J. Phys. Chem., 35, 2315 (1931).

49. Redlich, O., J. Phys. Chem., 44, 619 (1940).

50. Redlich, O. and Mayer, D., Chem. Rev., 64, 221 (1964).

51. Baxter, G. P. and Wallace, C. C., J. Am. Chem. Soc., 38, 70 (1916).

52. Noyes, R. M., J. Am. Chem. Soc., 86, 971 (1964).

53. Fajans, K. and Johnson, O., J. Am. Chem. Soc., 64, 668 (1942).

54. Padova, J., J. Chem. Phys., 39, 1552 (1963).

55. Redlich, O. and Rosenfeld, P., Z. physik. Chem., A155, 65 (1931).

56. Owen, B. B., Miller, R. C., Milner, C. E., and Cogan, H. L., J. Phys. Chem., 65, 2065 (1961).

57. Kruis, A., Z. physik. Chem., B34, 1 (1936).

58. Owen, B. B. and Brinkley, S. R., Jr., Ann. N.Y. Acad. Sci., 51, 753 (1949).

59. Lewis, G. N. and Randall, M., "Thermodynamics", 2nd ed., McGraw-Hill Book Company, Inc., New York, New York, 1961.

60. Mukerjee, R., J. Phys. Chem., 65, 740 (1961).

61. Benson, S. W. and Copeland, C. S., J. Phys. Chem., 67, 1194 (1963).

62. Blandamer, M. and Symons, M., J. Phys. Chem., 67, 1304 (1963).

63. Stokes, R. H., J. Am. Chem. Soc., 86, 979 (1964).

64. Buckingham, A. D., Discussions Faraday Soc., 24, 151 (1957).

65. Hepler, L. G., J. Phys. Chem., 61, 1426 (1957).

66. Desnoyers, J. E., Verrall, R. E., and Conway, B. E., J. Chem. Phys., 43, 243 (1965).

67. Hepler, L., Stokes, J., and Stokes, R., Trans. Faraday Soc., 61, 20 (1965).

68. Lamb, A. B. and Lee, R. E., J. Am. Chem. Soc., 35, 1666 (1913).

69. Geffchen, W., Beckmann, C., and Kruis, A., Z. physik. Chem., B20, 398 (1933).

70. Hall, N. F. and Jones, O. T., J. Am. Chem. Soc., 58, 1915 (1936).

71. Hall, N. F. and Alexander, O. R., J. Am. Chem. Soc., 62, 3455 (1940).

72. Geffchen, W. and Price, D., Z. physik. Chem., B26, 81 (1934).

73. Dorsey, N. Ernest, "Properties of Ordinary Water-Substance", Reinhold Publishing Corporation, New York, New York, 1940.

74. MacInnes, D. A., Dayhoff, M. O., and Ray, B. R., Rev. Sci. Instr., 22, 642 (1951).

75. Spedding, F. H. and Jaffe, S., J. Am. Chem. Soc., 76, 884 (1954).

76. Heiser, David Judson, "A Study of Thermodynamic Properties of Electrolytic Solutions of Rare-Earths", Unpublished Ph.D. thesis, Library, Iowa State University of Science and Technology, Ames, Iowa, 1958.

77. Pearce, J. N. and Pumplin, G. G., J. Am. Chem. Soc., 59, 1221 (1937).

78. Gibson, R. E. and Kincaid, J. F., J. Am. Chem. Soc., 59, 25 (1937).

79. Pauling, L., "The Nature of the Chemical Bond", 3rd ed., Cornell University Press, Ithaca, New York, 1960.

80. Worthing, A. G. and Geffner, J., "Treatment of Experimental Data", John Wiley and Sons, Inc., New York, New York, 1943.

81. Morgan, L. O., J. Chem. Phys., 38, 2788 (1963).

82. Hoard, J. L., Proc. Intern. Conf. Co-ord. Chem., 8th, 135 (1964).

83. Grenthe, I., Acta Chem. Scand., 18, 293 (1964).

84. Fitzwater, D. R. and Rundle, R. E., Z. Krist., 112, 362 (1959).

85. Marezio, M., Plettinger, H. A., and Zachariasen, W. H., Acta Cryst., 14, 234 (1961).

86. Van Wazer, J. R., Lyons, J. W., Kim, K. Y., and Colwell, R. E., "Viscosity and Flow Measurement", Interscience Publishers, New York, New York, 1963.

87. Poiseuille, J. L. M., Compt. rend., 11, 961 (1840).

88. Barr, G., "A Monograph of Viscometry", Oxford University Press, London, England, 1931.

89. Swindells, J. F., Coe, J. R., Jr., and Godfrey, T. B., J. Res. Natl. Bur. Stand., 48, 1 (1952).

90. Cannon, M. R., Manning, R. E., and Bell, J. D., Anal. Chem., 32, 355 (1960).

91. Cannon, M. R. and Fenske, M. R., Ind. Eng. Chem. Anal. Ed., 10, 297 (1938).

92. Ubbelohde, L., J. Inst. Petrol., 19, 376 (1933).

93. Ubbelohde, L., J. Inst. Petrol., 22, 37 (1936).

94. Ubbelohde, L., J. Inst. Petrol., 23, 427 (1937).

95. "Standard Method of Test for Kinematic Viscosity: D445-61", in Am. Soc. for Testing Materials, "ASTM Standards on Petroleum Products and Lubricants", Am. Soc. for Testing Materials, Philadelphia, Pa., 1961.

96. Poiseuille, J. L. M., Ann. chim. phys., Ser. 3, 21, 76 (1847).

97. Arrhenius, S., Z. physik. Chem., 1, 285 (1887).

98. Grüneisen, E., Wiss. Abh. Phys. Techn. Reichsanstalt, 4, 151 (1905). Original not available; cited in Jones, G., and Dole, M., J. Am. Chem. Soc., 51, 2950 (1929).

99. Applebey, M. P., J. Chem. Soc., 97, 2000 (1910).

100. Jones, G. and Dole, M., J. Am. Chem. Soc., 51, 2950 (1929).

101. Jones, G. and Talley, S., J. Am. Chem. Soc., 55, 624 (1933).

102. Jones, G. and Stauffer, R., J. Am. Chem. Soc., 62, 335 (1940).

103. Jones, G. and Colvin, J., J. Am. Chem. Soc., 62, 338 (1940).

104. Cox, W. M. and Wolfenden, J. H., Proc. Roy. Soc. London, A145, 475 (1934).

105. Nightingale, E. R., Jr., J. Phys. Chem., 66, 894 (1962).

106. Lengyel, S., Tamás, J. Giber, J., and Holderith, J., Magyar Kém. Folyóirat, 70, 66 (1964).

107. Campbell, A. N., Gray, A. P., and Kartzmark, E. M., Canad. J. Chem., 31, 617 (1953).

108. Campbell, A. N., Debus, G. H., and Kartzmark, E. M., Canad. J. Chem., 33, 1508 (1955).

109. Miller, M. L. and Doran, M., J. Phys. Chem., 60, 186 (1956).

110. Falkenhagen, H. and Dole, M., Physik. Z., 30, 611 (1929).

111. Falkenhagen, H. and Vernon, E., Physik. Z., 33, 140 (1932).

112. Falkenhagen, H. and Kelbg, G., Z. Electrochem., 56, 834 (1952).

113. Pitts, E., Proc. Roy. Soc., 217A, 43 (1953).

114. Einstein, A., Ann. Phys., 19, 289 (1906).

115. Vand, V., J. Phys. Chem., 52, 277 (1948).

116. Vand, V., J. Phys. Chem., 52, 300 (1948).

117. Vand, V., J. Phys. Chem., 52, 314 (1948).

118. Hardy, R. C. and Cottington, R. L., J. Res. Natl. Bur. Stand., 42, 573 (1949).

119. Kaminsky, M., Z. physik. Chem., 8, 173 (1956).

VIII. ACKNOWLEDGEMENTS

The author wishes to thank Dr. F. H. Spedding for his guidance throughout the course of this research. He also wishes to express his appreciation to his wife for her patience and constant encouragement. The assistance rendered by the author's associates in preparing and analyzing a number of the solutions studied in this research is also greatly appreciated.